# LABORATORY INVESTIGATION OF THE TREATMENT OF CHROMIUM CONTAMINATED GROUNDWATER WITH IRON-BASED PERMEABLE REACTIVE BARRIERS

A THESIS SUBMITTED TO
THE GRADUATE SCHOOL OF NATURAL AND APPLIED SCIENCES
OF
MIDDLE EAST TECHNICAL UNIVERSITY

BY

BURCU UYUŞUR

IN PARTIAL FULFILLMENT OF THE REQUIREMENTS
FOR
THE DEGREE OF MASTER OF SCIENCE
IN
ENVIRONMENTAL ENGINEERING

AUGUST 2006

Approval of the Graduate School of Natural and Applied Sciences

_____
Prof. Dr. Canan Özgen
Director

I certify that this thesis satisfies all the requirements as a thesis for the degree of Master of Science.

_____
Prof. Dr. Filiz B. Dilek
Head of Department

This is to certify that we have read this thesis and that in our opinion it is fully adequate, in scope and quality, as a thesis for the degree of Master of Science.

_____
Prof. Dr. Kahraman Ünlü
Supervisor

Examining Committee Members

| | | |
|---|---|---|
| Assist. Prof. Dr. Ayşegül Aksoy | (METU, ENVE) | _____ |
| Prof. Dr. Kahraman Ünlü | (METU, ENVE) | _____ |
| Prof. Dr. Gürdal Tuncel | (METU, ENVE) | _____ |
| Prof. Dr. Filiz B. Dilek | (METU, ENVE) | _____ |
| Prof. Dr. Nurkan Karahanoğlu | (METU,GEOE) | _____ |

I hereby declare that all information in this document has been obtained and presented in accordance with academic rules and ethical conduct. I also declare that, as required by these rules and conduct, I have fully cited and referenced all the material and results that are not original to this work.

Name, Last Name: Burcu Uyuşur

Signature:

# ABSTRACT

## LABORATORY INVESTIGATION OF THE TREATMENT OF CHROMIUM CONTAMINATED GROUNDWATER WITH IRON-BASED PERMEABLE REACTIVE BARRIERS

Uyuşur, Burcu

M.Sc., Department of Environmental Engineering

Supervisor: Prof. Dr. Kahraman Ünlü

August 2006, 99 pages

Chromium is a common groundwater pollutant originating from industrial processes such as metal plating, leather tanning and pigment manufacturing. Permeable reactive barriers (PRBs) have proven to be viable and cost-effective systems for remediation of chromium contaminated groundwater at many sites. The purpose of this research presented in this thesis is to focus on two parameters that affect the performance of PRB on chromium removal, namely the concentration of reactive media and groundwater flux by analyzing the data obtained from laboratory column studies. Laboratory scale columns packed with different amounts of iron powder and quartz sand mixtures were fed with 20 mg/l chromium influent solution under different fluxes. When chromium treatment efficiencies of the columns were compared with respect to iron powder/quartz sand ratio, the amount of iron powder was found to be an important parameter for treatment efficiency of PRBs. The formation of $H_2$ gas and the reddish-brown precipitates throughout the column matrix were observed, suggesting the reductive precipitation reactions. SEM-EDX analysis of the iron surface after the breakthrough illustrated chromium precipitation. In addition to chromium; calcium and significant amount of

iron-oxides or -hydroxides was also detected on the iron surfaces. When the same experiments were conducted at higher fluxes, an increase was observed in the treatment efficiency in the column containing 50% iron. This suggested that the precipitates may not be accumulating at higher fluxes which, in turn, create available surface area for reduction. Extraction experiments were also performed to determine the fraction of chromium that adsorbed to ironhydroxides. The analysis showed that chromium was not removed by adsorption to oxyhydroxides and that reduction is the only removal mechanism in the laboratory experiments. The observed rate of Cr(VI) removal was calculated for each reactive mixture which ranged from 48.86 hour$^{-1}$ to 3804.13 hour$^{-1}$. These rate constants and complete removal efficiency values were thought to be important design parameters in the field scale permeable reactive barrier applications.

# ÖZ

## KROMLA KİRLENMİŞ YERALTI SULARININ DEMİR İÇEREN GEÇİRGEN REAKTİF BARİYER SİSTEMİYLE ARITIMININ LABORATUAR KOŞULLARINDA İNCELENMESİ

Uyuşur, Burcu

Yüksek Lisans, Çevre Mühendisliği Bölümü

Tez Danışmanı: Prof. Dr. Kahraman Ünlü

Ağustos 2006, 99 sayfa

Krom metal kaplama, deri tabaklama, boya maddesi imalatı gibi endüstriyel işlemlerden kaynaklanan yaygın bir yeraltı suyu kirleticisidir. Geçirgen reaktif bariyerler (GRBler) kromla kirletilmiş yeraltı sularının arıtımında geçerli ve ekonomik olarak uygun sistemlerdir. Bu tezde sunulan araştırmanın amacı laboratuvar kolon çalışmalarından elde edilen verileri analiz ederek GRBlerin performansını etkileyen reaktif madde derişimi ve akış hızı gibi önemli iki parametre üzerinde yoğunlaşmaktır. Farklı miktarlarda demir tozu ve kuvars kum içeren karışımlarla doldurulan laboratuvar ölçekli kolonlar 20 mg/l krom iceren giriş suyu ile farklı akış hızlarında beslenmiştir. Kolonların verimleri demir tozu/kuvars kum oranlarına göre karşılaştırıldığında demir tozu miktarının GRBlerin giderim verimliliği açısından önemli bir parametre olduğu görülmüştür. Hidrojen gazı oluşumu ve kolon boyunca kırmızımsı-kahverengi çökeltiler gözlenmesi indirgeyici-çökelme tepkimelerin varlığına işaret etmektedir. Kolon kapasitesine erişildiğinde elde edilen SEM-EDX analizleri krom çökelmesini göstermiştir. Demir yüzeylerinde kromun yanısıra, kalsiyum ve ciddi miktarda demir oksit veya –hidroksit tespit edilmiştir. Aynı deneyler daha yüksek akış hızlarında tekrar edildiğinde, % 50 demir içeren kolonun giderim veriminde artış gözlenmiştir. Bu durum çökeltilerin yüksek akış oranlarında birikmediğini ve bu nedenle indirgeme tepkimeleri için daha fazla yüzey alanı

oluşturduğunu düşündürtmektedir. Ayrıca, demir oksitlere absorbe edilmiş krom oranını belirlemek amacıyla ekstraksiyon deneyleri yapılmıştır. Bu analizler sonucunda kromun demir oksitlere absorbe edilerek giderilmediği ve tek giderim mekanizmasının indirgeme olduğunu göstermiştir. 48.86 saat$^{-1}$ ve 3804.13 saat$^{-1}$ arasında değişen krom(VI) giderim oranları her reaktif karışım için hesaplanmıştır. Bu oranlar ve tam giderim verim değerlerinin saha ölçekli geçirgen reaktif bariyer çalışmaları için önemli dizayn parametreleri olabileceği düşünülmektedir.

Anahtar Kelimeler: Krom(VI), sıfır değerlikli demir, yeraltı suyu, geçirgen reaktif bariyer

# ACKNOWLEDGEMENTS

# TABLE OF CONTENTS

# LIST OF TABLES

**TABLES**

# LIST OF FIGURES

**FIGURES**

# LIST OF ABBREVIATIONS

$b$ :Minimum thickness of barrier in the direction of groundwater flow

$C_o$ :Contaminant concentration entering the permeable reactive barrier

$C_T$ :Target contaminant concentration downgradient of permeable reactive barrier

$\varepsilon$ :Bed void fraction

$k$ :Reaction rate constant

$k_{obs}$ :First-order reaction rate constant

$k_{SA}$ :Surface area normalized rate constant

$P_o$ :Initial concentration of Cr(VI)

$P$ :Concentration of dissolved Cr(VI)

$PRB$ :Permeable Reactive Barrier

$PV$ :Pore Volume

$q$ :Flux

$Q$ :Liquid flow rate

$t$ :Contact time between Cr(VI) solution and zero-valent iron

$t_{res}$ : Residence time

$x$ :Fraction of sand in the reactive mixture

$ZVI$ : Zero-Valent Iron

$\rho_b$ :Bulk density

$\rho_{sand}$ :Particle density of quartz sand

$\rho_s$ :Particle density of column mixture

$\rho_{iron}$ :Particle density of zero-valent iron

$v$ :Groundwater velocity through the barrier

$V$ :Reactor volume

$\phi$ :Porosity

$\rho_m$ :Surface area of zero-valent iron particles per solution volume

50*IR*   :Column containing 50% zero-valent iron

25*IR*   :Column containing 25% zero-valent iron

10*IR*   :Column containing 25% zero-valent iron

# CHAPTER 1

## INTRODUCTION

### 1.1. Overview

Groundwater is the most abundant and reliable freshwater resource on earth. Most of the drinking water is supplied from groundwater resources in many countries; 26% in Canada, more than 50% in USA, up to 80% in Europe and Russia, and even more in North Africa and the Middle East. Despite its vital importance, a lack of adequate attention to groundwater sustainability resulted in depletion and contamination of groundwater worldwide. Contaminated sites have become a major concern for communities who rely on groundwater for their water supply. Traditional approaches to treating contaminated groundwater have involved removing the source, pumping, and treating the contaminant plumes or isolating the source area with low permeability barriers or covers. However, these methods are costly and often ineffective in meeting long term long-term protection standards (Travis and Doty, 1990; Gillham and Burris, 1992; National Research Council, 1994; U.S.EPA, 2000a). Instead of these ex-situ approaches, the use of subsurface permeable reactive barriers (PRBs) for cleaning up contaminant plumes has become established as an economical technology for the in situ treatment of contaminated groundwater in 1990s. A PRB is an engineered zone of reactive material placed in an aquifer that allows the passage of groundwater while retaining or degrading the contaminants (Morrison et al., 2002). The major advantage of permeable reactive barriers over other conventional groundwater remediation approaches are the reduced operation and maintenance costs and enhanced technical

efficacy, particularly compared with pump-and-treat approaches (Thomas and Ward, 1995; Clark et al., 1997) and this advantage is the main driving factor for its applications. To date, there may be as many as 200 PRB installations worldwide (ITRC, 2005). PRBs have been used to treat a range of contaminants in groundwater such as organohalogen compounds (e.g. TCE, PCE, DCE); metals (e.g. chromium and arsenic); nitrate and radionuclides (e.g. uranium) and a range of reactive materials have been used such as metals (e.g. zero valent iron), granular activated carbon, organic materials (e.g. wood chip, compost), modified clays, chelators, zeolites, chemical oxidants and reducing agents (Environment Agency, 2002).

Chromium is one of the widely used metals (Barnhart, 1997) and contamination with anthropogenic Cr(VI) has been experienced in numerous soils, waste sites, surface waters and groundwaters (Calder, 1988; Palmer and Wittbrodt, 1991; Buerge, 1997). The treatment of Cr(VI) by zero-valent iron (ZVI) PRBs involves reduction of Cr(VI) to Cr(III) coupled with the oxidation of $Fe^0$ to Fe(II) and Fe(III) and the subsequent precipitation of sparingly soluble Fe(III)-Cr(III) oxyhydroxides and hydroxides (Wilkin et al., 2005). The extend and rate of Cr(VI) removal by ZVI has been studied in batch tests (Gould, 1982; Cantrell et al., 1995; Powell et al., 1995; Alowitz and Scherer, 2002;), column tests (Blowes et al., 1997; Astrup et al., 2000; Gandhi et al., 2002; Kaplan and Gilmore, 2004; Lo et al., 2006), pilot scale field trials (Puls et al., 1995) and in a number of full-scale demonstrations (Puls et al., 1999). The results of these studies indicated that the rate of Cr(VI) by ZVI is sufficiently rapid for use in groundwater remediation systems.

## 1.2. Scope

Generally, the design and the implementation of field scale PRBs have been preceeded by laboratory treatability tests. Column tests are used to evaluate the fate of contaminant(s) under dynamic flow conditions to simulate field conditions. Using the residence time and the flow velocity, the thickness of the treatment wall can be determined. It is also possible to evaluate a variety of parameters such as reactive media type and concentration, groundwater flow velocity, pH, initial concentration of

contaminant(s) and solution chemistry for their effect on the reactivity and the longevity of the system under dynamic flow conditions. Since the design parameters of the PRB is generally derived from column studies, it is crucial to investigate these parameters for a reliable design.

The main goal of this study to measure Cr(VI) removal efficiency by ZVI under flow conditions. In the first part of the study, the performance of PRBs under different groundwater flow velocities and ZVI concentrations were the scope to be studied. Also, the morphology of ZVI surface was studied by surface analytical techniques to identify the precipitates. In the second part, the data was analyzed in terms of reaction rate constants. The first-order Cr(VI) removal rate constants were found for complete removal phase. Lastly, the applicability of these findings was discussed in terms of field scale PRB applications.

## 1.3. Objectives

Despite the extensive research and wide applications of Cr(VI) removal by different types of iron species, there is still an information gap about the role of various components that control the effectiveness and longevity of the treatment of Cr(VI) by PRBs such as ZVI surface concentration and groundwater velocity. Furthermore, most of the treatability studies were carried out in batch mode, which does not simulate the dynamic groundwater flow environment properly. The specific objectives of this study were:

- To determine the Cr(VI) removal efficiency with respect to groundwater flux and ZVI concentration.

- To investigate the reaction kinetics of Cr(VI) removal by elemental iron as a function of groundwater flux and ZVI concentration.

- To recommend general design parameters for guiding field scale PRB applications.

**CHAPTER 2**

**LITERATURE SURVEY**

**2.1. Chromium in the Environment**

Chromium is one of the most widely used metals worldwide. Meanwhile, this large scale usage also brings about environmental problems because, it can exist in forms that are toxic and can be hazardous to the environment. Thus, it is important to know sources, transformation mechanisms and fate and transport of chromium in the environment.

**2.1.1. Source and Extend of Contamination in the Environment**

Chromium is an important industrial metal used in diverse products and processes (Nriagu, 1998). On a worldwide basis, about 80% of the mined chromium goes into metallurgical applications, mostly into manufacture of stainless steel. About 15% is used in the manufacture of chromium chemicals, and the remainder is used in refractory applications (Barnhart, 1997). In metallurgical applications, chromium is introduced into iron, steel and other alloys with ferrochromium, which is produced by the "pyro-metalurgical reduction" of chromite with carbon and/or silicon in high temperature electric arc furnaces. In chemical applications, sodium dichromate is produced from chromite ore following a kiln roasting process with soda ash. Derivative chemicals are then produced from the bulk chemical (Allen, 2003). At the end of the processing of the ore for the manufacture of Cr(VI) compounds, there is a waste residue or "mud" that contains $CaCrO_4$, calcium aluminochromate ($3CaO. Al_2O_3. CrO_4$), tribasic calcium chromate [($Ca_3(CrO_4)_2$], and the basic ferric chromate [$Fe(OH)CrO_4$] that dissolve and add hexavalent chromium to percolating waters (Gansy and Wamser, 1965; Palmer and Wittbrodt, 1991). Natural materials such as leather, wood and timber are stabilized for durability and long service by chromium salts that also allow permanent fixing of other

compounds such as colorful dyes, fungicides, and insecticides. Leather tanning is the largest chemical use, and timber preservation with the well-known CCA (Copper, Chromium, and Arsenic) product (ICDA, 2003). Due to the operation procedures at that time, nearly all wood preserving plants 20 years or older present some degree of soil and groundwater contamination (U.S. EPA, 2000b). Chromium pigments used in paints, inks, and plastics coloring are the second largest use. Zinc and strontium chromates are used in corrosion resistant priming paints. Other uses include chromium electro-plating, alternative surface coatings, catalysts, drilling muds, water treatment, textile dyes, and refractories.

As noted, industrial applications most commonly use chromium in oxidized form (Cr(VI)) (U.S. EPA, 2000b). Cr(VI) does not always readily reduce to Cr(III) and can exist over an extended period of time. Consequently, the resulting waste can introduce high concentrations of toxic and carcinogenic chromium in the environment (see next section for chromium chemistry). In fact, chromium is among the most common groundwater contaminants (NRC, 1994; Hellerich, 2005). Leakage, poor storage and improper disposal practices at manufacturing and ore processing facilities have released chromium to the environment, causing contamination of groundwater and surface water (Calder, 1988; Palmer and Wittbrodt, 1991). Several contaminated sites can be found in the literature. Two recent examples of chromium contaminated sites are as follows:

o Shawfield Glassgow Site, Scotland: Groundwater recovered from this site showed Cr(VI) concentrations three order magnitude in excess of Environmental Quality Standard in drinking waters (Farmer et al., 2002) which is derived from a former chromium salt production factory. Over 2.5 million tones of waste, called chromium ore processing residue (COPR), were generated from chromite ore treatment activities and this material has subsequently been used for infilling quarries and low lying areas in and around Glasgow and also for the construction of various earthworks such as terracing surrounding sports fields. These sites have been recorded as heavily contaminated by chromium (Farmer et al., 1999).

According to Glasgow City Council's 2004 report, a GIS system has been developing in further assessment.

o Hudson County, New Jersey: Waste material was created by three chromite ore smelting facilities that operated in Hudson City form 1900s to 1970s. Approximately, 2 to 3 million tons of this slag, which still contained hazardous levels of chromium, was used as a fill material in residential, recreational, public, commercial, and industrial areas. Until 1994, more than 160 separate waste sites containing chromium smelting slag had identified in or around Hudson City. Many of the sites have undergone remediation to decrease human exposure to and environmental contamination with chromium (Chromium Medical Surveillance Project, Summary of Final Technical Report, 1994).

Though not common, Cr(VI) can also be released into the environment through natural processes as well as anthropogenic activities (Palmer and Wittbrodt, 1991). For example, naturally elevated levels of hexavalent chromium have been found in Paradise Valley Arizona (Robertson, 1975), and Atacama Desert in Chile (Ericksen, 1983).

## 2.1.2. Chromium Chemistry

Chromium has a unique geochemical behavior in natural water systems (U.S. EPA, 2000b). It exists in oxidation states ranging from +6 to -2, however only the +6 and +3 oxidation states are commonly encountered in the environment. Redox and pH conditions are the main determining factors for the speciation of chromium in the environment. Under oxic conditions, hexavalent chromium, Cr(VI), exists as Cr(VI) oxyanions, $HCrO_4^{2-}$ (bichromate ion) at $pH \leq 6$ and $CrO_4^{2-}$ (chromate ion) at pH>6. Under reducing environments, Cr(III) predominates at ionic ($Cr^{3+}$) at pH values less than 3.0. At pH values above 3.5, hydrolysis of Cr(III) in a Cr(III)-water system yields trivalent chromium hydroxyl species ($CrOH^{2+}$, $Cr(OH)_2^+$, $Cr(OH)_3^0$, and $Cr(OH)_4^-$) (U.S. EPA, 2000b).

Cr(VI) is known to be toxic, mutagenic, teratogenic and carcinogenic. It is also very soluble, mobile, and moves at a rate essentially the same as the groundwater (Palmer and Puls, 1994). Unlike Cr (VI), Cr(III) has relatively low toxicity and very stable except in the presence of oxidized Mn, and are not oxidized by atmospheric $O_2$ until pH>9. Under most natural environmental conditions, Cr(III) readily precipitates as $Cr(OH)_3$ or as the solid solution $Fe_xCr_{1-x}(OH)_3$ (Rai et al., 1987; Sass and Rai, 1987; Puls et al., 1999a).

Natural oxidized chromium (chromate) is rare. However, industrial applications most commonly use chromium in the Cr(VI) form, which can introduce high chromate into the environment. Meanwhile, it is a strong oxidizing agent and is reduced to Cr(III) in the presence of electron donors. Electron donors commonly found in soils include aqueous Fe(II), ferrous iron minerals, reduced sulfur, and soil organic matter (Palmer and Puls, 1994). The reduction of Cr(VI) to the less soluble and less mobile Cr(III) valence state by a variety of reductants is thermodynamically favorable and kinetically rapid (Schroeder and Lee, 1975; Hem, 1977; Eary and Rai, 1988; Palmer and Wittbrodt, 1991; Palmer and Puls, 1994; Wittbrodt and Palmer, 1994; U.S. EPA, 1999). This property is the primary factor for the viability of natural attenuation (Palmer and Puls, 1994) and/or in situ treatment approaches using reactive zone technology (U.S. EPA, 2000b).

## 2.2. Permeable Reactive Barrier Technology

### 2.2.1. Technology Description

Permeable reactive barrier is a permeable zone of reactive material placed in subsurface in which contaminants in the plume are either removed or transformed into environmentally desirable phase while passing through it. The barrier is a barrier to contaminants; however, it is more permeable than the aquifer to enable the passage of the plume in a reasonable time. The treatment zone can be created directly using reactive materials or indirectly using materials designed to stimulate contaminant treatment

through physical, chemical or biological ways. A permeable reactive subsurface barrier is defined as:

*An emplacement of reactive materials in the subsurface designed to intercept a contaminant plume, provide a flow path through the reactive media, and transform the contaminant(s) into environmentally acceptable forms to attain remediation concentration goals downgradient of the barrier* (Powell and Powell, 1998; Powell and Puls, 1997, U.S. EPA, 1998).

PRBs have originally used to intercept and treat only contaminant plumes. Currently, however, they can also be installed near the source to reduce mass flux by a given percent with the idea that natural attenuation or some other remedy will address the downgradient residual contamination. Consequently, PRBs can be designed with different site specific objectives in mind. Figure 2.1 illustrates the examples of PRB configurations in use today (ITRC, 2005). Besides its employment independently, PRBs can also be used as part of an integrated treatment train approach, incorporating a range of active and passive remedial measures (Environment Agency, 2002).
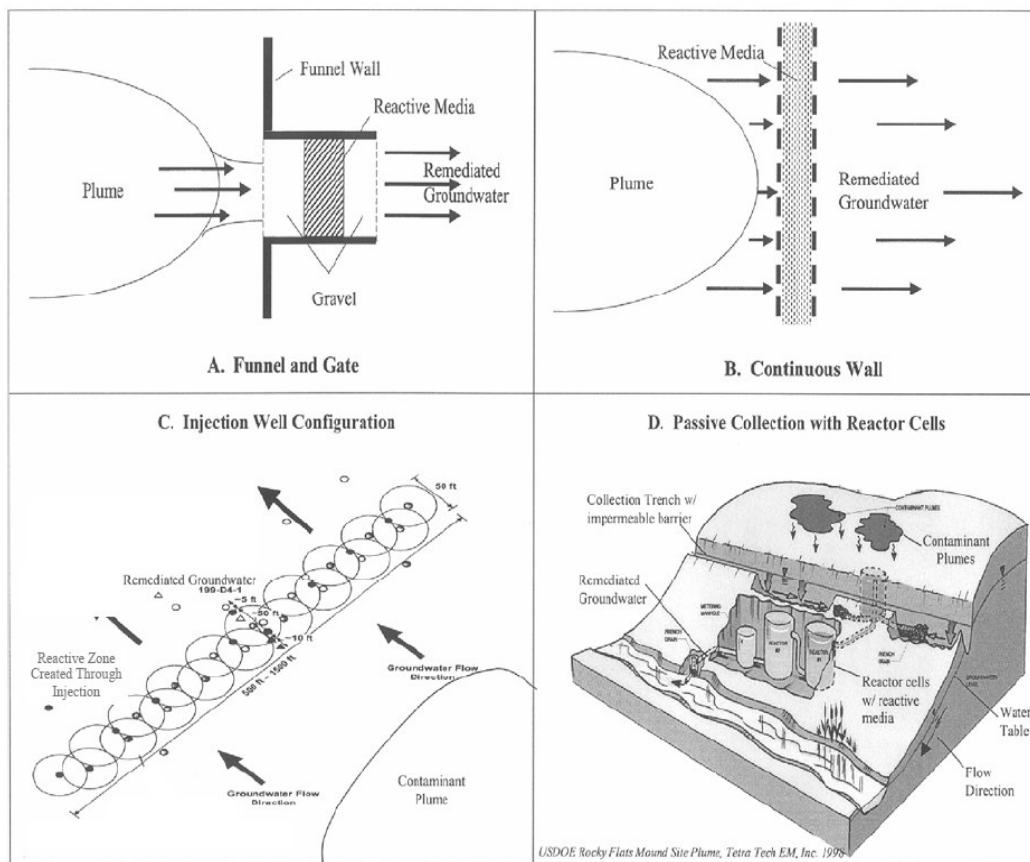
Figure 2.1. Examples of PRB configurations (ITRC, 2005).

The typical advantages and disadvantages of PRBs can be summarized as (Sharma and Reddy, 2004):

Advantages

- PRBs can remediate plume even when the source of the plume cannot be located.
- PRBs can degrade or immobilize contaminants in situ without having to bring contaminated groundwater to the surface,
- Energy requirements are low because natural groundwater flow is used to carry contaminants through the treatment zone,

- Only periodic replacement or rejuvenation of the reaction medium may be required,
- No effluents are generated that require permits and treatment, and
- Environmental impacts may be reduced because there is minimal disturbance to surface activities.

Limitations
- Plume must be very well characterized and delineated, for example, no fractured rock or excessive depth to contaminant plume,
- Limited long-term field testing data is available and field monitoring is in its infancy.
- Limited field data concerning longevity of wall reactivity or loss of permeability due to precipitation.
- Blockage of the pore space with products of reaction processes, particularly with injection based systems.

A brief review of the treatment media, treatable contaminants and design issues are given in the following sections.

### 2.2.2. Contaminants and Reactive Materials in PRB Applications

PRBs are capable of treating a number of contaminants in different removal mechanisms. These mechanisms include (ITRC, 2005),

- ✓ Reductive Dechlorination: chemical dehalogenation process causes highly reducing conditions in the presence of ZVI which brings about substitution of chlorine atoms by hydrogen in the structure of chlorinated hydrocarbons.

✓ pH Control: the solubility, thus the mobility of many inorganic contaminants-such as chromium, copper, zinc, and nickel- decreases in a range of neutral to slightly basic pH and increases in either very acidic or basic pH solutions. pH control process, which has long been applied for certain projects such as acid-mine drainage, applies this specialty in PRB concept.

✓ Oxidation Reduction: modifying redox reactions, through the modification of the state of the redox sensitive elements is the goal in PRB applications employing redox reactions. Use of tools such as Pourbaix diagrams, or Eh-pH diagrams, to evaluate groundwater systems for the anticipated concentration of various aqueous species under certain geochemical conditions is important in assessing which treatment materials might be effective for a contaminant.

✓ Sorption: keys to the use of effective sorption techniques in PRBs include selecting materials that are relatively hydrophobic and insoluble. Materials that simply biodegrade or adsorb water are not considered as feasible choices. Also, the effects of potential desorption, or reversed ion-exchange, should be considered for all potential uses of these materials.

✓ Bioremediation: many of the primary chemicals of concern, such as VOCs, inorganic constituents and radioactive materials can be treated through biological reactions promoted by PRBs. It is important to sustain the conditions required for biological reactions to proceed until achieving the target concentration.

The list of materials and treatable contaminants in PRB applications is given in Table 2.1.

Table 2.1.  Reactive materials and corresponding treatable contaminants in PRB applications (Adapted from ITRC, 2005)

| Treatment Material Category | Example Materials | Constituents treated |
|---|---|---|
| Reductive dechlorination for organic compounds | Zero valent metals (Fe) | Chlorinated ethenes, ethanes, methanes, and propanes; chlorinated pesticides, Freons, nitrobenzene |
| Reduction for metal contaminants | Zero valent metals (Fe), basic oxygen furnace slag, ferric oxides | Cr, U, As, Tc, Pb, Cd, Mo, U, Hg, P, Se, Ni |
| Sorption and ion exchange | Zero-valent iron, granular activated carbon, apatite (and related materials), bone char, zeolites, peat, humate | Chlorinated solvents (some), BTEX, Sr-90, Tc-99, U, Mo |
| pH control | Limestone, lime-based materials, compost, zero valent iron | Cr, Mo, U, acidic water |
| In situ redox manipulation | Sodium dithionite, calcium polysulfide | Cr, chlorinated ethenes |
| Enhancements for bioremediation (including carbon, oxygen, and hydrogen sources) | (Includes solid, liquid, and gaseous sources) Oxygen-release compounds, hydrogen-release compounds, carbohydrates, lactate, zero-valent iron, compost, peat, sawdust, acetate, | Chlorinated ethenes and ethanes, nitrate, sulfate, perchlorate, Cr, MTBE, polyaromatic hydrocarbons |

## 2.2.3. Design Considerations

The design variables that often can be controlled to optimize the design of a PRB include the reactive media, PRB dimensions, PRB orientation, PRB location, PRB configuration and safety factors (Gavaskar, 1999; ITRC, 2005). Table 2.2 summarizes the parameters that are needed in the design process.

Table 2.2. Summary of Parameters that need to be determined in the design process (Adapted from Environment Agency, 2002).

| Design Parameter | | Comment |
|---|---|---|
| Reactive media | Chemical composition<br>Surface Area<br>Grain size<br>Hydraulic conductivity<br>Strength | Design optimization for the reactivity and hydraulic conductivity of a PRB is vital. |
| Barrier Dimensions | Thickness | Dependent on residence time and velocity |
| | Depth<br>Width | Intercept the entire contaminant plume |
| Barrier Orientation | | Simulation of a wide range of hydraulic conditions enables an optimum design. |
| Barrier Location | | |
| Barrier Configuration | Continuous<br>Funnel-and-gate | |
| Safety Factors | | Uncertainties associated with design should be taken into account |

Reactive media

Besides its treatability of the contaminant(s) in the field, the selection of reactive media also includes specification of chemical composition, grain size, surface area, hydraulic conductivity and strength.

Chemical composition is vital for a design not only for reactivity but also for the risk of any potential contaminants (impurities) which may be harmful. The permeability of the reactive material is, in general, be proportional to the square of grain size, however, the surface area (hence the rate of reaction) is inversely proportional to grain size. Where there is a risk of fouling or precipitation of secondary mineral phases, the effect of this on the hydraulic performance of the PRB is likely to be more adverse for smaller grain sizes. The design therefore represents a compromise between reactivity (smaller grain size), permeability (larger grain size) and the effect of clogging (Environment Agency, 2002).

Barrier dimensions

The three barrier dimensions that need to be designed are the thickness, width and depth. The thickness and length depend partly on the selected configuration (continuous versus funnel-and gate) and are somewhat interrelated.

Reaction rates or half lives of contaminants in contact with the reactive medium are necessary to determine the reactive cell thickness that will provide sufficient residence time for the contaminants to degrade to their targeted concentrations. Because continuous tests better simulate the dynamic groundwater flow environment, testing in columns is by far the most common method. For each column at each velocity, contaminant concentrations are plotted as a function of distance along the column. The flow rate is used to calculate the residence time at each sampling position (relative to influent) for each profile. The contaminant degradation or disappearance rate

constants are calculated for each contaminant in the influent solution, using kinetic models.

The required residence time for a contaminant in the PRB will depend on the reaction rate and the required reduction in contaminant concentration. This is illustrated for first-order by the following equation:

$$t_{res} = \left[ \frac{\ln(C_T / C_0)}{-k} \right] \quad (2.1)$$

where,

$t_{res}$ = residence time (T)
$C_0$ = contaminant concentration entering the PRB (M/L$^3$)
$C_T$ = target concentration downgradient of the PRB (M/L$^3$)
$k$ = reaction rate constant (T$^{-1}$)

The minimum barrier thickness can be estimated from the following expression (Environment Agency, 2002):

$$b = v.t_{res} \quad (2.2)$$

where,

$b$ = minimum thickness of PRB in direction of water flow (L)
$v$ = groundwater velocity throughout the barrier (L/T)

Although the residence time requirement is relatively fixed based on the contaminant reaction rates, it should be noted that the groundwater velocity in this equation is the

velocity through the reactive cell and not the velocity in the aquifer. This reactive cell velocity may vary based on the relative porosties and hydraulic conductivities of the aquifer and the reactive cell, as well as the length of the funnel in a funnel-and-gate system and funnel-to-gate ratio. These variables have to be optimized to determine design dimensions of the gate (Gavaskar, 1999).

The primary physical function of the PRB is to capture the targeted groundwater (and plume) and provide it with sufficient residence time in the reactive media to achieve desired clean up goals. Consequently, the other parameter of concern when designing PRB is hydraulic capture width. Capture zone width refers to the width of the zone of groundwater that will pass through the reactive cell or gate rather than pass around the ends of the barrier or beneath it. Capture width is proportional to groundwater flow rate and residence time is inversely proportional to groundwater flow rate. The design will represent a balance between achieving sufficient capture width to capture the plume and ensuring sufficient residence time for the treatment process  The width of capture zone will increase or decrease as the ratio of reactive media hydraulic conductivity to aquifer hydraulic conductivity increases or decreases, respectively (Environment Agency, 2002). Sufficient hydraulic capture of the plume can be accomplished by ensuring that the particle size range (and the permeability) of the reactive media is significantly greater than that of the surrounding aquifer (ITRC, 2005). Different widths of a continuous reactive barrier, gate, or funnel can be simulated to evaluate any trade-offs that may occur between various design parameters (e.g., increased hydraulic capture width versus longer residence time in the reactive cell) (Gavaskar et al., 2000).

Barrier Orientation

A barrier orientation perpendicular to the groundwater flow ensures that the most efficient capture of the targeted portion of the groundwater (or the plume) is obtained. The uncertainty in this scenario is the groundwater flow direction. Determining the

exact groundwater direction in a much localized setting may be difficult, especially at sites with relatively flat gradients. Even if the regional groundwater flow direction is known, localized flow in the immediate vicinity of the barrier may vary. In addition, flow direction may change seasonally. At times when the groundwater flow is not exactly perpendicular to the face of the barrier, part of the plume may flow around the barrier, even though the barrier is still capturing approximately the same amount of water. To overcome these difficulties, examination of historical water levels to determine the variation in flow direction under seasonal high flow and low flow conditions is necessary. Furthermore, modeling multiple hydrologic scenarios to account for anticipated changes in seasonal flow directions and any unanticipated deviations in flow direction due to the uncertainty in defining localized flow is necessary (Gavaskar, 1999).

Barrier Location

Once the targeted plume has been adequately mapped out, determining a suitable location for the barrier depends on hydrologic, geotechnical, and administrative considerations.

Hydrologic considerations generally dictate that the barrier be placed just downgradient from the edge of the plume and oriented perpendicular to the groundwater flow for the most efficient capture of the plume. In this way, all of the contaminant can be treated and the plume is prevented from moving any further toward potential receptors. The presence of preferential plume pathways (such as sand channels) may also guide the location of the barrier.

Geotechnical considerations for locating the barrier may include the presence of underground utilities, cobbles and highly consolidated sediments. These factors will increase the difficulty of installation. The presence of buildings or other aboveground structures may also impede installation in certain areas.

Administrative considerations for guiding the location of the barrier may include a situation where the plume has moved off the property boundaries (Gavaskar, 1999).

Barrier Configuration

A PRB may be installed as a funnel-and-gate or a continuous system. A funnel-and-gate system consists of (Figure 2.1.A) an impermeable section (or funnel) that directs the captured groundwater flow towards the permeable section (or gate). This configuration sometimes allows better control over reactive cell placement and plume capture. At sites where the groundwater flow is very heterogeneous, a funnel-and-gate system can allow the reactive cell to be placed in the more permeable portions of the aquifer. At sites where the contaminant distribution is very non-uniform, a funnel-and-gate system can better homogenize the concentrations of contaminants entering the reactive cell. A continuous reactive barrier (Figure 2.1. B) consists a reactive cell containing the permeable reactive medium (USACE, 1997). Both of these techniques require some degree of excavation and limited to fairly shallow depths of sixteen to twenty-one meter or less. Newer techniques for emplacing the reactive media, such as injection wells (Figure 2.1 C) and passive collection with reactive cells (Figure 2.1. D) may serve to overcome some of these emplacement limitations.

Safety Factors

One way of ensuring that sufficient residence time is available in the future is to incorporate a safety factor in the designed flow through thickness of the reactive media in the PRB (ITRC, 2005). The uncertainties include seasonal and long term variations in the groundwater flow velocity and direction, variations in the contaminant concentration if the plume continues to develop, decrease in the bulk density of the reactive cell due to differential compaction in field applications and the change in the reaction rate due to temperature differences in the laboratory and field

applications (Gavaskar et al., 1999). Because of these uncertainties, it is probably sufficient to use a reasonable safety factor, in the range of about 2 to 3 times the calculated flow thickness at most sites (Environment Agency, 2002)

### 2.2.4. PRB Implementation

Successful remediation of contaminated groundwater using PRB technology requires the steps shown in Figure 2.2. These steps involve the determination of (Gavaskar, 1999):

- Suitability of a site for permeable reactive barrier application,
- Site characteristics affecting barrier design,
- Reaction rates or half lives (through column testing),
- Location, configuration and dimensions of the barrier,
- Longevity,
- Monitoring strategy,

The suitability of a site for PRB application follows a preliminary assessment that is designed to ensure that whether a PRB is likely to be an effective remedial option. After preliminary assessment, the necessary site characterization data is obtained. A good conceptual and, most often, a computerized model of the groundwater flow system should be generated with the site characterization data to aid the design. After this step, reaction rates or half lives of contaminants in contact with the reactive medium are necessary to determine the reactive cell thickness that will provide adequate residence time for the contaminants to degrade to their MCLs. The location, configuration, dimensions of the barrier and longevity issues are mainly based on site characterization data. Monitoring strategy includes groundwater monitoring well installation and development, sample collection, sample preservation and shipment, analytical procedures and chain-of custody control. These steps are detailed in the following parts.
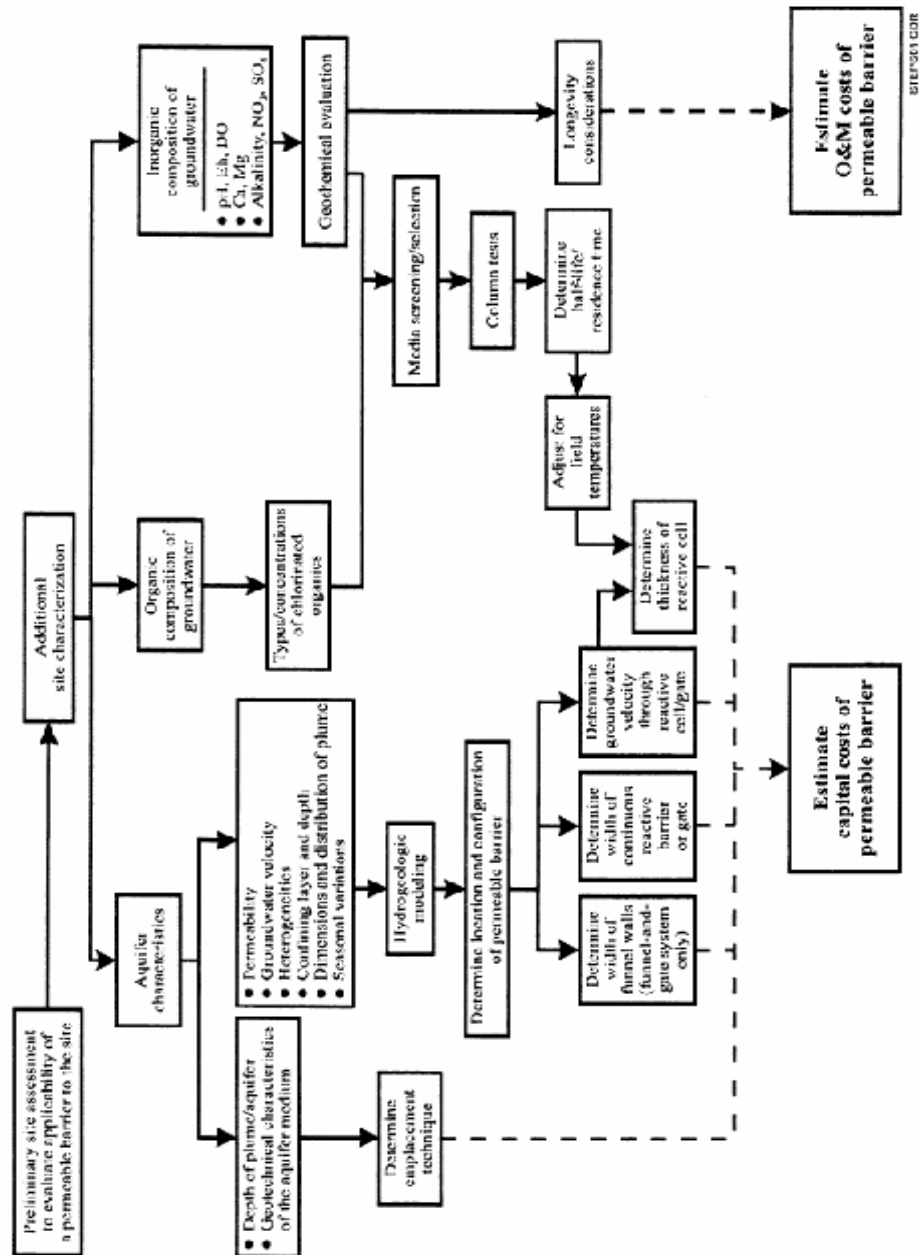
Figure 2.2. Steps in the Design of a Permeable Reactive Barrier (USACE, 1997; Gavaskar, 1999)

*Preliminary assessment:* Generally, a review of existing site documents, such as Remedial Investigation/Feasibility Study (RI/FS) reports and a visual examination of the layout of the site form the basis for a preliminary assessment of the feasibility of a permeable reactive barrier (Gavaskar, 1999). A preliminary assessment, as detailed in Figure 2.3., should be made to determine the suitability of a site for PRB application. Although an unfavorable response to any of the factors in the figure does not necessarily rule out a permeable reactive barrier, such a response can make the application more costly and difficult (USACE, 1997).
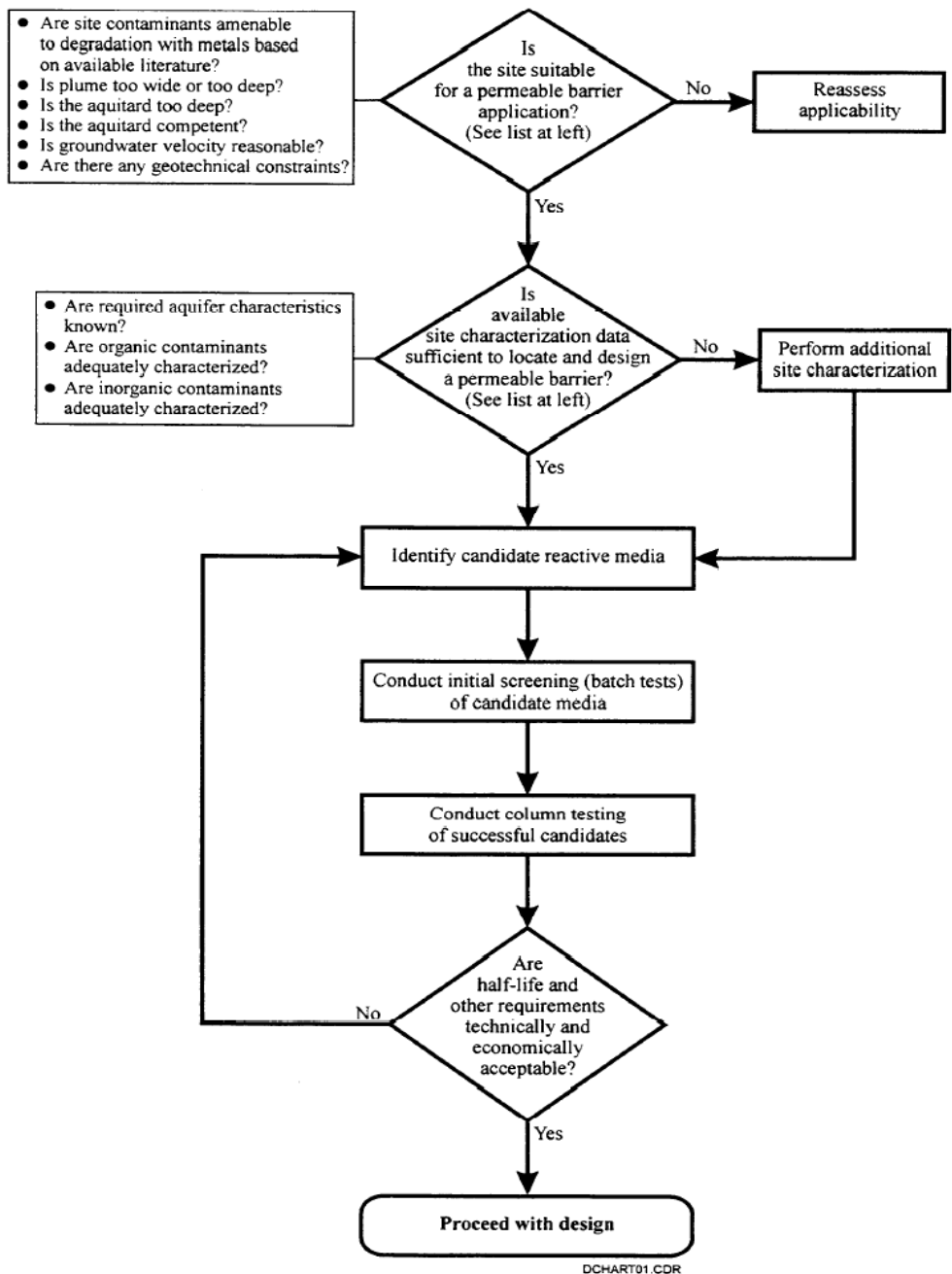
Figure 2.3. General approach for preliminary assessment of PRB design (USACE, 1997).

*Size characterization:* If the preliminary assessment shows that the site is suitable, a detailed site characterization should be conducted to determine aquifer and groundwater characteristics. The important site information required includes the contaminant distribution of the groundwater, hydrogeology of the site, geochemical composition of groundwater and geotechnical and topographic considerations. Contaminant distribution in the groundwater covers information on spatial distribution of the contaminants and temporal changes of contaminant concentration. Size characterization on hydrogeology of the site involves getting information about local hydrogeology of the site and determining groundwater velocity. Geochemical composition of groundwater is monitored through measuring parameters such as pH, dissolved oxygen and redox potential in the groundwater. This step is mainly for the purpose of determining whether conditions in the site can cause precipitate formation in the presence of reactive medium (Gavaskar et al, 2000).

*Selection of Reactive Media.* In treatability testing, batch test is employed for a quick screening of multiple reactive media whereas column tests are employed for final selection of the reactive media and obtaining design information such as contaminant half lives or reaction rates. The following issues should be taken into consideration in selecting the appropriate reactive media (USACE, 1997):

- ➤ Reactivity: the candidate medium should be bale to degrade the contaminant(s) in a reasonable period of time.
- ➤ Stability: the candidate material should retain its reactivity and hydraulic conductivity over time.
- ➤ Availability and Cost: the price of candidate material should be reasonable since large quantities of reactive material may be needed in the construction.

- ➢ Hydraulic Performance: lower particle size results in better reactivity because of increased surface area, but it will decrease the conductivity of the media; consequently, an optimization should be made for the particle size of the media.
- ➢ Environmental Compatibility: the media should not cause any adverse chemical reactions or by products when reacting with constituents in the contaminant plume, and should not act as a possible source of contaminant itself.

Following identification of the reactive media, batch tests could be performed to quickly screen several candidates. If only one or two candidates have been identified, screening by batch testing could be foregone in favor of batch testing. Column tests are more representative then batch tests and provide more accurate design information. Column tests are conducted to select the final reactive medium and determine half lives or residence times. It is recommended that column tests be performed with groundwater obtained from the site in order to generate representative design data. Half-lives calculated through column tests may require adjustments for field groundwater temperatures and the potentially lower field bulk density of the reactive medium. The flow through thickness of the reactive cell is determined by residence time requirements and the local groundwater flow velocity through the reactive cell.

*Modeling.* While treatability testing is being conducted, hydrogeologic modeling and geochemical evaluation of the site can begin. Hydrogeologic modeling can be used to define many aspects of the design. Several hydrogeologic models are available for modeling the permeable reactive flow and transport system. Widely available and validated models such as MODFLOW and its enhancements are generally sufficient to achieve permeable barrier design objectives. Hydrogeologic

modeling, along with site characterization data, is used for the following purposes (USACE, 1997):

--Location of the barrier

--Barrier configuration

--Barrier dimensions

--Hydraulic capture zone

--Design-trade offs.

--Media selection

--Longevity scenarios

--Monitoring plan

Geochemical evaluation of the site can also commence when treatability tests are in progress, although knowledge of the inorganic composition of the influent and effluent from column tests is helpful to the evaluation. Geochemical evaluation may consist simply of a qualitative assessment of the potential for precipitate formation in the reactive cell based on site characterization and treatability data. Numerical geochemical codes may or may not be used depending on site objectives.

The design can also be enhanced using probabilistic modeling to incorporate the variability of the input design parameters.

*Performance and Compliance Monitoring:* Once the PRB has been designed and constructed, the system has to be monitored as long as plume exists. The primary objective of monitoring is verify that groundwater quality downgradient of the PRB is in compliance with the target clean up objectives agreed to by site managers and regulators. Monitoring is generally comprised of two objectives; compliance monitoring and performance monitoring.

Performance Monitoring

Performance monitoring of PRBs includes the evaluation of physical, chemical and mineralogical parameters over time. It should address verification of emplacement and be able to detect loss of reactivity, decrease in permeability, and decrease in contaminant residence time in reaction zone, and short circuiting or leakage. Performance monitoring is conducted to some degree at most sites because it can alert site managers of any problems that may occur in the future, before the problems are identified by contaminant monitoring (that is, before plume breakthrough or bypass actually occurs).

Performance monitoring generally involves measurement of water levels, field parameters (ORP, pH, DO, and conductivity), and inorganic constituents in the groundwater monitoring wells in the PRB and its vicinity. Water levels and field parameters are simple measurements to perform and most site managers conduct these on a quarterly basis, along with groundwater sampling for contaminants. Quarterly monitoring also indicates any seasonal changes in contaminant distribution, groundwater flow, or geochemistry. Certain inorganic constituents can contribute to the formation of chemical or biological byproducts, which may take place over several years (or several pore volumes of flow). Therefore, groundwater sampling for inorganic parameters is generally conducted on an annual or biannual schedule (Gavaskar et al., 2000).

Compliance Monitoring

Compliance monitoring requirements for PRB applications are similar to those of other remediation technologies, however, the placement and design of the monitoring wells and the methods used to sample groundwater may be different.

Normal compliance monitoring involves target contaminants, their degradation products and general water quality parameters.

For compliance monitoring system design, well placement and design are important to ensure adequate assessment of system performance. Groundwater modeling should be used as a tool for the determination of monitoring well locations (ITRC, 1999). The number of the wells will depend on system design and size. In addition to the wells located at upgradient, downgradient and within PRB, wells should be located at each end of the PRB to ensure that contaminated water is not flowing around, under, or over the barrier wall. Installation of monitoring well clusters (multiple discretely screened wells within a single boring) may be appropriate if more than one aquifer is present or in case of heterogeneity development due to the compaction of the iron fines and the formation of corrosion products or precipitates within the pore spaces (ITRC, 1999).

The frequency with which compliance samples are collected should be based on the hydrogeologic character of the aquifer, the proximity of sensitive receptors such as water supply wells, and the risk posed by the contaminant(s). The amount or rate at which groundwater should be purged should be determined case-by case basis. Groundwater velocity is a key component in designing and establishing a monitoring schedule. Generally, if the groundwater velocity is low, a low frequency schedule is set-up. Sampling within and around a PRB requires special techniques to collect representative samples. For groundwater sampling within the PRB, methods that ensure consistent groundwater residence times and flow rates and that minimize disruption of the groundwater flow field during sampling and between sampling events are recommended. Low-flow sampling and purging techniques (Puls and Barcelona, 1996) and passive sampling devices such as passive diffusion bag samplers are recommended where appropriate to accomplish these goals (U.S. EPA, 1998).

It is also important to thoroughly understand the reactions which cause the transformation of destruction/immobilization of contaminants to be able to monitor for undesirable degradation or transformation products as part of the compliance sampling program. For instance, in the case of chromium and ZVI, the reaction product is an insoluble hydroxide mineral phase. This can only be confirmed using advanced surface analytical techniques, but can be inferred from non-detection of Cr(VI) and minute or non-detection of Cr(III) in aqueous samples together with ground-water quality data and geochemical parameters.

### 2.2.5. Advances in PRB

There are a number of innovative reactive media that show promise for use in PRBs. One group of these media is iron foam and colloidal iron (USACE, 1997). Also, bimetallic systems (metal couples) prepared by plating a second metal onto a ZVI surface have been shown to accelerate treatment rates relative to untreated iron metal. Bimetallic systems (metal couples) prepared by plating a second metal onto a zero-valent iron surface, including Fe/Cu, Fe/Ni (Sivavec et al., 1997) and Fe/Pd (Muftikian et al., 1995), have been shown to accelerate solvent degradation rates relative to untreated iron metal. Palladized iron has been shown to be effective in dechlorinating halogenated aromatic compounds such as polychlorinated biphenyls (PCBs) in addition to chlorinated aliphatic compounds (Grittini et al., 1995). The rate enhancement observed in bimetallic systems may be attributed to corrosion-inducing effects promoted by the second, higher reduction potential metal and possibly some catalytic effects. However, some investigators have found the enhanced reactivity of these systems to diminish relatively quickly, whereas others have found no apparent loss of reactivity. These differences may be related to ground-water chemistry or the method used for plating the iron, but further investigation is needed. It is important to note that ZVI

systems have not shown similar losses in reactivity in long-term laboratory, pilot and field investigations (U.S. EPA, 1998).

Various construction techniques are now available for PRB applications. These techniques generally comprise injection based construction methods which aim at thin and deeper PRBs. Injection methods can be listed as vertical fracturing, jetting columnar, jetting-panels diaphragm, pneumatic fracturing, and direct push. The selection of the technique depends on characteristics of the site.

An expansion of PRB technology is to use reductive reactive media (e.g. ZVI) to treat source zones. This approach not only eliminates the contamination at the source but also prevents the development of a plume in the downgradient of the source. Source area treatment of high-concentration groundwater using iron is different from PRB treatment. In the source area treatment, an iron material is injected, mixed or used as backfill to facilitate treatment. Sometimes, iron is mixed with a stabilizing agent such as clay to retard the flow through the source zone and to homogenize soils. Source area treatment has many applications in field scale using several emplacement methods. Contaminants treated include chlorinated solvents, Cr(VI), TCE, and chlorinated volatile organic compounds (ITRC, 2005).

## 2.3. Remediation of Chromate Contaminated Groundwater with Iron-based PRBs

### 2.3.1. Laboratory Scale Applications

Zero-valent iron (ZVI) is a mild reductant and serves as electron donor for the reduction of oxidized species under certain conditions. The thermodynamic instability of the iron metal can drive oxidation-reduction reactions without

external energy input, if suitable coupled reactions can occur to prevent accumulation of electric charge (Evans, 1960; Powell et al., 1995). Previous investigations have shown that soluble Cr(VI) may be removed from the solution via reduction to Cr(III) in the presence of ZVI according to equation 2.3 (Powell et al., 1995; Astrup et al., 2000; Mayne and Pryor, 1949; Gould, 1982; Buerge and Hug, 1998; Anderson et al., 1994; Melitas et al., 2001):

$$Fe^0 + CrO_4^{2-} + 2H_2O \leftrightarrow Cr(OH)_3 + Fe(OH)_3 + 2OH^- \qquad (2.3)$$

In addition to precipitation of $Cr(OH)_3$ solid, Cr(III) may also form $Cr_2O_3$ solid or coprecipitate with Fe(III) to form mixed Fe(III)-Cr(III) hydroxide solid solution (Eary and Rai, 1988; Puls et al., 1994; Powell et al., 1995; Blowes et al., 1997) or mixed Fe(III)-Cr(III) (oxy)hydroxide solid (Schwertmann, 1989) according to reactions 2.2 and 2.3, respectively.

$$(1-x)Fe^{3+} + xCr^{3+} + 3H_2O \leftrightarrow (Cr_xFe_{1-x})(OH)_{3(s)} + 3H^+ \qquad (2.4)$$

$$(1-x)Fe^{3+} + xCr^{3+} + 2H_2O \leftrightarrow Fe_{1-x}Cr_xOOH_{(s)} + 3H^+ \qquad (2.5)$$
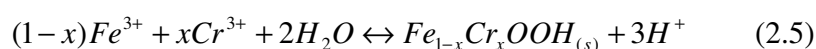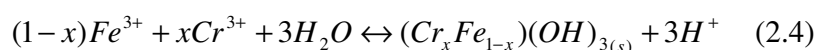
Reduction of Cr (VI) by ZVI has been extensively demonstrated by a number of laboratory studies. The experiments generally utilized batch reactors or flow through columns with a focus on the parameters affecting the rate and treatment efficiency of Cr(VI) such as pH, ZVI concentration, groundwater velocity, initial Cr(VI) concentration and groundwater chemistry.

pH has been extensively investigated as a key parameter affecting chromium reduction and it was shown that Cr(VI) reduction vary significantly depending on pH. Corrosion has been known to diminish at pH range 9.5-12.5 (Pourbaix, 1966,

Powell and Puls, 1997). Therefore, corrosion intensity and consequently Cr(VI) reduction, should be enhanced by lower pH. Generally, it was observed that Cr(VI) reduction rate increases with the decrease in pH (Gould, 1982; Eary and Rai, 1988, Alowitz and Scherer, 2002). On the other hand, James (1996) argued that redox reactions may also be inhibited at pH values as low as 6 due to the existence of different chromium species at different pH values. Geochemistry of aquifer materials have also shown to affect the reaction rates (Powell and Puls, 1993; Powell et al., 1994; Powell et al., 1995) by dissolution of aluminosilicates would lower the pH favorable for corrosion. The protons can also serve as electron acceptor at the iron surface, allowing the corrosion reactions to proceed more rapidly (Powell and Puls, 1997).

Increasing the surface area concentration of ZVI basically increases rate of remediation. On the other hand, having an extra non-reactive support surface such as sand for precipitation products formed in the column may in theory lead to higher capacities, since the reactive surfaces will be covered to a less extend than in a pure iron system. Batch and column experiments have shown that the reaction rates depend on the type of iron present and linearly related to the available surface area concentration for a given type of iron (Gould, 1982; Blowes et al., 1997; Alowitz and Scherer, 2002; Ponder et al., 2000). Still, the corrosion of iron, and thereby the pH increase is stated to be a limiting factor in the amount of ZVI and the amount of ZVI is stated to be system specific (Fernandez-Sanchez, et al., 2004).

If the reaction stoichiometry is considered, it follows that the increase in Cr(VI) concentration increases the reaction rate. Previous investigators have shown the increase in reaction rate with the increase in Cr(VI) concentration. The kinetic expression found by Gould (1982) is 0.5 order in Cr(VI) concentration. Lee et al., (2003) showed that when Cr(VI) concentrations were less than 20 mg/L, the rate

constant dramatically increased. Similar rate dependence was also reported by Ponder et al., (2000). On the other hand, very high concentrations of Cr(VI) can cause inhibition effects as shown by Melitas et al., (2001). Their experiments indicated that the rate of iron corrosion decreased with increasing Cr(VI) concentrations between 0 and 5000 $\mu$g/L.

An additional consideration for Cr(VI) reduction is the groundwater geochemistry. Mineral precipitation is expected based on groundwater chemistry (Mackenzie et al., 1999). Mineral precipitation decreases hydraulic conductivity by taking up pore spaces by coating ZVI surfaces or unattached fine precipitates (Liang et al., 2003) and reactivity (Mackenzie et al., 1999). Hardness and carbonate effects on the reactivity of ZVI iron for Cr(VI) has been investigated by Lo et al., (2006). A slight decrease in the Cr(VI) removal capacity was found in the presence of calcium ions. Cr(VI) removal was dropped by 17% when magnesium hardness was present at low to moderately hard level. Furthermore, there was a 33% decrease in the Cr(VI) removal capacity of ZVI when both carbonate and hardness ions were present. Likewise, in another study, calcium and magnesium had significant impact on Cr(VI) removal reducing ZVI capacity by 45% at hardness levels up to 140 mg/l as $CaCO_3$ (Karvonen, 2004). On the contrary, Kaplan and Gilmore (2004) observed little or no effects of background solution chemistry (0.2 M $NaHCO_3$, distilled water, and a carbonate dominated groundwater) on the reaction rate coefficients.

Another governing factor for the remediation of Cr(VI) by ZVI is the groundwater flow velocity. The residence time in a PRB is the ratio of the flow through thickness of a PRB to the groundwater flow velocity. Hence, the degradation efficiency and thickness of the PRB is directly proportional to the flow velocity. The effect of flow velocity on the efficiency of PRBs is complicated. In theory, longer residence times seem to enhance the degradation rate. Under lower velocity

conditions, transport to the reactive iron surfaces is enhanced by the increased time available for diffusion through coatings on the ZVI and accordingly, the extend of treatment is dependent on the degree of contact between the dissolved Cr(VI) and ZVI surface (Blowes et al., 1997). Conversely, increased flow rates decrease the rate of product accumulation, which in turn decreases the precipitate formation and enhancing surface reactivity. Furthermore, under flow conditions, the elevated reactant concentrations may be too short lived to permit the formation of a precipitate i.e. the formation of a precipitate may be kinetically hindered (Kaplan and Gilmore, 2004).

Although the rate of reduction of Cr(VI) is important, the rate of removal of formed Cr(III) is also crucial for permeable reactive barrier applications. The solubility product of Cr(OH)$_3$ is 6.3x10$^{-31}$ at 25$^{o}$C and readily precipitates at pH 7 (Karvonen, 2004). In addition, for mixed hydroxide precipitates, Eary and Rai (1988) found a stoichiometry of $Cr_{0.25}Fe_{0.75}(OH)_3$ and concluded that at pH values between 5 and 11, precipitation of a mixed Cr(III)-Fe(III) hydroxide phase generally limits total dissolved concentrations of Cr(III) to values less than 10$^{-6}$M.

### 2.3.2. Field Scale PRB Applications

Although the number of full scale applications of ZVI is growing, the technology is still relatively new. Therefore, there are limited published data on the performance of full-scale PRBs in the field. The following part summarizes information about the field scale PRB applications used to treat chromium plumes with ZVI.

U.S. Coast Guard Support Center, Elizabeth City

The field site is located on a U.S. Coast Guard air base near Elizabeth City, North Carolina. A plating shop had been operated at this site for 30 years before its closure in 1984. The shop was known to discharge acidic chromium solution and associated organic solvents. Sediments beneath the plating shop floor were found to contain up to 14,500 mg/kg Cr. The contaminated sediments were removed at that time but further site investigations also revealed a well defined plume of groundwater containing Cr(VI) extended from the electroplating shop to the Pasquotank River containing groundwater concentrations of 28 mg/L near the source in 1988 (U.S. EPA, 2000b). Concentrations in excess of 10 mg/l Cr had been detected in the groundwater at the site since 1991 (Puls et al., 1999).

The contaminated surficial aquifer has consisted of Atlantic coastal plain sediments. Borehole log data indicated that the surficial aquifer is complex and heterogeneous, composed of varying amounts fine sand and silty clay (Parsons Engineering Science, 1993; U.S. EPA, 1999). Cone penetrometer tests indicated that the surficial aquifer contained fine sands interfingered with silty clay lenses. The thickness of these lenses varied from 0.3 meter to more than 3 meters. The aquifer is underlain at approximately 18 meters depth by dense clay of the Yorktown Confining unit (U.S. EPA, 1999). Groundwater velocity is variable with depth, with a highly conductive layer at roughly 5 to 6 meter below ground surface. This layer coincides with the highest aqueous concentrations of chromate and chlorinated organic compounds. The groundwater table ranges from 1.5 to 2.0 meter below ground surface and the average horizontal hydraulic gradient varies from 0.0011 to 0.0033. Slug tests conducted on monitoring wells with 1.5 meter screened intervals between 3 and 6 meter below ground surface indicate hydraulic conductivity values of between 0.3 and 8.6 m/day. (Sabatini et al., 1997; Puls et al., 1999).

Laboratory investigations and a field scale pilot study using ZVI led to the installation of a PRB at the site to remediate chromium and portions of TCE. Continuous wall design was selected because for the Elizabeth City site, there was no hydraulic advantage of funnel-and-gate design in terms of both increased capture area and increased residence time. The full scale of wall was entirely comprised of ZVI in the form of iron filings. The selection was based on suitable reaction rates, desirable hydraulic properties, and lower cost. The installed barrier was 46 m long, 5.5 m in depth and 0.6 m wide to capture the entire plume and to prevent penetration of a fine grained geologic unit present at approximately 8 m depth. An estimated 3.2 $m^3$ of iron filings were emplaced per linear meter and about 280 ton of iron was installed (Puls et al., 1999). The total cost of the reactive barrier including site assessment, design, construction, materials, and preliminary and follow up work was approximately 985,000 $ (U.S. EPA, 2000b).

The monitoring network was installed with piezometers and monitoring wells to collect samples. Performance and compliance monitoring was performed based on analysis for pH, Eh, electrical conductivity, turbidity, alkalinity, Cr(VI), dissolved Fe(II), total sulfide and dissolved and total inorganic constituents. After eight years of application, PRB was effective in reducing Cr(VI) from average values of 1500μm/L to <1 μg/L within and hydraulically downgradient of PRB. Chromium removal occurred within the aquifer upgradient and at the leading edge of the inside PRB.

Vertical and angle cores have also been collected to examine changes to the iron surface and evaluate the formation of secondary precipitates which can effect the wall performance in time. The regions where chromium removal occurred showed the greatest amount of secondary mineral formation. Cr(III) has been detected on the cores by X-ray absorption near-edge structure (XANES) spectroscopy

confirming reduction processes. XANES spectra and microscopy results suggested that Cr is, in part, associated with iron sulfide grains formed as a consequence of microbially mediated sulfate reduction in and around the PRB (Wilkin et al., 2005).

Haardkrom Site, Kolding, Denmark

The Haardkrom site formerly operated as an electroplating facility in Kolding, Denmark, where chromium, nickel, zinc and degrasing agent, TCE was used. The groundwater consequently has been contaminated with high levels of TCE and Cr(VI). Concentrations of TCE in the groundwater ranged from 40-1,400 $\mu g/L$ while Cr(VI) concentrations in groundwater ranged from 8 to 110 mg/L (Bronstein, 2005).

Site characterization studies showed that the upper 2-3 meter of the ground at the site consisted of a low permeability, heterogeneous mixture of sandy and clayey loam interspersed with local lenses of sandy layers. The aquifer in these upper layers was less than 2 m below ground and was not continuous throughout the site. Although the direction of groundwater flow is mainly north to northeast, the direction seems to change with seasons.

The availability of construction techniques in Denmark and cost considerations weighed heavily in the selection of the PRB design, which consists of a continuous trench. 50 m long, 1-3 m deep, and 1 m thick continuous PRB trench was installed in 1991. An excavation box was used to install the trench because of the low permeability of the soil. The PRB designers accounted for the limited capacity of chromate removal in PRBs and set the dimensions of the trench to accommodate all of the Cr(VI) in the plume. Laboratory experiments showed chromate reduction capacities to be in the order of 1-3 mg Cr(VI)/1 g ZVI. Bypass trenches and

recirculation pipes were incorporated into the design to enhance water flow through the heterogeneous aquifer. The design cost was $108,000, and the installation cost was $250,000 (RTDF, 2002).

The results of the first year of operation suggested that the design is not effectively controlling the uneven distribution of contaminants along the PRB, especially Cr(VI). Heterogenous loading of the PRB and dispersion of the contaminant plume have contributed to the exhaustion of iron-chromate removal capacity in the wall. (Vidic, 2001).

The literature reveals that in the last ten years, a lot of progress has been made about PRBs and the remediation of Cr(VI) with ZVI reactive media. Researches have improved the understanding of the longevity and performance of PRBs. Field data has begun to be published. New reactive media are under investigation. In terms of the remediation of Cr(VI) with ZVI, the chemistry of corroding iron has been studied extensively and is well understood. Much effort has gone into the investigation of secondary phases which form on the $Fe^0$ surfaces.  The effect of different variables (such as the amount of reactive media, groundwater velocity, pH, groundwater chemistry) on the removal efficiency and long term reactivity of PRBs has been investigated in laboratory studies. These works showed that many questions remain to be answered about how the groundwater velocity affects the removal capacity of a PRB. Also, the ratio of reactive media to bulking agent inert media has been overlooked. In fact, this issue is believed to be more important as field scale applications ages when clogging is experienced. The reaction kinetics of Cr(VI) removal by ZVI has generally been studied in batch reactors except some flow through experiments. Furthermore, to the best of our knowledge, the implications of the experimental data have not been put forward in any PRB design studies. Consequently, this study has focused on issues relatively weakly addressed                   so                   far          in          the                literature.

# CHAPTER 3

## MATERIALS AND METHODS

### Description of Column Studies

### 3.1.1. Materials and Solutions

The reactive ZVI material used in the experiments was a reduced iron powder; Alfa Aesar, -20 mesh (size<0.841 mm). The particle density of the iron powder was 7.87 g/cm$^3$. Brunauner-Emmett Teller (BET) specific surface area analysis of the iron was performed by METU Central Laboratory using Quantachrome Autosorb-1-C/MS. The specific surface area of the iron was 0.04 m$^2$/g. Iron powder was used as received without using any chemical (acid washing) or mechanical (sonication) pretreatment. In the construction of iron-based PRBs, it is a common practice to mix sand with elemental iron to decrease the cost and to increase the permeability of the reactive media. Consequently, inert quartz sand was considered as the bulking agent with similar size to iron powder. The sand fraction used in this study passed through 20 mesh but retained by 30 mesh based on sieve analysis.

To simulate a carbonate containing groundwater, $CaCO_3$ saturated water was used as the background solution. This background solution was prepared by adding reagent-grade $CaCO_3$ to deionized water in excess of its solubility. Then, the solution was bubbled with $CO_2$ to promote dissolution of the $CaCO_3$, and allowed to equilibrate and degas at atmospheric $P_{CO2}$ for 4-5 days. The solubility of $CaCO_3(s)$ in deionized water open to an atmosphere with $P_{CO2}=10^{-3.5}$ atmosphere and the concentration of

the species in the system can be calculated from mass and charge balances. According to these calculations, the theoretical value of this pH buffer is 8.3. However, due to the factors such as pressure and temperature, the pH of the background solution used in the experiments ranged between 7.3 and 8.1.

Column influent solutions were prepared by adding reagent-grade salts [$K_2CrO_4$ for chromate solution and NaCl for Cl solution] to background solution. Initial Cr(VI) concentration was 20 mg/l. This concentration was selected considering the typical initial Cr(VI) concentration in plumes (U.S. EPA, 1999; U.S. EPA, 2000b) as well as in an effort to prevent the inhibition of reaction rates through increased surface passivation due to high concentrations of Cr(VI).

### 3.1.2. Experimental Setup

Laboratory columns used in the experiments were made of glass, measuring 15 cm in length and 3 cm in diameter. Columns were packed with three different amounts of iron powder/quartz sand mixtures. The column mixtures, flow rates and fluxes are listed in Table 3.1. The ratio of iron surface area to solution volume (surface area concentration of iron, $m^2$ $mL^{-1}$) was found from the product of the ZVI solids concentration in the reactive media (g $mL^{-1}$) and the specific surface area of iron ($m^2$ $g^{-1}$).

Table 3.1.  Reactive mixtures and flow rates used in column experiments

| Column Name | 50IR | | | 25IR | | | 10IR | | | 100QS |
|---|---|---|---|---|---|---|---|---|---|---|
| Column reactive mixture | 50%Iron Powder (w/w) 50%Quartz Sand (w/w) | | | 25%Iron Powder (w/w) 75%Quartz Sand (w/w) | | | 10%Iron Powder (w/w) 90%Quartz Sand (w/w) | | | 100% Quartz Sand |
| Flow rate (ml/min) | 0.5 | 0.9 | 1.2 | 0.5 | 0.9 | 0.4 | 0.5 | 0.9 | 0.4 | 0.4 |
| Flux (ml/cm$^2$. min) | 0.07 | 0.127 | 0.17 | 0.07 | 0.127 | 0.057 | 0.07 | 0.127 | 0.057 | 0.057 |

Porosity of the columns was calculated from the bulk density and particle density of the reactive mixtures as follows:

$$\phi = 1 - \frac{\rho_b}{\rho_s} \qquad (3.1)$$

where $\rho_b$ is the bulk density (g cm$^{-3}$) and $\rho_s$ is the particle density (g cm$^{-3}$) of the column mixtures. Particle density of the reactive mixtures was calculated by multiplying the density of iron and sand with their ratios and adding the products such that:

$$\rho_s = x\rho_{sand} + (1-x)\rho_{iron} \qquad (3.2)$$

where $\rho_s$ is the particle density of the column mixture, $\rho_{sand}$ is the density of quartz sand (2.65 g cm$^{-3}$), $\rho_{iron}$ is the density of ZVI particles (7.87 g cm$^{-3}$), and x is the fraction of sand in the mixture.

The average residence time, $t_{res}$, of the columns was found through dividing the column length, $L$, by the groundwater flow velocity, $v$, in each column. That is,

$$t_{res} = \frac{L}{v} \qquad (3.3)$$

A control experiment containing 100% quartz sand was also conducted. The reactive mixtures were placed in the columns in 2 cm lifts with periodic tapping to avoid air pockets and layering. Once each column was filled, the top was sealed with teflon tape. The influent solutions were pumped through the columns in an up-flow manner through teflon tubing using a multi-channel peristaltic pump (MasterFlex, Cole Parmer). Several pore volumes of background solution were passed through the columns prior to introduction of influent solutions. These two steps ensured that the columns become fully saturated. The basic experimental set-up illustrated in Figure 3.1 was employed in all the experiments at room temperature.

Column flow rate was periodically measured by collecting the effluent from each column in a graduated cylinder to determine the flow velocity in the column.

a)
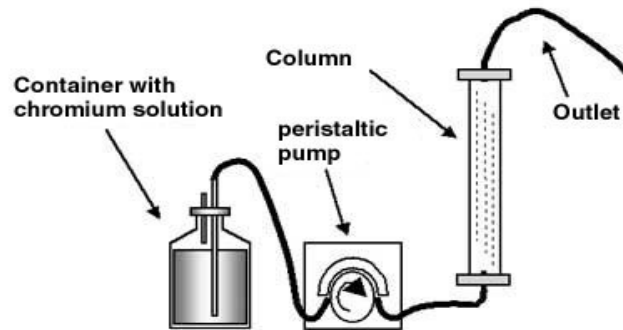


b)



Figure 3.1. A schematic (a) and pictorial (b) view of experimental set-up of columns

### 3.1.3. Column Operations

The flow rates of columns in the experiments were selected with the intention of simulating typical groundwater velocities in sandy aquifers. The first set of column tests was started with a flow rate of 0.5 ml/min; yielding a Darcy flux of 0.07 ml/cm$^2$.min and groundwater flow velocity range of 153.8 cm/day to 196.1 cm/day in the reactive mixtures (Table 3.1). When the capacity of the reactive mixtures were exhausted (i.e. $C_{influent} \cong C_{effluent}$), they were emptied and refilled with the same iron powder/quartz sand ratios for running the second set tests. The second set of tests was conducted with a higher flow rate of 0.9 ml/min. This flow rate yielded a Darcy flux of 0.127 ml/cm$^2$.min and groundwater flow velocity range of 260.2 cm/day to 340 cm/day in the reactive mixtures. The third (and last) flow rates of the column experiments were selected based on the treatment efficiencies of the first two sets. Accordingly, columns containing 25% and 10% iron powder (25IR and 10IR) were run with a flow rate of 0.4 ml/min (Darcy flux of 0.057 ml/cm$^2$.min and groundwater flow velocities of 129.7 cm/day and 148.6 cm/day, respectively); whereas column containing 50% iron (50IR) was run with a flow rate of 1.2 ml/min (Darcy flux of 0.17 ml/cm$^2$.min and groundwater flow velocity of 389.2 cm/day). Also, at the beginning of each experimental set, Cl$^-$ solution was pumped through the columns to determine the dispersivity of each reactive mixture at a given flow rate. The Cl$^-$ solution was then flushed through the columns with background solution before chromate solution was introduced.

In the literature it was reported that besides reduction, Cr(VI) may be adsorbed to the oxyhydroxides rusts that are formed in the columns (Powell et al., 1995; Palmer and Puls, 1994). To determine the fraction of adsorbed Cr(VI), sequential extractions were done at the end of a column study. An initial water extraction served to remove remaining pore water. Following the water extraction, a phosphate extraction was applied to the reactive mixture. Phosphate, as a strong

adsorbate, would compete for adsorption sites and desorbs the adsorbed chromate. The test was conducted by adding 0.01 M potassium phosphate ($KH_2PO_4$) to the reactive mixture and equilibrating at 120 rpm for 24 hours. The water was then separated from the slurry by centrifuge and Cr(VI) was measured in the liquid phase. The increase in the chromate concentration, if any, was taken as the amount of "exchangeable chromate".

### 3.1.4. Solid Phase Characterization

At the completion of column studies, the reactive mixtures were removed from highly oxidized edges of the column, gently washed with acetone, filtered, washed repeatedly with additional acetone to dry the sample as quickly as possible. Then, the reactive mixtures dried under nitrogen gas to minimize contamination of surfaces by atmospheric gases. This method was shown to minimize the formation of oxides due to oxidation at the iron surface. Scanning electron micrographs were generated using a JSM-6400 Electron Microscope (JEOL) equipped with NORAN System 6 X-ray Microanalysis System & Semafore Digitizer. The weight and atomic percentage of the elements present on the reactive mixture were determined using Energy Dispersive X-Ray Analysis (EDX). Solid phase characterization experiments were done in the Department of Metallurgical and Materials Engineering Scanning Electron Microscopy (SEM) Laboratories at METU.

### 3.2. Analytical Methods

Cr(VI) was determined using a Hach DR 2010 spectrophotometer and Hach method 8023. This method uses 1,5 diphenylcarbohydrazide, which reacts with Cr(VI) to form a magenta complex that is measured at a wavelength of 540 nm. Total Cr was measured using flame atomic adsorbtion spectroscopy (ATI Unicam

929) and Cr(III) was determined by subtracting the Cr(VI) from total Cr concentrations. Redox potential (Eh) was determined using a combination Ag/AgCl reference electrode with a platinum button (Sensorex, S500C-ORP). The electrode reading was confirmed with Quinhydrone standard solution. Millivolt readings were converted to Eh using the electrode reading and the standard potential of Ag/AgCl electrode (SHE) at $25^{\circ}$C. The pH measurements were made using a combination of pH/reference electrode (Cole Parmer, EW-55520-08) connected to a pH meter (EUTECH, CyberScan500) and standardized with the buffer 7 and 10. $Cl^{-}$ was measured using argentometric method (APHA, 1989). All measurements were performed in duplicate for quality control. Dispersion coefficients were calculated by fitting the $Cl^{-}$ concentration versus time data to the one-dimensional advection-dispersion equation using CXTFIT, a non linear least square algorithm program (Parker and van Genuchten, 1984).

# CHAPTER 4

# RESULTS AND DISCUSSIONS

## 4.1. Control Column Experiment

The control column experiment containing 100 % quartz sand was performed for testing the possibility of reduction in Cr(VI) concentration due to the bulking agent quartz sand (Table 3.1, column 100QS). Chloride, as a conservative tracer, was passed through the sand column for nearly 3 pore volumes at a flux of 0.057 ml/cm$^2$.min. In the control column, breakthrough of Cr(VI) was observed at one pore volume and coincided with the breakthrough of Cl$^-$ (Figure 4.1). Tailing behavior was observed in both the Cl$^-$ and Cr(VI) curves indicating immobile water phase probably resulting from the non-uniformity of the quartz sand. The results showed that no loss of Cr(VI) occurred due to adsorption onto sand particles or due to Fe$^{2+}$ release from sand particles and thus Cr (VI) removal can be attributed only to the presence of zero-valent iron in the system. It is also worth pointing out that actually neither of these mechanisms was likely to take place under the operative conditions of the columns, where particle size is relatively large for adsorption phenomena to take place and influent water pH is relatively high for the dissolution of Fe$^{2+}$ ions from sand particles.
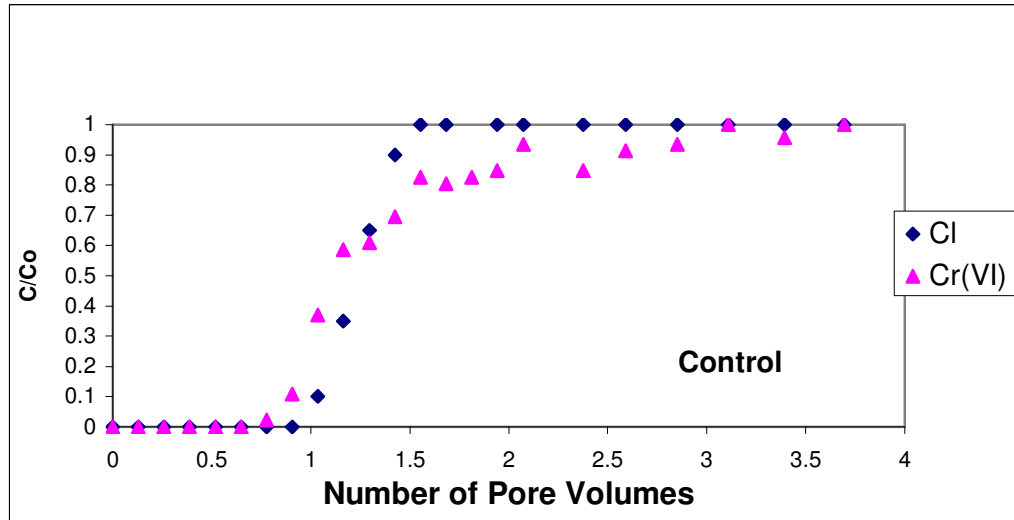
Figure 4.1. Control column experiment containing 100% quartz sand and with flux of 0.057 ml/cm$^2$.min.

Furthermore, the possibility of Cr(VI) absorption to iron oxides has been tested by sequential water and phosphate extractions at the end of one of the runs performed with zero-valent iron. The phosphate removes adsorbed chromate by both directly competing for the adsorption sites in the soil and indirectly (in some cases) by increasing the pH (U.S. EPA, 1994). At the end of the extractions, no recovery of Cr(VI) by $PO_4^{3-}$ desorption was obtained. As a result of this finding, it was confirmed that Cr(VI) was not removed by adsorption to oxyhydroxides and that reduction is the only removal mechanism in the laboratory experiments.

## 4.2. Visual Observations in Time

Clear and distinct visual changes were observed in the columns as the reductive precipitation reactions had taken place in time. The position of reactive front (operationally defined as visible limit of ferric oxyhyroxide precipitates by Fryar and Schwartz, 1998) was observed and photographed for column 50IR operated at a flux of 0.07 ml/cm$^2$.min (Figure 4.2). Reddish brown corroded regions were appeared at the inlet first and migrated in upward direction during the treatment. However, the precipitates mostly and uniformly accumulated around the inlet of the column and their intensity and uniformity were gradually decreased along the upward column length. Cr(VI) was first detected in the effluent when the reactive front reached to the end of the column. Although the removal capacity of the column was exhausted, there was still unreacted iron especially in the upper parts of the column at the end of the run. The removal of Cr(VI) and the formation of these precipitates constitute the evidence of reductive precipitation reactions. The results also suggested that the initial removal capacity was decreased gradually due to formation of precipitates around the iron particles, which blocked the available surface area preventing the use of unreacted iron in the column. In addition, the exit of gas bubbles was observed in the effluent port, which was attributed to H$_2$ gas formation due to the anaerobic corrosion of iron (see equation 4.3). Hydrogen generation associated with the corrosion reactions is reported to be generally noticeable in batch and oftentimes column experiments with ZVI after 1 or 2 days of water contact (Reardon, 2005) and this finding is supported by field observations. For example, reduced conditions observed in the Elizabeth City are deduced to the reduction of water to H$_2$ gas (Weisener et al., 2005). Also, hydrogen gas can accumulate as films on granular iron. For instance, gas accumulations in granular iron of 10% to 15% (Mackenzie et al., 1999), 20% (Repta, 2001) and 10% (Zhang and Gillham, 2005) of the initial porosity have been reported.

Figure 4.2. Column 50IR showing the reactive front

## 4.3. Mineralogical Characterization

A potential limitation of the reactive iron barrier is the deterioration of the ZVI material by corrosion and subsequent precipitation of minerals that may cause cementation, decreased reactivity and permeability of the ZVI barrier. The geochemical changes in reactive media, depending on the inorganic characteristics

of water can result in the in the formation of iron oxides, carbonate minerals, and other solid phases (Roh et al., 2000).

Under the anaerobic conditions that exist in the bulk of the media, iron is reduced by water as shown in the following reaction:

$$Fe^0 + 2H_2O \leftrightarrow Fe^{2+} + H_2(g) + 2OH^- \qquad (4.1)$$
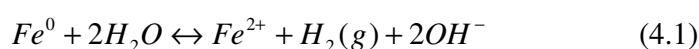
The resultant rise in the pH can lead to the precipitation of ferrous hydroxide as:

$$Fe^{2+} + 2OH^- \leftrightarrow Fe(OH)_2(s) \qquad K_{Fe(OH)_2(s)} = 8x10^{-6} \quad (4.2)$$
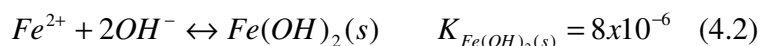
Ferrous hydroxide, (reaction 4.2) is thermodynamically unstable and may be further oxidized to magnetite according to the reaction

$$3Fe^{2+} + 4H_2O(l) \leftrightarrow Fe_3O_4(s) + 6H^+ + H_2(g) \qquad (4.3)$$
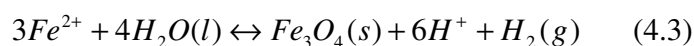
at a pH higher than 6-7 (Pourbaix, 1973; Mackenzie et al., 1999). In aerobic conditions, iron is oxidized by available oxygen as shown in the following reaction (Powell et al., 1995):

$$Fe^0 + 1.5O_2 + 6H^+ \leftrightarrow Fe(OH)_3 + 1.5H_2 \qquad (4.4)$$
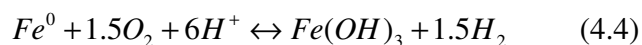
Furthermore, in carbonate containing waters, the rise in pH from the anaerobic corrosion of iron will shift the carbonate-bicarbonate equilibrium and lead to the precipitation of ferrous carbonate (siderite) and calcium carbonate (aragonite and calcite):

$$HCO_3 + OH^- \leftrightarrow CO_3^{2-} + H_2O \qquad pK_a = 10.3 \qquad (4.5)$$

$$Fe^{2+} + CO_3^{2-} \leftrightarrow FeCO_3(s) \qquad K_{FeCO_3} = 3.2x10^{-11} \qquad (4.6)$$

$$Ca^{2+} + CO_3^{2-} \leftrightarrow CaCO_3(s) \qquad K_{CaCO_3} = 2.8x10^{-19} \qquad (4.7)$$

Thus, potential likely mineral phases formed under the conditions of this study include mixed Cr(III)-Fe(III) (oxy)hydroxide solids resulting from the coprecipitation of iron and reduced chromium, various Fe oxides, hydroxides and oxyhydroxides, and carbonate precipitates such as siderite ($FeCO_3$), aragonite and calcite ($CaCO_3$) which most likely formed due to the high concentration of carbonate in the background solution.

Formations of these precipitated phases were detected by Scanning Electron Microscopy (SEM) and Energy Dispersive X-Ray Analysis (EDX). Figure 4.3 (a) and (b) show two SEM images of the iron powder prior to reaction with Cr (VI) solution and Figure 4.3 (c) shows the EDX analysis results.

a)

b)



(c)
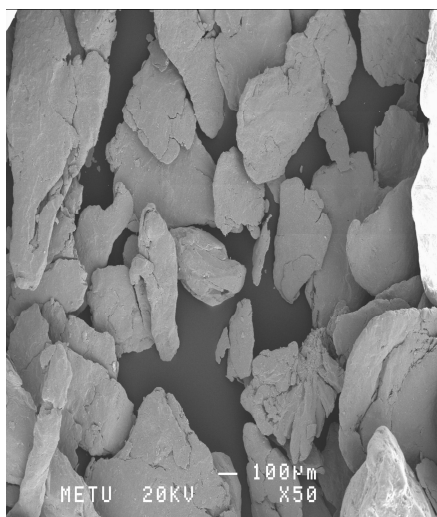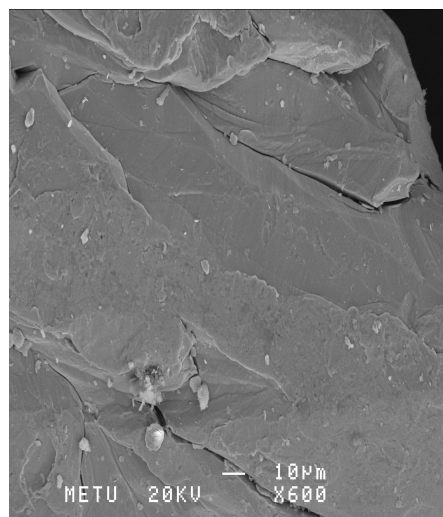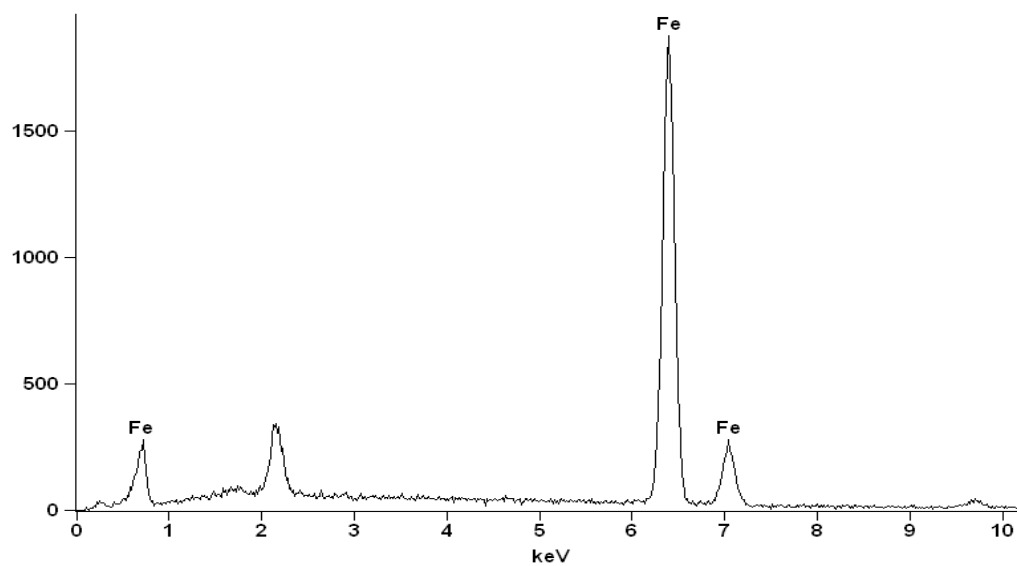


Figure 4.3. (a and b) SEM pictures and (c) EDX analysis of the virgin iron powder.

As shown in Figure 4.3, the iron powder used in this study was irregular in shape and had a lower surface area compared to the morphologies of the previously reported SEM results of the zero valent iron (Gandhi et al., 2002; Gu et al., 1998). EDX analysis showed that it was almost pure iron with a small fraction of oxidation on the surface.

At the end of the first experimental set, which was conducted at a flux of 0.07 ml/cm$^2$.min, the column containing 50% iron powder (50IR) was opened for mineralogical characterization after the exhaustion of its Cr(VI) removal capacity, that is effluent Cr(VI) concentration approached influent concentration. Column was divided into two as "upward" and "downward" sections and samples were taken from the selected parts of reacted and cemented regions of each section. Figure 4.4 and 4.5 show the SEM-EDX results of the iron surfaces from two samples taken from "downward" section of the 50IR column and Figure 4.6 shows the SEM-EDX results of the "upward" section of the 50IR column. Since Au and Cu were used in sample preparation for SEM and EDX analysis, EDX analysis also contained Au and Cu and their signals in the EDX spectra were deleted.

a)                                    b)



(c)

| Element | Net Counts | Weight Conc % | Atom Conc % | Compound Conc % | Formula |
|---------|------------|---------------|-------------|-----------------|---------|
| Si | 906 | 2.22 | 4.22 | 2.22 | Si |
| Ca | 3007 | 6.26 | 8.32 | 6.26 | Ca |
| Cr | 884 | 2.46 | 2.52 | 2.46 | Cr |
| Fe | 21263 | 89.06 | 84.95 | 89.06 | Fe |
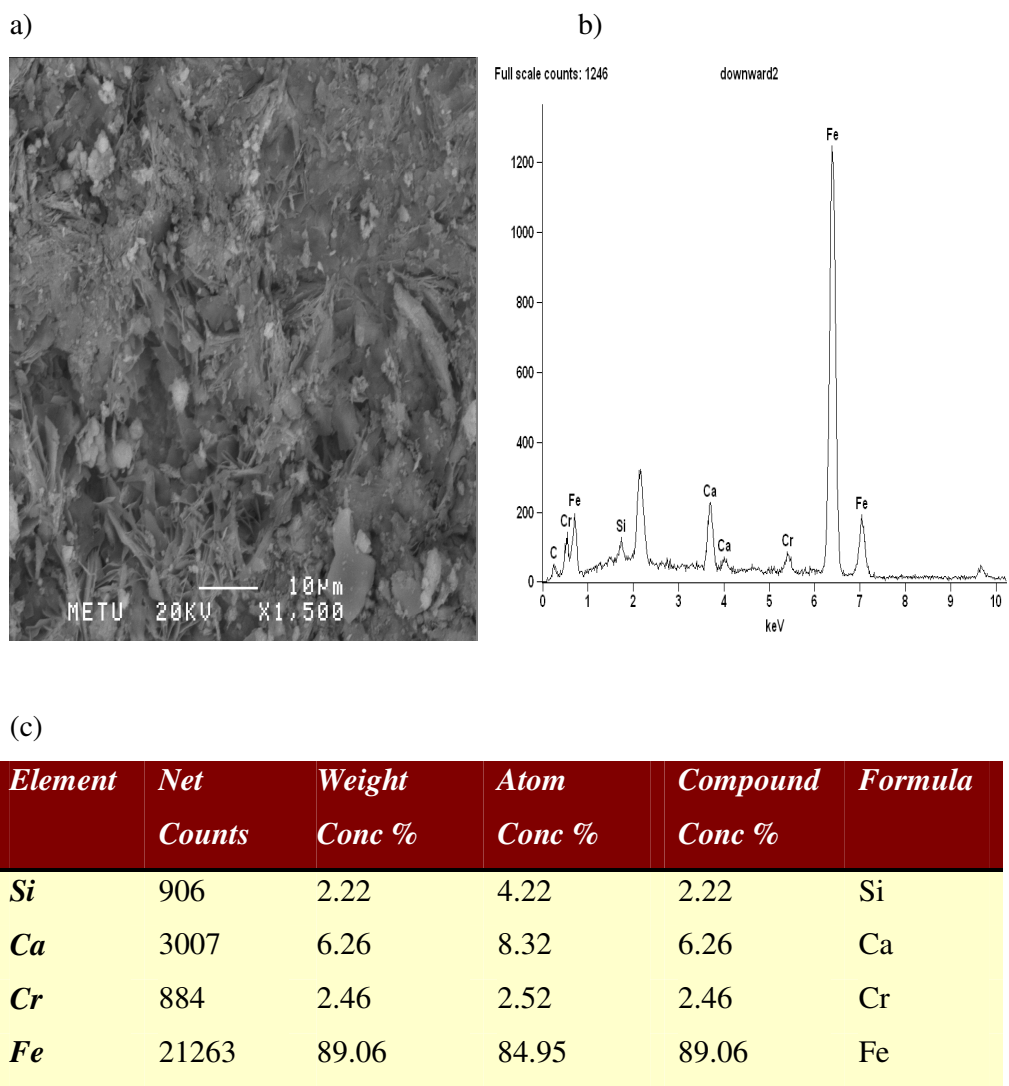
Figure 4.4. (a) Iron surface of the "downward" section of the column 50IR analyzed by SEM after exposure to 453 pore volumes of Cr (VI) solution. (b, c) EDX analysis of the elements on the surface.

a)



b)



(c)

| Element | Net Counts | Weight Conc % | Atom Conc % | Compnd Conc % | Formula |
|---------|-----------|---------------|-------------|---------------|---------|
| Ca | 2139 | 5.22 | 7.09 | 5.22 | Ca |
| Cr | 2195 | 7.26 | 7.60 | 7.26 | Cr |
| Fe | 17649 | 87.52 | 85.31 | 87.52 | Fe |
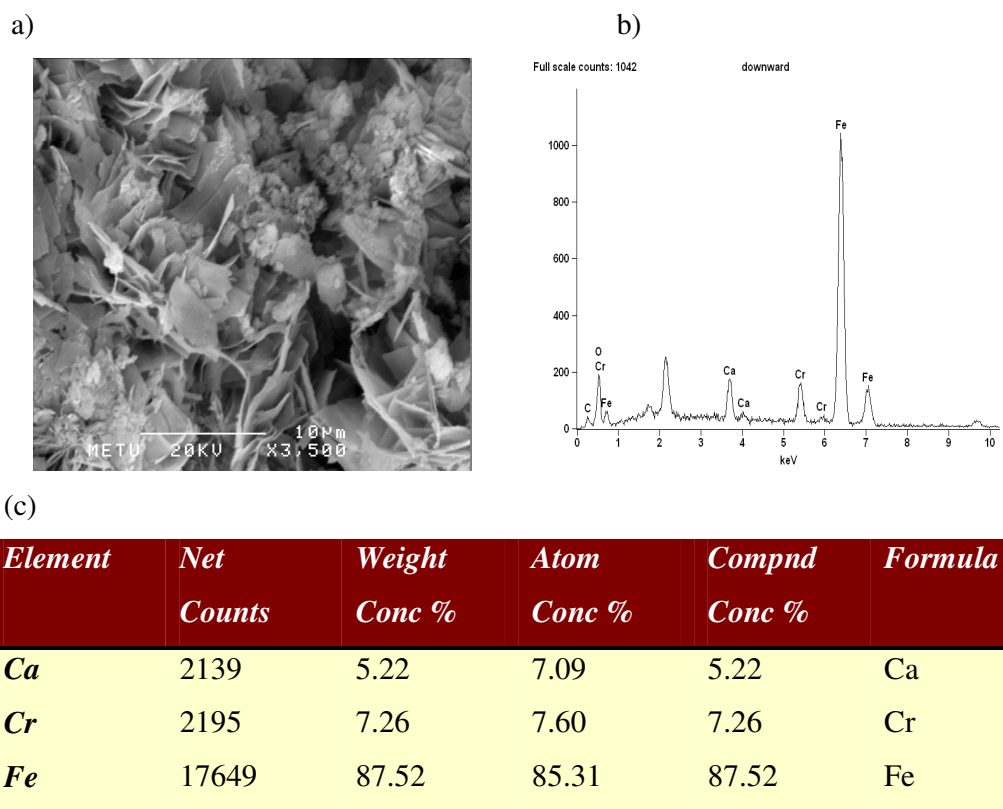
Figure 4.5. (a) Another iron surface of the "downward" section of the column 50IR analyzed by SEM after exposure to 453 pore volumes of Cr (VI) solution. (b, c) EDX analysis of the elements on the surface.

Visual comparison of iron structure before and after the reaction with Cr(VI) (Figure 4.3a, 4.4a and 4.5a) revealed that the iron surface were covered with (oxy)hydroxides that were produced by reduction-precipitation reactions. EDX analysis has shown distributed Fe, Cr, Ca and Si on the surface of the specific particle analyzed with ratios of 2.22 weight percentage of (wt %) Si, 6.26 wt % Ca, 2.46 wt % Cr and 89.06 wt % Fe in the first sample and, 5.22 wt % Ca, 7.26

wt % Cr and 87.52 wt % Fe in the second sample. The presence of Ca indicated $CaCO_3$ precipitation. Si content in the first sample is most likely resulted from the dissolution of quartz sand. In fact, ferrihydrite is known to strongly absorb Si, which stabilizes ferrihydrite and retards the further oxidation to ferric oxyhydroxides (Benali, et al., 2001; Fredrickson et al., 1998; Mayer and Jarrell, 1996; Furukawa et al., 2002). Consequently, it can be inferred that the specific surface in the first sample is coated with ferrihydrite.

a)                                                  b)



c)

| Element | Net Counts | Weight Conc % | Atom Conc % | Compnd Conc % | Formula |
|---------|-----------|---------------|-------------|---------------|---------|
| Ca | 476 | 0.87 | 1.21 | 0.87 | Ca |
| Cr | 1024 | 2.37 | 2.53 | 2.37 | Cr |
| Fe | 26333 | 96.76 | 96.26 | 96.76 | Fe |
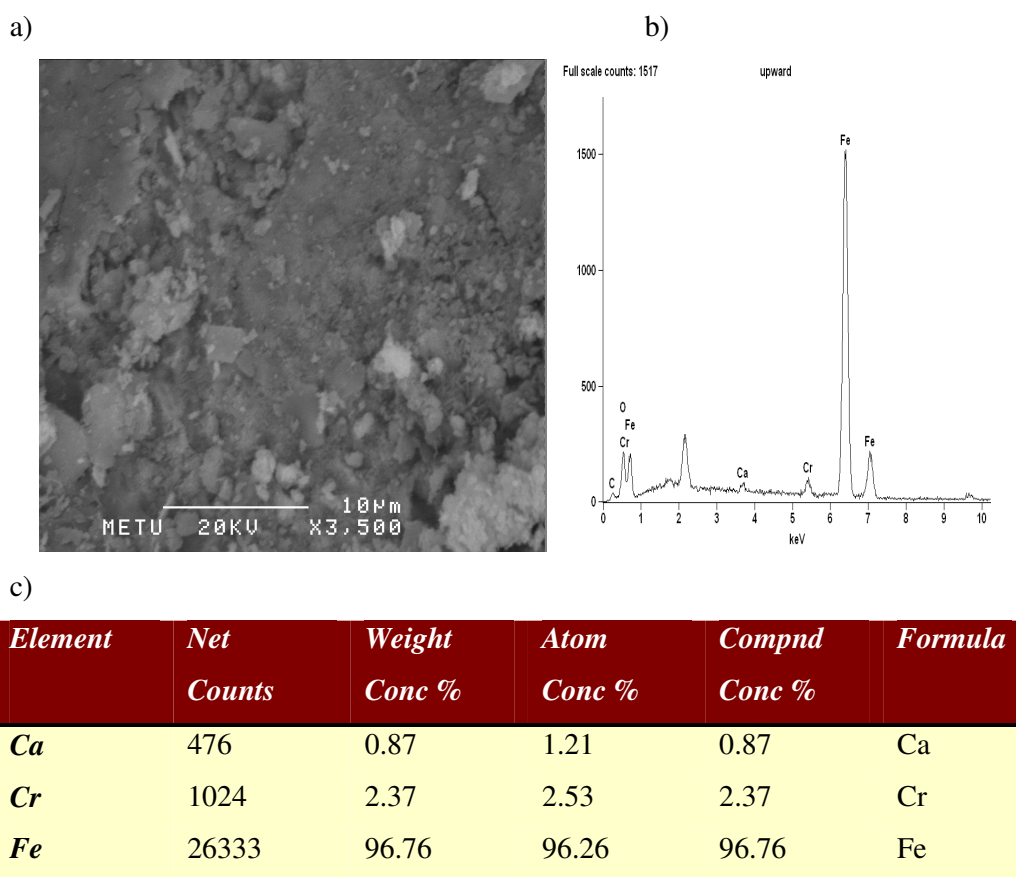
Figure 4.6. (a) Iron surface of the "upward" section of the column 50IR analyzed by SEM after exposure to 453 pore volumes of Cr (VI) solution.
(b, c) EDX analysis of the elements on the surface.

Samples taken from the "upward" section of the 50IR column also confirmed the formation of Fe (hydr)oxides. Fe in the "upward" sample showed stronger signals than the "downward" samples with a weight percentage of 96.76 which may be due to the lesser amount of Ca and Cr precipitation. The analysis also showed a lower concentration of calcium in the upward samples with a weight percentage of only 1.21 suggesting that $CaCO_3$ precipitation occurred when the chromate solution first entered the column. This preferential precipitation in the upgradient reactive media is consistent with laboratory applications (Kamolpornwijit et al., 2003; Kamolpornwijit et al., 2004; Zhang and Gillham, 2005) and field applications (Furukawa et al., 2002; Liang et al., 2003). Lower amount of Cr accumulation was detected in this sample compared to downward ones. Since only 2.37 wt % of Cr was present in the sample, only a thin layer of Fe-Cr precipitates on the ZVI surface is suspected (Lo et al., 2006).

In terms of comparison between the two sections, Cr and Fe are correlated in different ratios in upper and lower sections (Figure 4.4c, 4.5c and 4.6c). The "upward" section has shown less amount of Cr in the samples than the "downward" samples. This may be attributable to the preferential flow development in upward sections because of precipitation. If samples in the "upward" section were selected from the parts where the flux was less, the amount of Cr was also expected to be low in these areas. This result is consistent with visual observations, since less and non-uniform cementation have been observed in the "upward" section. In the "lower" section, Ca sink is more dominant compared to the upper section. From this information, it may be inferred that mineral precipitates mostly accumulate at the upgradient of a PRB where the plume first enters the barrier. On the other hand, in both sections, weight percentage of Cr in the solid sample was far less compared to that of Fe. This is consistent with the study of Blowes et al., 1997 conducted with Cr(VI) and ZVI. However, Cr/Fe ratio is dependent on many factors such as influent Cr(VI) concentration, batch versus column experiment, flow rate, and the type and

amount of ZVI used in the experiments. Consequently, it is difficult to make a direct comparison between different studies.

## 4.4. System Hydraulics

Besides reactivity, long term permeability is also a critical factor in the performance of ZVI PRBs. The hydraulics of a PRB is mainly affected by two factors, namely mineral precipitation and gas formation. Mineral precipitation forces water to flow through the column circumference and forms a preferential, tortuous high velocity flow path (Liang et al., 2003). Because the gas phase is the non-wetting fluid, hydrogen gas formed, accumulates in the largest pores that are most effective in transmitting water (Zhang and Gillham, 2005). Thus, due to these two phenomena (i.e. increased tortuosity of flow path and reduction in conductive porosity) system hydraulics is subject to change as a PRB ages and hydraulic flow properties are important parameters for the performance of PRBs.

During the experiments, the flux has been checked from time to time by measuring the amount of sample in a volumetric flask and recording the elapsed time interval. The precipitates and the probable hydrogen gas formation did not appear to significantly affect porosity and in turn the hydraulic performance of the system (Figure 4.7. a, b and c) since flux measurements showed no significant fluctuations. The percent flux changes during the runs ranged between 0.71% and 29.05%. The highest change occurred in the flux was 29.05% decrease in column 25IR operated at a flux of 0.057 ml/cm$^2$.min. This drop was recorded at the beginning of the run. However, later the fluxes increased after this sudden decrease for this column. Therefore, it is suspected that the glass filter supporting the media was clogged at the beginning of this run and allowing less amount of flow through the column. The subsequent increase can be attributable to the precipitation which caused the water to follow a preferential and high velocity pathway as mentioned above. Column 10IR has shown the steadiest flux during the runs. This is probably due to high amount of

sand in the column mixture. High amount of sand, which is creating pores with large size, prevented the precipitation to affect the fluxes. For column 50 IR, variations in the flux were recorded mostly in the column having the average flux of 0.07 ml/cm$^2$.min. In fact, the variations were larger for column 50IR compared to other columns operated at the same flux. This is likely due to the porosity values of the columns (Table 4.1). The non-uniformity of pore sizes of the reactive mixtures are expected to increase as their iron contents increases. Hence, the system hydraulics was more prone to disturbances in column 50IR compared to columns 25IR and 10IR.

However, it should be noted that this study was conducted at short columns and flow rates were higher than normally encountered flow rates under many field conditions. Furthermore, sand and sand size iron was selected for use in reactive mixtures. This improved the hydraulic conductivity of the columns as well as enabling a more uniform distribution of flow through the columns. Consequently, clogging in the reactive media was not very serious in the experiments of this study.

(a)
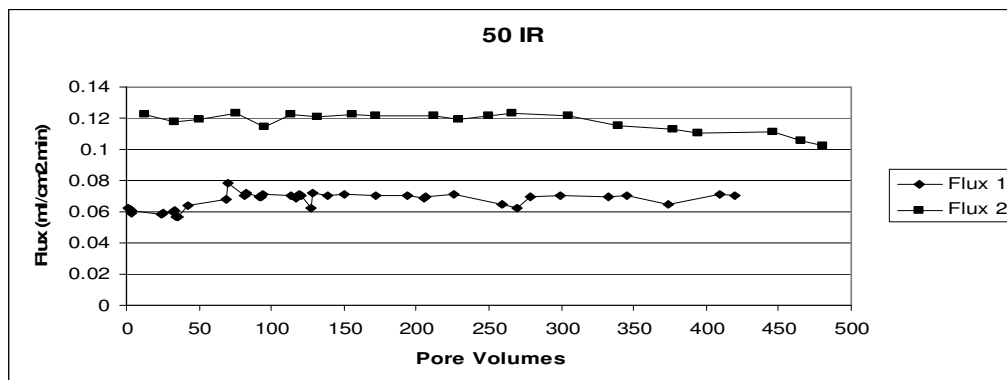


(b)
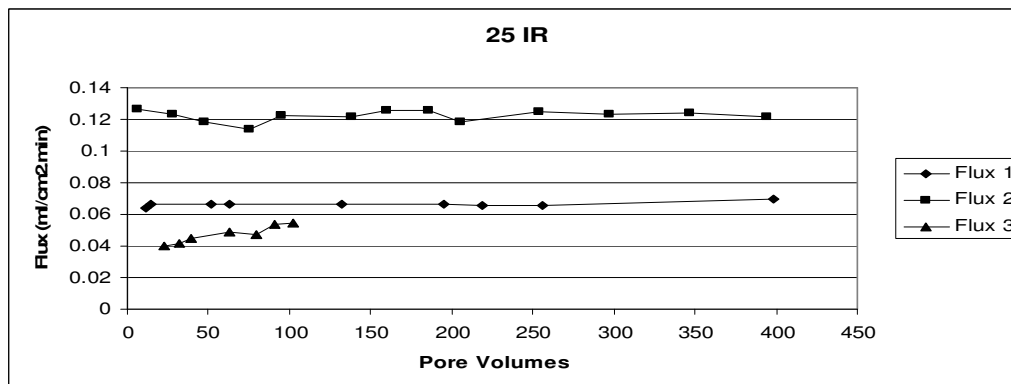


(c)
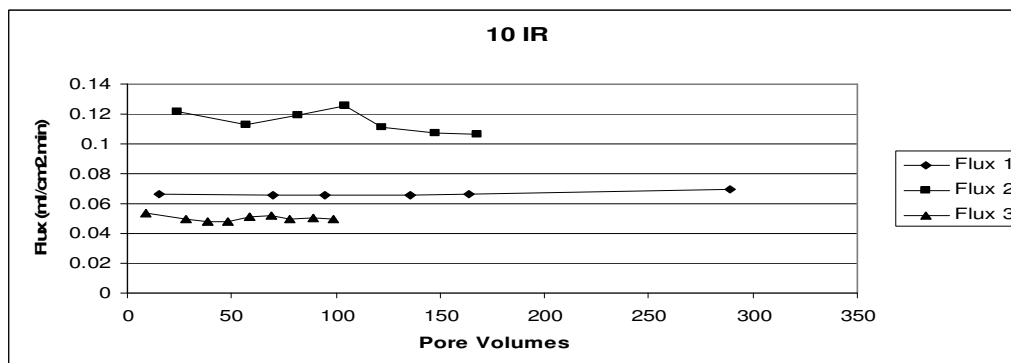


Figure 4.7. Evolution of fluxes versus pore volumes for reactive column mixtures.
(a) Column 50 IR (b) Column 25 IR (c) Column 10 IR. Flux 1=0.07 ml/cm$^2$.min,
Flux 2=0.127 ml/cm$^2$.min, Flux 3=0.057 ml/cm$^2$.min.

Table 4.1. Hydraulic Properties of Reactive Mixtures

| Property | 50 IR | | | 25 IR | | | | 10 IR | | 100 QS |
|---|---|---|---|---|---|---|---|---|---|---|
| Flux (ml/cm²·min) ($q$) | 0.07 | 0.127 | 0.17 | 0.07 | 0.127 | 0.057 | 0.07 | 0.127 | 0.057 | 0.057 |
| Flow Velocity ($v$) (cm/day)(m/year) | 153.80 561.37 | 260.19 982.55 | 389.19 1420.55 | 181.44 662.25 | 335.08 1223.03 | 129.74 473.57 | 196.13 715.87 | 340.03 1241.11 | 148.62 542.48 | 180.24 657.9 |
| Residence Time (hour)($t_{res}$) | 2.34 | 1.38 | 0.92 | 1.98 | 1.07 | 2.77 | 1.84 | 1.06 | 2.42 | 2 |
| Dispersion Coefficient (cm²/min)($D$) | 1.53 | 0.947 | 2.9 | 0.316 | 0.266 | 0.021 | 1.579 | 0.0252 | 0.0209 | 0.0789 |
| Pore Volume (ml) | 64.3 | | | 53.7 | | | | 49.8 | | 47.9 |
| Porosity ($\phi$) | 0.628 | | | 0.524 | | | | 0.486 | | 0.452 |
| Bulk density (g/cm³) ($\rho_b$) | 1.96 | | | 1.883 | | | | 1.629 | | 1.452 |
| Surface Area of Iron to Volume of Solution Ratio (m²/ml) ($\rho_m$) | 0.065 | | | 0.0365 | | | | 0.0137 | | NA |
| Surface Area of Iron (m²)($W$) | 4.178 | | | 1.960 | | | | 0.682 | | NA |

## 4.5. Effect of Iron Concentration on Cr(VI) removal

The effect of ZVI concentration on Cr(VI) reduction was studied in columns 50IR, 25IR and 10IR. Figure 4.8 (a), (b) and (c) show the Cr(VI) breakthrough curves for fluxes of 0.07, 0.127 and 0.057 ml/cm$^2$.min, respectively. The iron ratios in the columns were also reported as the ratio of surface area of iron to volume of solution (Table 4.1) in the figures. Note that 50IR was operated at 0.17 ml/cm$^2$.min for the third set.

At a flux of 0.07 ml/cm$^2$.min (Figure 4.8 (a)) the columns 50IR, 25IR and 10IR were operated for about 453, 399 and 289 pore volumes (PVs) passing through 29.1, 21.4 and 14.4 liters of influent solution, respectively. By comparing the breakthrough curves, it can be seen that the maximum treatment efficiency was measured in column 50IR. In this column, complete removal of Cr(VI) had prevailed for more than 120 PVs.

(a)
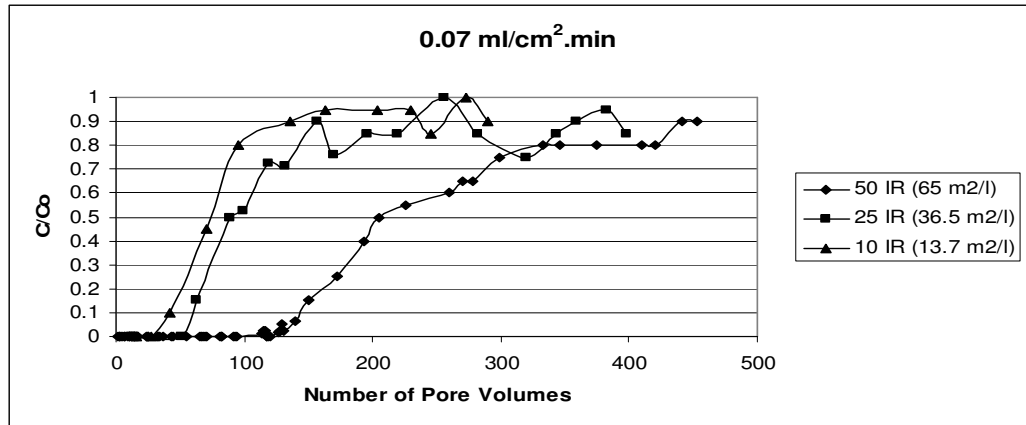


(b)
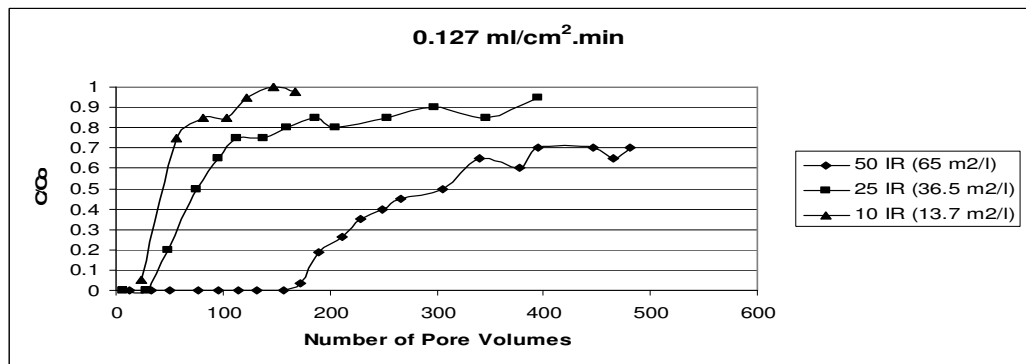


(c)



Figure 4.8. Breakthrough curves of Cr(VI) through the columns packed with different iron powder/quartz sand ratios. (a) Flux=0.07 ml/cm$^2$.min, (b) Flux=0.127 ml/cm$^2$.min, (c) Flux=0.057 ml/cm$^2$.min.

In 50IR column, dissolved Cr(VI) concentrations dropped from 20 mg/l in the influent to non detectable levels (<0.1 mg/l) in the effluent for about 120 PVs. At 127.2 PV, Cr(VI) was detected in the effluent. As the ZVI concentration halved (column 25IR), the treatment efficiency was nearly halved as well. Cr(VI) was detected at 62.9 PVs. In column 10IR, Cr(VI) was absent in the effluent only for 40PVs, showing the lowest treatment efficiency. In the second set of experiments, the same columns were operated at a flux of 0.127 ml/cm$^2$.min with the same influent solution. As shown in Figure 4.8 (b), the Cr(VI) reduction followed the same trend for the reactive mixtures with a decreasing capacity as ZVI concentration decreased with complete treatment of about 170 PVs of influent water. Column 50IR showed the highest treatment efficiency. However, column 25IR has treated much less Cr(VI) contaminated water giving a breakthrough at about 48 PVs. For column 10IR, breakthrough was observed at 23.8 PV. Finally, at a flux of 0.057 ml/cm$^2$.min (Figure 4.8 (c)), column 25IR showed better removal than 10IR but with a small difference in the efficiency.

It is apparent from these runs that the degree of treatment efficiency among the columns was more pronounced in column 50IR compared to those of 25IR and 10IR. Overall, at the same flux, increasing ZVI concentration increased the treatment efficiency and the effect became more observable at higher reactive media concentrations.

Another issue of concern is the reduction in treatment capacity during the transition period, which is the period starting with the first Cr(VI) detection in the effluent. During the transition period, in all of the experimental columns, there is a gradual increase in the effluent Cr(VI) concentration. In column 50IR, the slope of the curves is mild and it gets steeper as the amount of ZVI in the columns 25IR and 10IR decrease.

The results have shown that the efficiency Cr(VI) reduction by ZVI is significantly influenced by the amount of ZVI. When the capacities of the three columns were compared, it was seen that increasing the amount of ZVI extended the lifetime of complete treatment. The effect was more clearly seen in column 50IR compared to columns 25IR and 10IR which have relatively less amount of ZVI. These results indicated that mixing the reactive media with bulking agents may not be effective in creating an extra space for precipitates, but for keeping an adequate permeability between the particles. Also, in the transition period, column 50IR had a much smoother and prolonged curve. This suggests that $Fe^{3+}$ in the oxides may have reduced to $Fe^{2+}$ in this phase, enabling treatment of Cr(VI) and gradually decreasing the capacity of the medium.

In general, these results are consistent with the results reported in the literature where the rates of Cr(VI) reduction is found to be proportional to the iron surface area concentration (Gould, 1982; Blowes et al., 1997; Ponder et al., 2000; Alowitz and Scherer, 2002). Besides zero valent iron, other compounds containing iron has shown superior treatment at high concentrations. For example, at higher surface area concentrations of green rust (Bond and Fendorf, 2003) and carbonate green rust $[Fe^{II}_4 Fe^{III}_2 (OH)_{12}][4H_2O.CO_3]$ (Williams and Scherer, 2001), faster rates of Cr(VI) reduction were observed. Studies of published degradation rate data for individual halogenated hydrocarbons and chlorinated compounds also showed that the transformation rates are also proportional to iron surface area concentration (Jonhson et al., 1996; Matheson and Tratnyek, 1994; Sivavec et al., 1995; Agrawal and Tratnyek, 1996).

## 4.6. Effect of Groundwater Flux on Cr(VI) Removal

The effect of groundwater flux on the rates of Cr(VI) reduction was studied over the flux range of 0.057 ml/cm$^2$.min to 0.17 ml/cm$^2$.min. The experimental results were presented here to determine the relationship between the flux and the treatment efficiency. Figure 4.8 (a), (b) and (c) show the normalized Cr(VI) breakthrough curves of the columns having three different fluxes.

In Figure 4.9 (a), Cr(VI) removal efficiency of column 10IR at fluxes of 0.07 ml/cm$^2$.min, 0.127 and 0.057 ml/cm$^2$.min was compared. The treatment efficiencies were quite similar at 0.057 and 0.07 ml/cm$^2$.min fluxes (breakthrough at 38.4 and 41.9 PVs, respectively), while Cr(VI) breakthrough occurred much earlier at the flux of 0.127 ml/cm$^2$.min (23.8 PV). In contrast, column 25IR shows no significant difference in the treatment efficiency with respect to fluxes (Figure 4.9 (b)) with overlapping breakthrough curves. Complete Cr(VI) removal was occuring for more than 30 PVs, 50 PVs, and 30 PVs at flow rates 0.057, 0.07 and 0.127 ml/cm$^2$.min, respectively. The maximum treatment efficiency, therefore, occurred at 0.07 ml/cm$^2$.min. This suggests that there can be an optimum flux for the reduction of Cr(VI). Although 0.057 ml/cm$^2$.min flux allows more contact time within the column, this can also result in production of more H$_2$ gas which has an inhibitory effect for system hydraulics. In fact, column 25IR had changes in flux during the run with a decrease and then an increase back again. That is, if the production of H$_2$ gas caused occupying pores in the media, this might as well affect the flux and treatment efficiency.

(a)
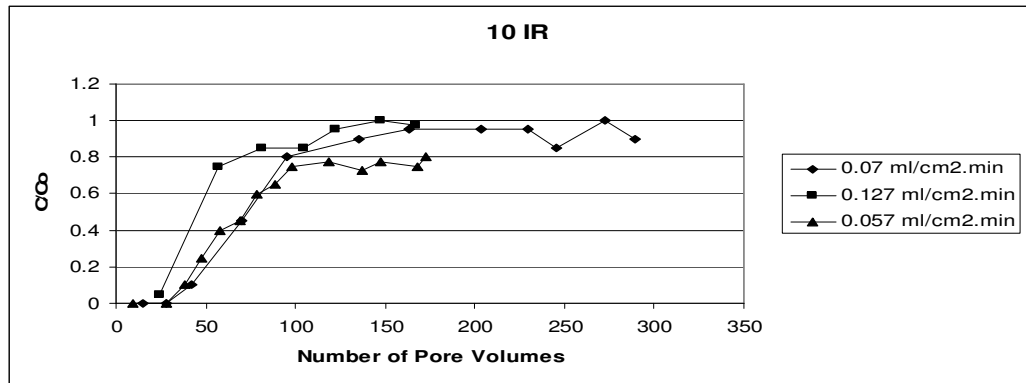


(b)
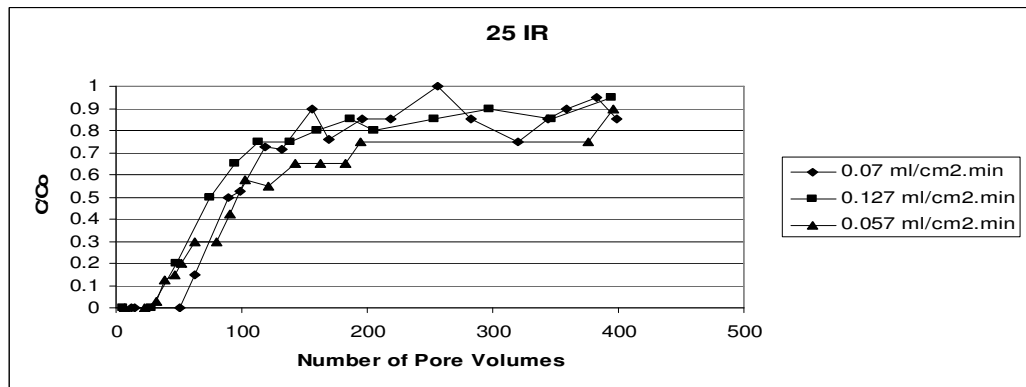


(c)



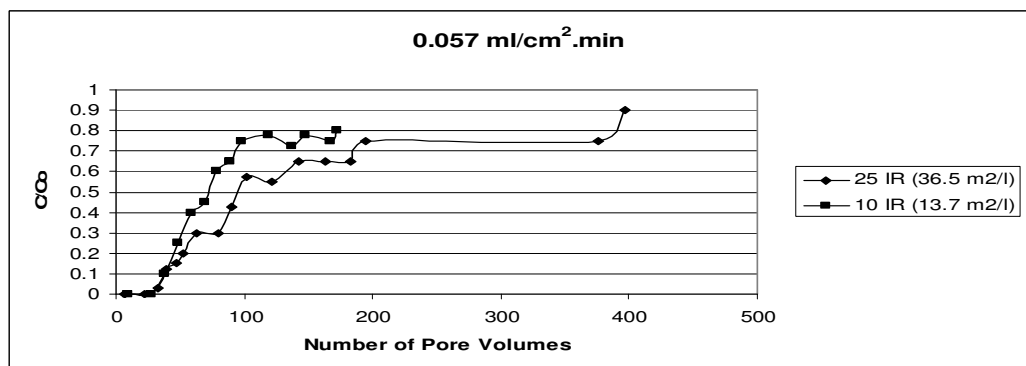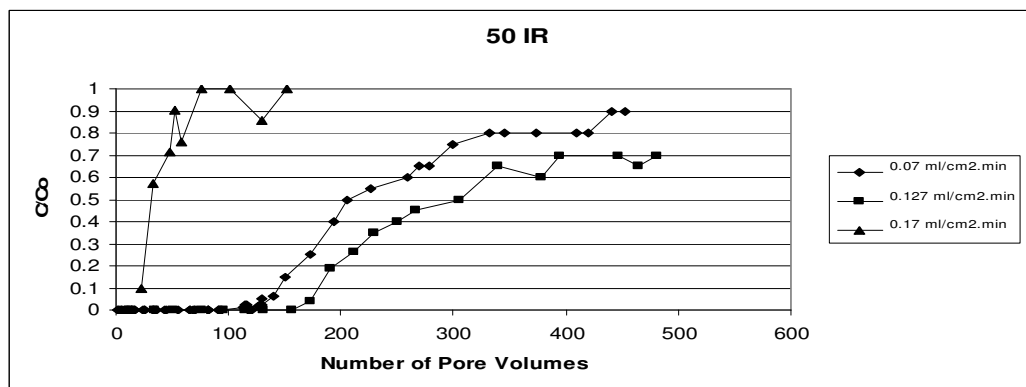Figure 4.9. Breakthrough curves of Cr(VI) through the columns packed with different iron powder/quartz sand ratios. (a) Iron powder/Quartz Sand=10%, (b) Iron powder/Quartz Sand=25%, (c)Iron powder/Quartz Sand=50%.

Interestingly, column 50IR showed a different behavior than the other columns. The Cr(VI) removal capacity at a flux of 0.127 ml/cm$^2$.min was significantly higher than that of 0.07 ml/cm$^2$.min (Figure 4.9 (c)). Hence, it was decided to operate column 50IR at a much higher flux (0.17 ml/cm$^2$.min). At this flux, almost no reduction of Cr(VI) was observed which showed the most rapid breakthrough among all of the experimental columns.

It can be seen from these results that groundwater flux had a variable effect on Cr(VI) reduction. The residence time was the determining factor in column 10IR, since shorter residence time reduced the capacity and efficiency of ZVI to treat Cr(VI). No significant effect of flux was seen in column 25IR. The Cr(VI) reduction was not proportional to the residence time in column 50IR, showing superior removal at a flux of 0.127 ml/cm$^2$.min than at 0.07 ml/cm$^2$.min. However, when the column 50IR was operated at a much higher flux (0.17 ml/cm$^2$.min), nearly no treatment of Cr(VI) was observed. Most probably, insufficient residence time prevented Cr (VI) removal. Column 50IR did not appear to have significant corrosion and precipitation reactions.

Two explanations were suggested for the phenomenon in 50IR in which better efficiency was observed at a bigger flux. First, at higher fluxes, the precipitates that blocks available surface area for further reduction may not be accumulating. This condition apparently results in more available reactive surface for reduction. Iron oxides and hydroxides are common colloid formations in groundwater (McCarthy and McKay, 2004) and they can be transported at moderate to high groundwater velocities. Accordingly, this condition decreases the possibility of surface passivation of iron. Furthermore, as the flux increases, the concentration of the reaction products is lowered by dilution (Kaplan and Gilmore, 2004). This suggestion is also likely to explain the results in column 25IR and 10IR. The fluxes were probably high enough for the transport of the precipitates formed in

this column. Hence, the capacity was exhausted at similar pore volumes regardless of the value of the flux. With regard to column 10IR, on the other hand, the precipitation formation was possibly not intense enough to control the efficiency.

Second, it is thought that thicker oxide films were produced at lower fluxes. These thick oxide films may have prevented the diffusion of Cr(VI) transfer through the fresh ZVI in the column. At higher fluxes, the film thickness were much less resulting in unimpeded contact between Cr(VI) and ZVI. This explanation agrees with the results of other studies, indicating dependence on diffusion from bulk solution to ZVI surface (Wüst et al., 1999, Morrison et al., 2001).

## 4.7. pH and Oxidation-Reduction Potential

In the experiments, it is apparent that buffer solution, the amount of ZVI and flux have had impact on pH. The pH of the groundwater in which ZVI is undergoing corrosion is expected to increase (Matheson and Tratnyek, 1994; Kielemoes et al., 2000; Kamolpornwijit et al., 2003). On the other hand, the buffering capacity of the solution (the presence of carbonate species in the background solution) tends to buffer the pH of the effluent preventing very high pH values. As the pH increases, bicarbonate ($HCO_3^-$) in solution converts to carbonate ($CO_3^{2-}$) to buffer the pH increase. Also, the pH of the groundwater in contact with ZVI is controlled by the amount of ZVI dissolved into the water; the extent of ZVI dissolution is influenced by the relative rates of ZVI corrosion and the groundwater flow velocity (Liang et al., 2003).

In all of the columns, the pH of the effluent water was basic due to the bicarbonate background solution. The increase in pH is an expected result as ZVI reacts and dissolves (Matheson and Tratnyek, 1994; Stumm and Morgan, 1996; Liang et al.,

2003). However, high incrase in pH is prevented by the background carbonate solution since $OH^-$ ions react with bicarbonate species to buffer the pH. Generally, for the same reactive mixture when velocity was slow, a high pH was detected (longer residence time would be needed for pH rise to occur). When flow rate was higher a smaller rise in pH was detected because the short residence time did not allow production of enough $OH^-$ to raise the pH.

For column 50IR at fluxes of 0.07 and 0.127 ml/cm$^2$.min, the pH of the effluent solution first had a gradual increase to pH values of 9.9 and 8.9, respectively (Figure 4.10 a, b), then, it reached a steady value of near 7.9, coinciding with the end of the complete Cr(VI) removal time. This is attributed to the passivation of ZVI in the reactive mixtures, which result in reduced ZVI dissolution and, therefore, a smaller rise in pH (Kamolpornwijit et al., 2003). At the flux of 0.17 ml/cm$^2$.min, the column did not show a significant variation in pH, most probably due to the insufficient residence time to produce $OH^-$ ions (Figure 4.10 a, b, c). In column 25IR, the pH did not change much with respect to influent solution pH, ranging from 7.77 and 8.56 (Figure 4.11 a, b, c). Likewise, in column 10IR, the effluent pH values were nearly the same as the influent pH values at all three fluxes (Figure 4.12. a, b, c). The pH increase was not as significant in column 25IR and 10IR as was in 50IR, probably due to the less amount of dissolved Fe in the                                                                                                                        medium.

(a)
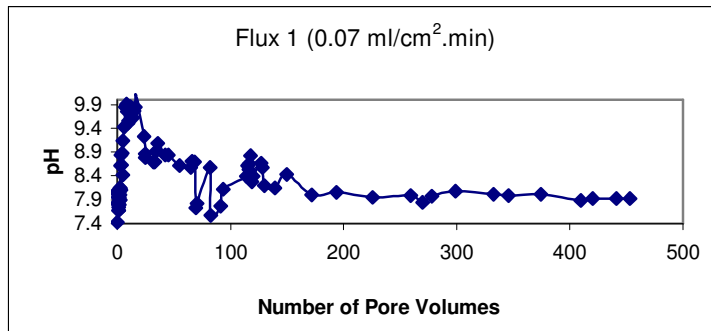


(b)
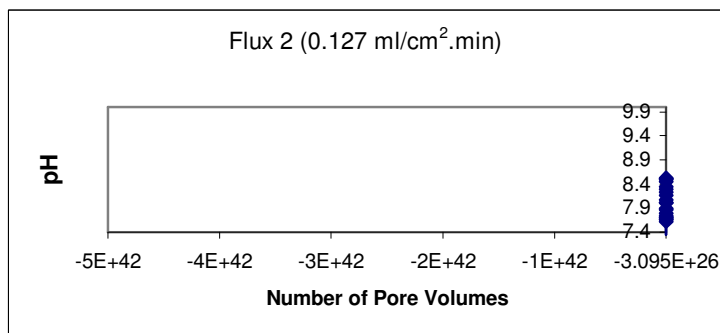


(c)
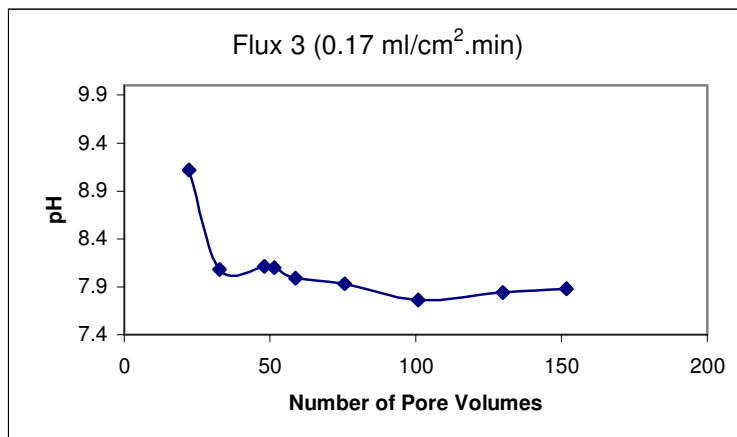


Figure 4.10. pH measurements for column 50IR(a) Flux 1 =0.07 ml/cm$^2$.min (b) Flux 2 = 0.127 ml/cm$^2$.min (c) Flux 3 = 0.17 ml/cm$^2$.min

(a)
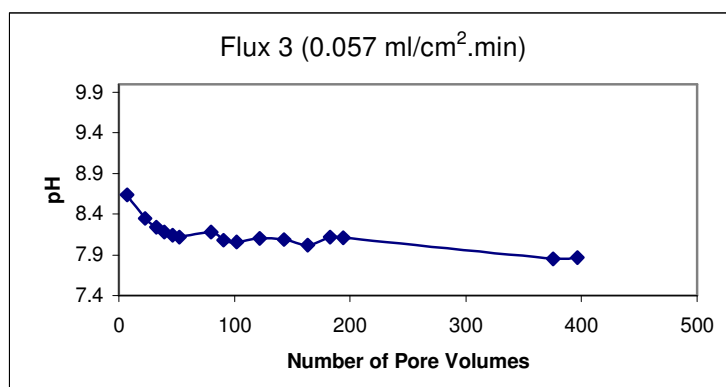


(b)
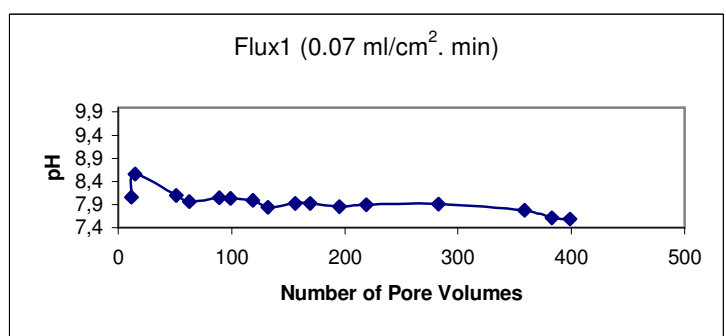


(c)
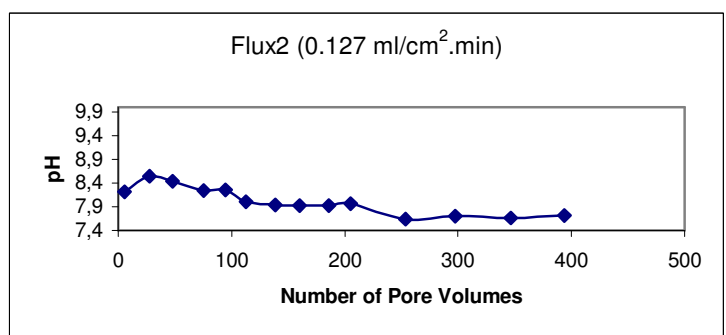


Figure 4.11. pH measurements for column 25IR. (a) Flux 3=0.057 ml/cm$^2$.min
(b) Flux 1=0.07 ml/cm$^2$.min (c) Flux 2 = 0.127 ml/cm$^2$.min

(a)

Flux 3 (0.057 ml/cm$^2$.min)

(b)

Flux 1 (0.07 ml/cm$^2$.min)

(c)
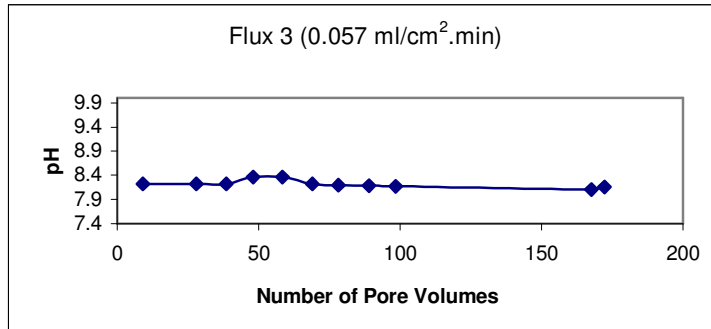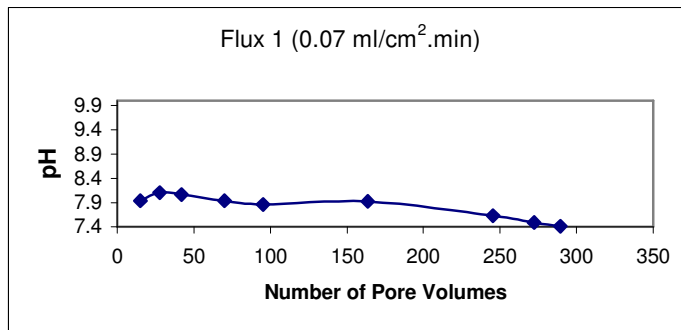
Flux 2 (0.127 ml/cm$^2$.min)
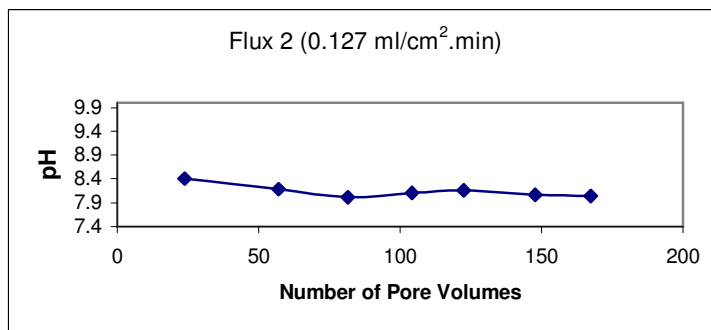
Figure 4.12. pH measurements for column 10 IR.(a) Flux 3 = 0.057 ml/cm$^2$.min (b) Flux 1 = 0.07 ml/cm$^2$.min (c) Flux 2 = 0.127 ml/cm$^2$.min

74

If corrosion occurs, the redox potential, $E_h$, at the surface of the corroding ZVI should approach that of the oxidation-reduction potential responsible for the dissolution of the metal surface, as shown in the following reaction equations

$$Fe^0 \leftrightarrow Fe^{2+} + 2e^- \qquad (4.8)$$

$$Fe^0 \leftrightarrow Fe^{3+} + 3e^- \qquad (4.9)$$
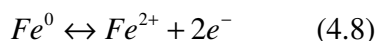
In a suspension, bulk $E_h$ should approach those near the reactive surface. However, this is the entire reactive surface, including both cathodic and anodic reactions. Therefore, the half reactions of the electron acceptors such as

$$2H^+ + 2e^- \leftrightarrow H_2(g) \qquad (4.10)$$

$$6H^+ + 1.5O_2 + 3e^- \leftrightarrow 3OH^- + 1.5H_2 \qquad (4.11)$$

$$CrO_4^{2-} + 4H_2O + 3e^- \leftrightarrow Cr(OH)_3 + 5OH^- \qquad (4.12)$$
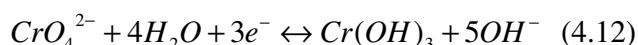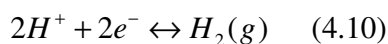
will also influence the measured $E_h$ as will any other active redox couples. This is called mixed potential (Powell et al., 1995). Redox potential measurements with platinum electrodes are generally useless except to estimate ferrous-ferric activity ratios or sulfide activities when the concentrations are greater than $10^{-5}$ M. Otherwise, the potential may drift according to the electrokinetic phenomena, mixed potentials or impurities at the metal electrode surface. Also, to determine the redox chemistry of a water sample, it is necessary to determine all the relevant redox species. These species can be expected to react in different ways and at different rates. Homogeneous redox reactions can be rather slow and heterogeneous redox reactions can be even slower (Wilkin et al., 2000).

The factors mentioned above probably affected the measured redox potential of the effluent samples. The measured Eh values in the effluent were moderately reducing, ranging between 171 mV and 474.4 mV (Appendix). No correlation of Eh values were found with the amount of ZVI or flow rate due to the mixed potential or small amount of dissolved Fe in the effluent. In fact, redox measurements were done only to have an idea about the general redox geochemistry of the effluent because of the difficulties and uncertainties in the redox measurements in the laboratory conditions.

## 4.8. Kinetic Considerations

In the literature, reduction of Cr(VI) is extensively modeled using pseudo-first order kinetics according to the following equation (Powell et al., 1995, Ponder et al., 2000, Alowitz and Scherer, 2002, Melitas and Farrell, 2002):

$$\frac{dP}{dt} = -k_{obs}P \qquad (4.13)$$

where P is the concentration of dissolved Cr(VI), t is the contact time between Cr(VI) solution and ZVI particles, and $k_{obs}$ is the first-order reaction rate constant. Integrating this equation yields

$$\ln\left(\frac{P_o}{P}\right) = -k_{obs}t \qquad (4.14)$$

where $P_o$ is the initial concentration of Cr(VI).

This equation can be modified by defining a surface area normalized reaction rate parameter which is independent of ZVI concentration and ZVI surface area, and in turn a more representative rate constant, as:

$$k_{obs} = k_{SA}\rho_m \qquad (4.15)$$

$$\ln\left(\frac{P_o}{P}\right) = -k_{SA}\rho_m t \qquad (4.16)$$

where $k_{SA}$ is defined as the surface area normalized rate coefficient and $\rho_m$ is the surface area of ZVI particles per solution volume (Alowitz and Scherer, 2002). For the case of steady state flow in a packed bed reactor, an expression analogous to the equation above may be derived by expressing the time (t) as the product of bed void fraction ($\varepsilon$) and the reactor volume (V), divided by the liquid flow rate (Q) through the bed (U.S. EPA, 1998), yielding the following expression

$$\ln\left(\frac{P_o}{P}\right) = \frac{k_{SA}\rho_m \varepsilon V}{Q} \qquad (4.17)$$

The term $\rho_m \varepsilon V$ is the total surface area of zero-valent iron, W, that the fluid encounters as it flows through the bed. With this substitution, and by representing the flow rate as the product of cross-sectional plume area (A), the aquifer porosity ($\phi$), and the average flow velocity (v), that is Q=Av$\phi$, the amount of iron required per unit cross-section of plume to realize the desired decrease in Cr(VI) concentration may be expressed as

$$\frac{W}{A} = \frac{v\phi}{k_{SA}}\ln\left(\frac{P_o}{P}\right) \qquad (4.18)$$

and rearranging yields

$$k_{SA} = \frac{v\phi A}{W} ln\left(\frac{P_o}{P}\right) \qquad (4.19)$$

This expression allows calculating the surface area normalized rate coefficient for each experiment at a specified time interval. It should be noted that the first-order kinetics are mostly reported for initial reaction rates and that the rates are increasingly deviated from the first-order kinetics with increasing time (Melitas and Farrell, 2002; Ponder et al., 2000). Hence, in our experiments, a pseudo first-order rate assumption was made for the first 100 PVs of the experiments. The surface area normalized rate coefficients were calculated for the first 100 PVs of each run. That is, P was taken as the effluent Cr(VI) concentration exactly at $100^{th}$ PV. If the Cr(VI) concentration measurement had not been made at $100^{th}$ PV, a linear interpolation was made between Cr(VI) concentrations of the two closest measurements to $100^{th}$ PV. $P_o$ was the Cr(VI) concentration in the influent solution, 20 mg/l. Porosity ($\phi$), average groundwater flow velocity (v) and W values are given in Table 4.1. Observed rate coefficients ($k_{obs}$) was obtained by multiplying $k_{SA}$ values with surface area of ZVI per solution volume ($\rho_m$). The $k_{obs}$ and $k_{SA}$ values obtained from each column are reported in Table 4.2.

Table 4.2.  Values of $k_{obs}$ and $k_{SA}$ constants calculated for reduction of Cr(VI) by ZVI.

| Column | Flux (ml/cm$^2$.min) | $k_{obs}$ (d$^{-1}$) | $k_{SA}$ (cm/h) |
|---|---|---|---|
| 10IR | 0.057 | 50.75 | 8.89 |
|  | 0.070 | 48.86 | 8.56 |
|  | 0.127 | 66.16 | 11.59 |
| 25IR | 0.057 | 93.17 | 6.13 |
|  | 0.070 | 126.23 | 8.30 |
|  | 0.127 | 155.20 | 10.21 |
| 50IR | 0.070 | 1635.83 | 60.40 |
|  | 0.127 | 3804.13 | 140.46 |
|  | 0.170 | NA | NA |

$k_{SA}$ values have ranged between 6.13 cm/h and 140.16 cm/hour giving the minimum at column 25IR operated at a flux of 0.057 ml/cm$^2$.min and the maximum at column 50IR operated at a flux of 0.127 ml/cm$^2$.min. As the formula indicates (equation 4.19), when the surface area normalized rate coefficients and observed rate constants were compared in each column, it was observed that as the velocity(flux) increased, $k_{SA}$ and $k_{obs}$ increased. On the other hand, when the $k_{SA}$ values were multiplied with $\rho_m$ to obtain observed rate coefficients, the observed Cr(VI) removal rate constants increased as the iron content increase at the same flux. Although there were differences in $k_{obs}$ values between columns 25IR and 10IR, the variability was modest, with about a 2-3 fold change. However, the difference was significant in column 50IR, which also showed much higher

treatment efficiency as compared to columns 25IR and 10IR. Since the column 50IR operated at a flux of 0.17 ml/cm$^2$.min has shown nearly no complete treatment (i.e., Cr(VI) was detected almost instantly in the effluent), it was not meaningful to calculate a rate constant for this case. In fact, this means a rate constant of nearly zero.

Once the surface area normalized rate constants or observed rate constants of Cr(VI) removal have been determined, designing the flow through thickness requires an accurate estimate of the residence time to achieve the desired concentration. After residence time is calculated, the thickness can be simply determined by multiplying it with the groundwater velocity. In addition, reactions between common ions and ZVI need to be considered in the context of kinetics and the relative rates at which flow and reactions occur in PRBs.

### 4.9. Field Scale Implications

The results presented in Section 4.8 can be of particular interest for the field scale applications in the design phase. $k_{obs}$ values calculated through column tests can be used in the calculation of the thickness of a PRB. On the other hand, there are two assumptions in the calculations of observed rate constant of Cr(VI) removal. First, Cr(VI) reduction reaction is assumed to be first-order. Second, a proportionality relationship was assumed to occur between observed rate constants and surface area concentration of ZVI in the column mixtures.

There is yet another design parameter that may be useful for field scale PRB installations. Table 4.3 summarizes the complete treatment efficiency of each reactive mixture for each flux. The difference between the treatment efficiencies of columns 10IR and 25IR was modest whereas treatment efficiency of column 50IR was much

higher as compared to these two columns. This shows that the treatment efficiencies of columns increase non-linearly after a certain value of iron content.

This table can also be used as a preliminary estimate of required amount of ZVI to treat a specific volume of plume at a specific groundwater flux. For example, it may be referred that a PRB containing 50% ZVI treat 120 PVs of Cr(VI) contaminated groundwater at a flux of 0.07 ml/cm$^2$.min. Similarly, it may treat 156 PVs at 0.127 ml/cm$^2$.min. To put in another way, a PRB containing equal or less than 50% ZVI can not treat a plume which has a size more than 156 pore volume. For an iron-based PRB having 25% ZVI, the expected life-time can not exceed 51.2 times its pore volume at a flux of 0.07 ml/cm$^2$.min. It should be noted, on the other hand, these data are transferable to field conditions provided that temperature, surface area of ZVI, influent Cr(VI) concentration and other conditions are similar to this study.

Table 4.3. Expected life times of ZVI PRB as a function of flux and ZVI concentration.

| Flux (ml/cm$^2$.min) | Reactive Column | | |
|---|---|---|---|
| | 50 IR | 25 IR | 10 IR |
| 0.057 | NA | 22.4 PV | 28 PV |
| 0.07 | 120 PV | 51.2 PV | 27.8 PV |
| 0.127 | 156 PV | 27.6 PV | ND |

ND: Not Detected, NA: Not Applicable

# CHAPTER 5

## CONCLUSIONS AND RECOMMENDATIONS

### 5.1. Conclusions

To date, it has been shown that ZVI based PRBs can be used as an effective remedial material for in situ remediation of groundwater contaminated with Cr(VI). This study aimed to investigate the effectiveness of a ZVI based PRB operated to remove Cr(VI) in a set of conditions which are likely to occur under field conditions. Visual observations, mineralogical characterization, pH and redox measurements and comparison of the column results with respect to concentration of ZVI in the columns and groundwater fluxes provided preliminary guidelines for the understanding of treatment of Cr(VI) ZVI based PRBs.

In the entire column experiments conducted in this study, iron corrosion and cementation were extensive at the inlet of the column and reduced gradually away from the inlet. Rusty stain was visible. The decline in the concentration of Cr(VI) and visual observation of oxyhydroxide formations were viewed as the evidence of the reductive precipitation of Cr(VI) by ZVI. Gas bubble formation was also observed, suggesting the anaerobic reduction of ZVI by water.

The amount to reactive media is a vital parameter in PRB applications to have sufficient treatment within the reactive medium and also significantly affect the remediation cost. It follows that increasing the surface area of the iron should also increase the rate of removal. On the other hand, it is sometimes necessary to include sand in the reactive media to increase the porosity because of hydraulic constraints. Having an extra non-reactive support surface such as sand for

precipitation products formed in the column may in theory lead to higher capacities, since the reactive surfaces will be covered to a less extend than in a pure iron system. One of the main focus of this study was to address the impact of ZVI amount on Cr(VI) removal. The amount of ZVI concentration was found to be an important parameter for the remediation of Cr(VI) contaminated groundwater by ZVI under flowing conditions. In all groundwater fluxes, the increase in the amount of ZVI resulted in better treatment efficiencies. The effect was more clearly observed as concentration of ZVI increased. That is, superior treatment was achieved by columns 50IR and 25IR more than column 10IR. Despite the fact that the surface area of the iron used was relatively low (0.04 m$^2$/g), high pore volumes of complete removal was achieved (more than 156 PVs maximum). Nevertheless, at later stages of the runs, the precipitates decreased the availability of iron surface preventing the diffusion of Cr(VI) to ZVI. Consequently, once the Cr(VI) was detected in the effluent, the amount of ZVI rarely affected the period to achieve the complete breakthrough of the column.

The groundwater fluxes used in the study simulated fast flowing sandy aquifers or flow of groundwater in the funnel of a PRB. In columns containing 10% and 25% ZVI showed superior treatment at low flow rates. Conversely, column containing 50% ZVI treated more pore volumes of Cr(VI) contaminated groundwater at higher flow rate. This revealed that there are other factors about the flow rate besides residence time. These factors included the mobility of precipitates at higher fluxes that result in available iron surface area and the thickness of oxide film formation, which in turn affects the effectiveness of diffusion.

The buffer solution appeared to be effective at maintaining pH conditions in the columns. The pH of the influent solution was between 7.3 and 8.1 whereas effluent pH was slightly basic (7.32<pH<10.09). It should be noted that buffering may be

significant over longer time scales since $Ca^{2+}$ and $CO_3^{2-}$ ions contribute to the mineral precipitation affecting both the reactivity and the hydraulic conductivity of the columns. Oxidation reduction potential of the effluent was moderately reduced in all runs. Still, the results of redox measurements were not taken as routine determination of the electroactive species in the samples due to the probable interferences and limitations in the measurement.

The mineralogical characterization study clearly revealed the mineral precipitates that result from the changes in chemical conditions. $Ca^{2+}$ was detected in EDX analysis of the reacted column samples indicating calcium carbonate precipitation. However, hydraulic performance of the columns was not affected significantly by precipitation. This is most probably due to the fact that iron was mixed with quartz sand and groundwater fluxes were quite high for porosity reduction to occur.

The observed rate constants of Cr(VI) removal can be an important parameter for the design studies since PRB performance is mainly dependent on the Cr(VI) removal rate. Also, complete removal efficiency values of each run can be used to represent field conditions that have similar groundwater flow velocity and buffering capacity. For instance, the complete treatment results of this study suggested that a PRB containing 50% iron designed to treat a Cr (VI) plume can treat a plume with a size of about 127.23 pore volumes of the aquifer at an average groundwater flow velocity of 153.8 cm/day. Despite the fact that this is a preliminary estimation, it provides a means of studying the expected life time of the constructed PRB and seems to be transferable to field conditions.

## 5.2 Recommendations

In this study, it has been shown with SEM and EDX analysis that chromium was incorporated into the (oxy)hydroxide precipitates. In a further study, the extent of

chromium leaching from the chromium containing precipitates contained in the column can be studied. Previous research has shown that it may be possible to regenerate the iron reactive media by flushing the wall with clean or mild reductant. Therefore, flushing solutions for the removal of precipitates can also be analyzed in terms of maintenance issues.

As PRB installations get older, long term reactivity and permeability issues gain more attention. Information on inorganic geochemical changes in the reactive media is useful in terms of longevity. Evaluation of longevity of a PRB system can be examined using long term column tests. Tracer tests can be conducted at the beginning and during or at the end of the treatability tests and the breakthrough curves can be compared to see how the porosity changes over time.

In this research, the complete treatment phase was assumed to follow a first order reaction kinetics and rate coefficients were calculated with respect to this assumption. The investigation of reaction kinetics needs improvement in this sense. In further studies, as concentrations of contaminants and the inorganic change with the distance traveled through the reactive media, they can be measured by installing a number of intermediate sampling ports along the length of the column. When the flow rate and porosity are known, distances through the column can be converted easily to residence time. A graph of contaminant concentration versus time can then be created which will be used to estimate the order of reaction rates.

New reactive media and/or reactive media combinations are being researched for PRB applications. Treatability tests for new reactive media are needed to be developed. In many sites, a mixture of contaminants which can not be treated by a single reactive material can occur. Sequential treatment system with multiple reactive zones for different contaminants is a good alternative for these types of

contaminated sites. Laboratory tests for these kinds of conditions can be informative.

Probabilistic design methodology should be incorporated when evaluating the variability of input parameters such as aquifer properties, influent contaminant concentration, and reaction rates. Modeling tools can be further developed to incorporate uncertainty in the design.

Source zone treatment has also gained attention in recent years. The applicability and obstacles of this method can be further explored.

# REFERENCES


Agrawal, A., Tratnyek, P.G., (1996) Reduction of nitro aromatic compounds by zero-valent iron metal. Environmental Science and Technology, 30: 153-160.

Allen, D., (2003) Material flows and waste streams: Chromium. ESM 282 Industrial Ecology Lecture Notes. The Bren School at UCSB.

Alowitz, M.J., Scherer, M.M., (2002). Kinetics of nitrate, nitrite and Cr(VI) reduction by iron metal. Environmental Science and Technology. 36 (3): 299-306.

Astrup, T., Stipp, S.L.S., Christensen, T.H., (2000). Immobilization of chromate from coal fly ash leachate using an attenuating barrier containing zero valent iron. Environmental Science Technology, 34: 4163-4168.

APHA (1989). Standard Methods for the Examination of Water and Wastewater. 20th Edition. American Public Health Association, American Water Work Association, Water Environment Federation, Washington, D.C.

Barnhart, J.,, (1997) Chromium chemistry and implications for environmental fate and toxicity. Journal of Soil Contamination, 6: 561-568.

Benali, O., Abdelmoula, M., Refait, P., Genin, J.M.R., (2001) Effect of orthophosphate on the oxidation products of Fe(II)-Fe(III) hydroxycarbonate transformation of green rust to ferrihydrite. Geochimica et Cosmochimica Acta, 65: 1715-1726.

Blowes, D.W., Ptacek, C.J., Jambor, J.L., (1997) In-Situ remediation of Cr(VI) contaminated groundwater using permeable reactive walls. Environmental Science and Technology, 31: 3348-3357.

Bond, D.L., Fendorf, S., (2003) Kinetics and structural constraints of chromate reduction by green rust. Environmental Science and Technology, 37: 2750-2757.

Bronstein, K., (2005) Permeable reactive barriers for inorganic and radionuclide contamination. U.S. Environmental Protection Agency Office of Solid Waste and Emergency Response Office of Superfund Remediation and Technology Innovation Washington, DC

Buerge, I.J., Hug, S.J., (1997) Kinetics and pH dependence of chromium(VI) reduction by iron(II). Environmental Science and Technology, 31: 1426-1432.

Buerge, I.J., Hug, S.J., (1998)  Influence of organic ligands on chromium(VI) reduction by iron(II). Environmental Science and Technology, 32: 2092-2099.

Calder, L.M., (1988).  Chromium contamination of groundwater, In: Chromium in the natural and human environments, Vol 20 (J.O. Nriagu and E. Nieboer, Eds.), John Wiley and Sons, New York, 1988, pp. 215-230.

Cantrell, K.J., Kaplan, D.I., Wietsma, T.W. (1995) Zero-valent iron for the in-situ remediation of selected metals in the groundwater. Journal of Hazardous Materials, 42: 201-212.

Chromium Medical Surveillance Project, Summary of Final Technical Report. October 1994. Environmental Health Services Division of Epidemiology, Environmental and Occupational Health Services. New Jersey Department of Health Services.

Clark, D. K., Darling, D. F., Hineline, T. L. and Hayden, P. H. (1997), Field Trial of the Biowall Technology at a Former Manufactured Gas Plant Site. 29th Mid-Atlantic Industrial and Hazardous Waste Conference, Presentation by Stearns and Wheler, LLC, Cazenovia, NY, U.S.A.

Eary, L.E., Rai, D.(1988). Chromate removal from aqueous wastes by reduction with ferrous iron. Environmental Science and Technology, 22: 972-977.

Environment Agency (2002) Guidance on the use of Permeable Reactive Barriers for remediating contaminated groundwater. National Groundwater & Contaminated Land Centre Report. NC/01/51.

Ericksen, G.E., (1983). The Chilean nitrate deposits. American Scientist, 71: 366-374.

Evans, U.R., (1960). The corrosion and oxidation of metals: Scientific Principles and Practical Applications, Edward Arnold (Publishers) Ltd.: London, p: 1094.

Farmer, J.G., Graham, M.C., Thomas, R.P., Licona-Manzur, C., Paterson, E., Campbell, C.D., Geelhoed, J.S., Lumsdon, D.G., Meeussen, J.C.L., Roe, M.J., Conner, A., Fallick, A.E., Bewley, R.J.F., (1999). Assessment of modeling of the environmental chemistry and potential for remediative treatment of chromium-contaminated land. Environmental Geochemistry and Health, 21: 331-337.

Farmer, J.G., Thomas, R.P., Graham, M.C., Geelhoed, J.S., Lumsdon, D.G., Paterson, E., (2002). Chromium speciation and fractionation in ground and surface waters in the vicinity of chromite ore processing residue disposal sites. Journal of Environmental Monitoring, 4: 235-243.

Fernandez-Sanchez, J.M., Sawvel, E.J., Alvarez, P.P.J., (2004). Effect of $Fe^0$ quantity on the efficiency of integrated microbial-$Fe^o$ treatment processes. Chemosphere, 54: 823-829.

Fredrickson, J.K., Zachara, J.M., Kennedy, D.W., Dong, H.L., Onstott, T.C., Hinman, N.W., Li, S.M., (1998) Biogenic iron mineralization accompanying dissimilatory reduction of hydrous ferric oxide by a groundwater bacterium. Geochimica Cosmochimica Acta, 62: 3239-3257.

Fryar, A.E., Schwartz, F.W., (1998) Hydraulic-conductivity reduction, reaction front propagation, and preferential flow within a model reactive barrier. Journal of Contaminant Hydrology, 32: 333-351.

Furukawa, Y., Kim, J., Watkins, J., Wilkin, R.T., (2002). Formation of ferrihyrite and associated iron corrosion products in permeable reactive barriers of zero-valent iron. Environmental Science and Technology, 36: 5469-5475.

Gandhi, S., Oh, B., Schnoor, J.L., Alvarez, P.J.J., (2002) Degradation of TCE, Cr(VI), sulfate and nitrate mixtures by granular iron in flow through columns under different microbial conditions. Water Research, 36: 1973-1982.

Gansy, A.B., Wamser, G.A. Suppression of water pollution caused by solid wastes containing chromium compounds. U.S. Patent No. 3, 981, 965.

Gavaskar, A., (1999). Design and construction techniques for permeable reactive barriers. Journal of Hazardous Materials, 68: 41-71.

Gavaskar, A., Gupta, N., Sass, B., Janosy, R., Hicks, J., (2000) Design Guidance for Application of Permeable Reactive Barriers for Groundwater Remediation, Battelle Press, Columbus, OH.

Gillham, R.W.; Burris, D.R., (1992). Recent developments in permeable in-situ treatment walls for remediation of contaminated groundwater. Proceedings, Subsurface Restoration Conference, June 21-24, Dallas, Texas.

Gould, J.P., (1982). The kinetics of hexavalent chromium reduction by metallic iron. Water Resources, 16: 871-877.

Grittini, C., Malcomson, M., Fernando, Q., Korte, N., (1995). Rapid dechlorination of polychlorinated biphenyls on the surface of a Pd/Fe bimetallic system. Environmental Science and Technology, 29: 2898-2900.

Gu, B., Liang, L., Dickey, M.J., Yin, X., Dai, S., (1998) Reductive precipitation of uranium(VI) by zero-valent iron. Environmental Science and Technology, 32: 3366-3373.

Gui, J., Devine, T.M., (1994) The influence of sulfate ions on the surface enhanced Raman spectra of passive films formed on iron. Corrosion Science, 36: 441-462.

Hellerick, L.A., Nikolaidis, N.P., (2005). Studies of hexavalent chromium attenuation in redox variable soils obtained from a sandy to sub-wetland groundwater environment. Water Research, 39: 2851-2868.

Hem, J.D., (1977). Reactions of metal ions at surfaces of hydrous iron oxide. Geochimica et Cosmochimica Acta, 41: 527-538.

International Chromium Development Association (ICDA), (2003) http://www.chromium-asoc.com/

ITRC (Interstate Technology & Regulatory Council). (1999). Regulatory Guidance for Permeable Reactive Barriers Designed to Remediate Chlorinated Solvents. Interstate Technology & Regulatory Council, Permeable Reactive Barriers Team. Available on the internet at www.itrcweb.org

ITRC (Interstate Technology & Regulatory Council). (2005). Permeable Reactive Barriers: Lessons Learned/New Directions. PRB-4. Washington, D.C.: Interstate Technology & Regulatory Council, Permeable Reactive Barriers Team. Available on the internet at www.itrcweb.org

James, B.R., (1996) The challenge of remediating chromium contaminated soil. Environmental Science and Technology, 30(6): 248A-251A.

Johnson, T.L., Scherer, M.M., Tratnyek, P.G., (1996) Kinetics of halogenated organic compound degradation by iron metal. Environmental Science and Technology, 30: 2634-2640.

Kamolpornwijit, W., Liang, L., West, O.R., Moline, G.R., Sullivan, A.B., (2003). Preferential flow path development and its influence on long term PRB performance: column study. Journal of Contaminant Hydrology, 66: 161-178.

Kamolpornwijit, W., Liang, L., Moline, G.R., Hart, T., West, O.R., (2004). Identification and quantification of mineral precipitation in $Fe^0$ filings from a column study. Environmental Science and Technology, 38: 5757-5765.

Kaplan, D.I., Gilmore, T.J., (2004) Zero-valent iron removal rates of aqueous Cr(VI) measured under flow conditions. Water, Air, and Soil Pollution, 155: 21-33.

Karvonen, A., (2004) Cation Effects on chromium removal in permeable reactive walls. Journal of Environmental Engineering, 130: 863-866.

Kielemos, J., Boever, P.D., Verstraete, W., (2000) Influence of denitrification on the corrosion of iron and stainless steel powder. Environmental Science and Technology, 34: 663-671.

Lee, T., Lim, H., Lee, Y., Park, J., (2003) Use of waste iron metal for removal of Cr(VI) from water. Chemosphere, 53: 479-485.

Liang, L., Sullivan, A.B., West, O.R., Moline, G.R., Kamolpornwijit, W., (2003) Predicting the precipitation of mineral phases in permeable reactive barrier. Environmental Engineering Science, 20: 635-653.

Lo, I.M.C., Lam, C.S.C., Lai, K.J.K. (2006). Hardness and carbonate effects on the reactivity of zero-valent iron for Cr(VI) removal. Water Research, 40: 595-605.

Mackenzie, P.D., Horney, D.P., Sivavec, T.M., (1999). Mineral precipitation and porosity losses in granular iron columns. Journal of Hazardous Materials, 68: 1-17.

Matheson, L.J., Tratnyek, P.G., (1994) Reductive dehalogenation of chlorinated methanes by iron metal. Environmental Science and Technology, 28: 2045-2053.

Mayer, T.D., Jarrell, W.M., (1996) Formation and stability of Iron(III) oxidation products under natural concentrations of dissolved silica. Water Resources, 30: 1208-1214.

Mayne, J.E.O., Pryor, M.J., (1949) The mechanism of inhibition of corrosion of ironby chromic acid and potassium chromate. Journal of Chemical Society, 1831.

McCarty, J.F., McKay, L.D., (2004). Colloid transport in the subsurface: Past, present and future challenges. Vadose Zone Journal, 3: 326-337.

McKenzie, P.D., Sivavec, T.M., Horney, D.P., (1997). Extending hydraulic lifetime of iron wall. In: International Containment Technology Conference Proceedings, Feb 9]12 1997, St. Petersburg, FL, p781-787.

Melitas, N., Chuffe-Moscoso, O., Farrell, J., (2001) Kinetics and soluble chromium removal from contaminated water by zero-valent iron media: Corrosion inhibition and passive oxide effects. Environmental Science and Technology, 35: 3948-3953.

Melitas, N., Farrell, J., (2002) Understanding chromate reaction kinetics with corroding iron media using Tafel analysis and electrochemical impedance spectroscopy. Environmental Science and Technology, 36: 5476-5482.

Morrison, S.J., Metzler, D.R., Dwyer, B.P., (2002). Removal of As, Mn, Mo, Se, U, V and Zn from groundwater by zero-valent iron in a passive treatment cell: reaction progress modeling. Journal of Contaminant Hydrology, 56: 99-116.

Morrison. S.J., Metzler, D.R., Carpenter, C.E., (2001) Uranium Precipitation in a permeable reactive barrier by progressive irreversible dissolution of zerovalent iron. Environmental Science and Technology, 35: 385-390.

Muftikian, R., Fernando, Q., Korte, N., (1995) A method for the rapid dechlorination of low molecular weight chlorinated hydrocarbons in water. Water Research, 29(10): 2434-2439.

National Research Council (NRC) (1994). Alternatives for groundwater cleanup. National Academy Press, Washington, D.C.

Nriagu, J.O., (1998) Production and uses of chromium. Chromium in the Natural and Human Environments. Volume 20 (J.O. Nriagu and E. Nieboers editors). John Wiley & Sons, New York: 81-104.

Palmer, C.D., Wittbrodt, P.R., (1991) Processing affecting the remediation of chromium-contaminated Sites. Environmental Health Perspectives, 92: 25-40.

Palmer, C.D., Puls, R.W., (1994) Natural attenuation of hexavalent chromium in groundwater and soils. EPA Groundwater Issue. EPA/540/5-94/505.

Parker, J. C.; van Genuchten, M. Th. (1984) Virginia Agriculture Experimental Station Bulletin 84-3; 96 pp.

Parsons Engineering Science (1993) RCRA Facility Investigation Work Plan, Rev. 0, October 1993.

Ponder, S.M., Garab, J.G., Mallouk, T.E. (2000). Remediation of Cr(VI) and Pb(II) aqueous solutions using supported, nanoscale zero-valent iron. Environmental Science and Technology, 34: 2564-2569.

Pourbaix, M., (1966) Atlas of Electrochemical Equilibria in Aqueous Solutions. Pergamon Press: Oxford, U.K.

Pourbaix, M., (1973) Lectures on Electrochemical Corrosion, Plenum, New York, p. 202.

Powell, R.M., Puls, R.W., (1993) Presented at Metal Speciation and Contamination of Aquatic Sediments Workshop, Jekyll Island, GA.

Powell, R. M.; Puls, R. W.; Paul, C. J., (1994) Innovative Solutions for Contaminated Site Management; Water Environment Federation: Miami, FL, pp 485-496.

Powell, R.M., Puls, R.W., Hightower, S.K., Sabatini, D.A., (1995) Coupled iron corrosion and chromate reduction: Mechanisms for subsurface remediation. Environmental Science and Technology, 29: 1913-1922.

Powell, R.M., Powell, P.D. (1998) Iron Metal for Subsurface Remediation. The Encyclopedia of Environmental Analysis and Remediation. Robert A. Myers, ed. John Wiley & Sons, Inc., New York. 8:4729-4761.

Powell, R.M., Puls, R. W. (1997) Permeable Reactive Subsurface Barriers for the Interception and Remediation of Chlorinated Hydrocarbon and Chromium (VI) Plumes in Ground Water". U.S. EPA Remedial Technology Fact Sheet. EPA/600/F-97/008.

Puls, Powell, R.M., Paul, C.J., (1995) In situ remediation of ground water contaminated with chromate and chlorinated solvents using zero-valent iron. A field study. In Proc. Div. Environ. Chem., Am. Chem. Soc., Anaheim, CA, April 2-7, 1995.

Puls, R. W., Barcelona, M.J., (1996). Low-Flow (Minimal Drawdown) Ground-Water Sampling Procedures. U.S. EPA Ground Water Issue. EPA/540/S-95/504.

Puls, R.W., Paul, C.J., Powell, R.M., (1999a) The application of in-situ permeable reactive (zero-valent iron) barrier technology for the remediation of chromate-contaminated groundwater. Applied Geochemistry, 14: 989-1000.

Puls, R.W., Blowes, D.W., Gillham, R.W., (1999b) Long-term performance monitoring for a permeable reactive barrier at the U.S. Coast Guard Support Center, Elizabeth City, North Carolina. Journal of Hazardous Materials, 68: 109-124.

Rai, D., Sass, B.M., Moore, D.A., (1987) Chromium(III) hydrolysis constants and solubility of chromium(III) hydroxide. Inorg., 26: 345-349.

Remediation Technologies Development Forum (RTDF). Permeable Reactive Barriers Team. November 6-7, 2002 Meeting Summary. http://www.rtdf.org/public/permbarr/minutes/110702/summary.html

Repta, C.J.W. (2001) Evaluation of nickel-enhanced granular iron for the dechlorination of trichlorethene. M.Sc. thesis, Department of Earth Sciences, University of Waterloo, Waterloo, Ontario.

Robertson, N., (1975) Hexavalent chromium in the Ground Water in Paradise Valley, Arizona. Ground Water, 16: 516-527.

Roh, Y., Lee, S.Y., Elless, M.P., (2000) Characterization of corrosion products in the permeable reactive barriers. Environmental Geology, 40: 184-194.

Sabatini, D.A., Knox, R.C., Tucker, E.E., Puls, R.W., (1997). USEPA Environmental Research Brief, EPA/600/S-97/005.

Sass, B.M., Rai, D., (1987) Solubility of amorphous chromium(III)-iron(III) hydroxide solid solutions. Inorganic Chemistry, 26: 2228-2232.

Schroeder, D.C., Lee, G.F., (1975). Potential transformations of chromium in natural waters. Water, Air, Soil Pollution, 4: 355-365.

Schwertmann, U., Gasser, U., and Sticher, H. (1989) Chromium-for-iron substitution in synthetic goethites. Geochimimica Cosmochimica Acta, 53: 1293-1297.

Sharma, H.D., Reddy, K.R., (2004) Geoenvironmental Engineering: Site Remediation, Waste Containment, and Emerging Waste Management Technologies. Wiley Publishers.

Sivavec, T.M., Mackenzie, P.D., Horney, D.P., (1997). Effect of groundwater on reactivity of bimetallic media: Deactivation of nickel-plated granular iron. ACS National Meeting, American Chemical Society, Division of Environmental Chemistry, Preprints of Extended Abstracts, 37: 83-85.

Stumm, W., Morgan, J.J., (1996) Aquatic Chemistry, 3rd Edition. New York, John Wiley and Sons.

Thomas, J.M., Ward, C.H., (1995). Ground water for bioremediation, New York, NY, Geotechical Special Publication, ASCE, pp. 1456-1466.

Travis, C.C.; Doty, C.B., (1990). Can contaminated aquifers at Superfund sites be remediated ? Environmental Science and Technology, 24: 1464-1466.

USACE, (1997) (U.S. Army Corps of Engineers), Design Guidance for the Application of Permeable Barriers to Remediate Dissolved Chlorinated Solvents. CEMP DG 1110-345-117, U.S. Department of Army, Washington, DC, Feb. 1997b.

U.S. EPA, (1994). Natural Attenuation of Hexavalent Chromium in Groundwater and Soils. EPA Groundwater Issue. U.S. Environmental Protection Agency, Office of Research and Development. EPA/540/5-94/505.

U.S. EPA, (1998). Permeable Reactive Barrier Technologies for Contaminant Remediation. U.S. Environmental Protection Agency, Office of Research and Development. EPA/600/R-98/125.

U.S. EPA, (1999). An In Situ Permeable Reactive Barrier for the Treatment of Hexavalent Chromium and Trichloroethylene in Ground Water: Volume 1 Design and Installation. U.S. Environmental Protection Agency, Office of Research and Development. EPA/600/R-99/095a.

U.S. EPA, (2000a). Field Demonstration of Permeable Reactive Barriers to Remove Dissolved Uranium From Groundwater, Fry Canyon, Utah. U.S. Environmental Protection Agency, 402-C-00-001.

U.S. EPA, (2000b). In situ treatment of soil and groundwater contaminated with Chromium, Technical Resource Guide. U.S. Environmental Protection Agency, EPA/625/R-00/005.

Vidic, R. D. (2001) Permeable reactive barriers: case study review." GWRTAC E-Series Technology Evaluation Report TE-01-01, Ground-Water Remediation Technologies Analysis Center, Pittsburgh, PA.

Weisener, C.G., Scott Sale, K., Smyth, D.J.A., Blowes, D.W., (2005) Field column study using zero-valent iron for mercury removal from contaminated groundwater. Environmental Science and Technology, 39: 6306-6312.

Wilkin, R.T., Ludwig, R.D., Ford, R.G., eds, Proceedings of the Workshop on Monitoring Oxidation-Reduction Processes for Ground-water Restoration, Dallas, Texas, April 25-27. 2000: Cincinnati. OH. U.S. Environmental Protection Agency. EPA/600/R-02/002. p. 43-47.

Wilkin, R.T., Su, C., Ford, R.G., Paul, C.J., (2005) Chromium-Removal Processes during Groundwater Remediation by a Zerovalent Iron Permeable Reactive Wall. Environmental Science and Technology, 39: 4599-4605.

Williams, A.G.B., Scherer, M.M., (2001) Kinetics of Cr(VI) reduction by Carbonate Green Rust. Environmental Science and Technology, 35: 3488-3494.

Wittbrodt, P.R., Palmer, C.D., (1994). Reduction of Cr(VI) by soil humic acids. European Journal of Soil Science, 48: 151-162.

Wüst, W.F., Köber, R., Schlicker, O., Dahmke, A., (1999) Combined zero- and first-order kinetic model of the degradation of TCE and cis-DCE with commercial iron. Environmental Science and Technology, 33: 4304-4309.

Zhang, Y., Gillham, R.W., (2005) Effects of Gas Generation and Precipitates on Performance of $Fe^o$ PRBs. Ground Water, 43(1): 113-121.

**APPENDIX**

**REACTIVE COLUMN DATA**

Table A.1. 50 IR Reactive Column Data, Flux 1=0.07 ml/cm$^2$.min

| Date | Time | PV | pH | Cr(VI) (mg/l) | C/Co | Flow (ml/min) | Flux (cm/min) | % Change in Flux | v (m/year) | v (cm/day) | Eh (mV) | Total Cr (mg/l) | Cr(III) (mg/l) |
|------|------|-----|------|------|------|------|------|------|------|------|------|------|------|
| 30-Mar | 10.3 | | 7.42 | 0 | 0 | | | | | | | 0.000 | 0.000 |
| 30-Mar | 10.45 | | 8.03 | 0 | 0 | | | | | | | 0.000 | 0.000 |
| 30-Mar | 11 | | 8.08 | 0 | 0 | | | | | | | 0.000 | 0.000 |
| 30-Mar | 11.15 | | 8.09 | 0 | 0 | | | | | | | 0.000 | 0.000 |
| 30-Mar | 11.3 | | 7.95 | 0 | 0 | | | | | | | 0.000 | 0.000 |
| 30-Mar | 11.45 | | 7.81 | 0 | 0 | | | | | | | 0.000 | 0.000 |
| 30-Mar | 12.15 | | 7.85 | 0 | 0 | | | | | | | 0.000 | 0.000 |
| 30-Mar | 12.3 | | 8.04 | 0 | 0 | | | | | | | 0.000 | 0.000 |
| 30-Mar | 12.45 | 1 | 7.67 | 0 | 0 | 0.44 | 0.06 | 11.91 | 521.40 | 142.85 | | 0.000 | 0.000 |
| 30-Mar | 13.45 | | 7.74 | 0 | 0 | | | | | | | 0.000 | 0.000 |
| 30-Mar | 14 | | 7.68 | 0 | 0 | | | | | | | 0.000 | 0.000 |
| 30-Mar | 14.3 | | 7.79 | 0 | 0 | | | | | | | 0.000 | 0.000 |
| 30-Mar | 14.45 | | 7.95 | 0 | 0 | | | | | | | 0.000 | 0.000 |
| 30-Mar | 15.15 | | 7.79 | 0 | 0 | | | | | | | 0.000 | 0.000 |
| 30-Mar | 15.3 | | 7.88 | 0 | 0 | | | | | | | 0.000 | 0.000 |
| 30-Mar | 17 | | 8.07 | 0 | 0 | | | | | | | 0.000 | 0.000 |
| 30-Mar | 17.15 | 2 | 8.1 | 0 | 0 | 0.44 | 0.06 | 12.50 | 517.91 | 141.89 | | 0.000 | 0.000 |
| 30-Mar | 17.45 | | 8 | 0 | 0 | | | | | | | 0.000 | 0.000 |
| 30-Mar | 20.15 | 3 | 8.61 | 0 | 0 | 0.42 | 0.06 | 16.67 | 493.25 | 135.14 | | 0.000 | 0.000 |
| 31-Mar | 14.15 | | 8.11 | 0 | 0 | | | | | | | 0.000 | 0.000 |
| 31-Mar | 15 | | 8.84 | 0 | 0 | | | | | | | 0.000 | 0.000 |
| 31-Mar | 16.3 | 4 | 8.63 | 0 | 0 | 0.43 | 0.06 | 14.61 | 505.44 | 138.48 | | 0.000 | 0.000 |
| 31-Mar | 17 | | 8.88 | 0 | 0 | | | | | | | 0.000 | 0.000 |

Table A.1. 50 IR Reactive Column Data, Flux 1=0.07 ml/cm$^2$.min (Continued)

| Date | Time | PV | pH | Cr(VI) (mg/l) | C/Co | Flow (ml/min) | Flux (cm/min) | % Change in Flux | v (m/year) | v (cm/day) | Eh (mV) | Total Cr (mg/l) | Cr(III) (mg/l) |
|------|------|------|-------|------|------|------|------|------|--------|--------|-------|-------|-------|
| 4-Apr | 13 | | 9.14 | 0 | 0 | | | | | | | 0.000 | 0.000 |
| 4-Apr | 14 | 6 | 9.42 | 0 | 0 | | | | | | | 0.000 | 0.000 |
| 4-Apr | 17 | 7 | 9.84 | 0 | 0 | | | | | | | 0.000 | 0.000 |
| 5-Apr | 13 | | 9.86 | 0 | 0 | | | | | | | 0.000 | 0.000 |
| 5-Apr | 14 | | 9.91 | 0 | 0 | | | | | | | 0.000 | 0.000 |
| 5-Apr | 15 | | 9.88 | 0 | 0 | | | | | | | 0.000 | 0.000 |
| 5-Apr | 16 | 9 | 9.75 | 0 | 0 | | | | | | | 0.000 | 0.000 |
| 5-Apr | 17 | | 9.51 | 0 | 0 | | | | | | | 0.000 | 0.000 |
| 5-Apr | 18 | | 9.78 | 0 | 0 | | | | | | | 0.000 | 0.000 |
| 5-Apr | 18.3 | 10 | 9.56 | 0 | 0 | | | | | | | 0.000 | 0.000 |
| 6-Apr | 12 | | 9.81 | 0 | 0 | | | | | | | 0.000 | 0.000 |
| 6-Apr | 14 | 11 | 9.79 | 0 | 0 | | | | | | | 0.000 | 0.000 |
| 6-Apr | 15 | | 9.85 | 0 | 0 | | | | | | | 0.000 | 0.000 |
| 6-Apr | 16.3 | 12 | 9.81 | 0 | 0 | | | | | | | 0.000 | 0.000 |
| 6-Apr | 17 | | 9.77 | 0 | 0 | | | | | | | 0.000 | 0.000 |
| 6-Apr | | 13 | 9.79 | 0 | 0 | | | | | | | 0.000 | 0.000 |
| 7-Apr | | 14 | 9.62 | 0 | 0 | | | | | | | 0.000 | 0.000 |
| 7-Apr | | 15 | 9.77 | 0 | 0 | | | | | | | 0.000 | 0.000 |
| 7-Apr | | 16 | 9.84 | 0 | 0 | | | | | | | 0.000 | 0.000 |
| 8-Apr | | 16.6 | 10.09 | 0 | 0 | | | | | | | 0.000 | 0.000 |
| 28-Apr | | 23.8 | 9.23 | 0 | 0 | 0.42 | 0.06 | 16.88 | 491.96 | 134.78 | | 0.000 | 0.000 |
| 28-Apr | | 24.8 | 8.86 | 0 | 0 | 0.42 | 0.06 | 16.67 | 493.25 | 135.14 | | 0.000 | 0.000 |
| 28-Apr | | 25 | 8.78 | 0 | 0 | | | | | 0.00 | | 0.000 | 0.000 |
| 29-Apr | | 32.2 | 8.7 | 0 | 0 | 0.43 | 0.06 | 14.75 | 504.58 | 138.24 | | 0.000 | 0.000 |
| 29-Apr | | 33 | 8.69 | 0 | 0 | 0.43 | 0.06 | 14.27 | 507.45 | 139.03 | | 0.000 | 0.000 |
| 29-Apr | | 34 | 8.92 | 0 | 0 | 0.40 | 0.06 | 19.33 | 477.46 | 130.81 | | 0.000 | 0.000 |
| 29-Apr | | 36 | 9.09 | 0 | 0 | 0.40 | 0.06 | 19.55 | 476.20 | 130.47 | 394.4 | 0.000 | 0.000 |
| 2-May | | 42.5 | 8.84 | 0 | 0 | 0.45 | 0.06 | 9.42 | 536.11 | 146.88 | 467.7 | 0.000 | 0.000 |
| 2-May | | 45 | 8.84 | 0 | 0 | | | | | | 456.5 | 0.000 | 0.000 |
| 3-May | | 55 | 8.61 | 0 | 0 | | | | | | 386.2 | 0.000 | 0.000 |
| 4-May | | 65 | 8.57 | 0 | 0 | | | | | | 400 | 0.000 | 0.000 |

Table A.1. 50 IR Reactive Column Data, Flux 1=0.07 ml/cm$^2$.min (Continued)

| Date | Time | PV | pH | Cr(VI) (mg/l) | C/Co | Flow (ml/min) | Flux (cm/min) | % Change in Flux | v (m/year) | v (cm/day) | Eh (mV) | Total Cr (mg/l) | Cr(III) (mg/l) |
|------|------|-----|------|------|--------|------|------|--------|--------|--------|-------|--------|--------|
| 4-May | | 65 | 8.57 | 0 | 0 | | | | | | 400 | 0.000 | 0.000 |
| 4-May | | 66 | 8.71 | 0 | 0 | | | | | | 380.2 | 0.000 | 0.000 |
| 6-May | | 68.3 | 8.69 | 0 | 0 | 0.48 | 0.07 | 4.10 | 567.65 | 155.52 | 365.3 | 0.000 | 0.000 |
| 6-May | | 69.4 | 7.73 | 0 | 0 | 0.56 | 0.08 | -11.11 | 657.66 | 180.18 | 406.8 | 0.000 | 0.000 |
| 7-May | | 70.4 | 7.82 | 0 | 0 | | | | | | 422.1 | 0.000 | 0.000 |
| 7-May | | 81.2 | | 0 | 0 | 0.50 | 0.07 | 0.00 | 591.90 | 162.16 | | 0.000 | 0.000 |
| 9-May | | 82.2 | 8.57 | 0 | 0 | 0.50 | 0.07 | -0.69 | 596.00 | 163.29 | 474.7 | 0.000 | 0.000 |
| 9-May | | 82.57 | 7.57 | 0 | 0 | 0.51 | 0.07 | -1.76 | 602.30 | 165.01 | 408.9 | 0.000 | 0.000 |
| 10-May | | 91.4 | 7.77 | 0 | 0 | 0.49 | 0.07 | 1.84 | 581.00 | 159.18 | 385.7 | 0.000 | 0.000 |
| 10-May | | 92.91 | | 0 | 0 | 0.49 | 0.07 | 1.97 | 580.26 | 158.98 | | 0.000 | 0.000 |
| 10-May | | 93.85 | 8.12 | 0 | 0 | 0.50 | 0.07 | -0.69 | 596.00 | 163.29 | 403.1 | 0.000 | 0.000 |
| 12-May | | 113.85 | 8.39 | 0.18 | 0.009 | 0.50 | 0.07 | 0.37 | 589.72 | 161.57 | | 2.225 | 2.045 |
| 12-May | | 114.85 | 8.61 | 0.5 | 0.025 | | | | | | 398 | 6.395 | 5.895 |
| 12-May | | 116 | 8.54 | 0.5 | 0.025 | | | | | | 414.2 | 6.580 | 6.080 |
| 13-May | | 117 | 8.66 | 0 | 0 | 0.48 | 0.07 | 3.03 | 573.96 | 157.25 | 380 | 0.670 | 0.670 |
| 13-May | | 118 | 8.83 | 0 | 0 | 0.50 | 0.07 | 0.32 | 590.00 | 161.64 | 331.7 | 1.480 | 1.480 |
| 17-May | | 119 | 8.28 | 0 | 0 | 0.50 | 0.07 | -0.17 | 592.88 | 162.43 | 383.6 | 0.585 | 0.585 |
| 17-May | | 120 | 8.39 | 0 | 0 | 0.50 | 0.07 | -0.02 | 592.00 | 162.19 | 374.6 | 0.000 | 0.000 |
| 18-May | | 127.23 | 8.67 | 0.4 | 0.02 | 0.44 | 0.06 | 11.43 | 524.25 | 143.63 | 171 | 4.150 | 3.750 |
| 18-May | | 128.23 | 8.57 | 0.5 | 0.025 | 0.51 | 0.07 | -1.26 | 599.35 | 164.21 | 184.7 | 8.850 | 8.350 |
| 18-May | | 129.44 | | 1 | 0.05 | | | | | | | 0.000 | -1.000 |
| 18-May | | 130 | 8.2 | 0.5 | 0.025 | | | | | | 281.9 | 0.000 | -0.500 |
| 19-May | | 139.3 | 8.15 | 1.25 | 0.0625 | 0.50 | 0.07 | 0.66 | 587.98 | 161.09 | 300.2 | 13.600 | 12.350 |
| 20-May | | 149.8 | 8.43 | 3 | 0.15 | 0.50 | 0.07 | -0.86 | 596.96 | 163.55 | 189.9 | 20.815 | 17.815 |
| 22-May | | 172 | 8 | 5 | 0.25 | 0.50 | 0.07 | 0.00 | 591.89 | 162.16 | 284 | 7.020 | 2.020 |
| 24-May | | 193.62 | 8.05 | 8 | 0.4 | 0.50 | 0.07 | 0.90 | 586.57 | 160.70 | 263.3 | 9.323 | 1.323 |
| 25-May | | 205 | | 10 | 0.5 | 0.48 | 0.07 | 3.03 | 573.96 | 157.25 | | 11.835 | 1.835 |
| 25-May | | 206 | | | | 0.49 | 0.07 | 1.43 | 583.42 | 159.84 | | 11.245 | |
| 27-May | | 225.9 | 7.95 | 11 | 0.55 | 0.50 | 0.07 | -0.83 | 596.79 | 163.50 | | 12.405 | 1.405 |

Table A.1. 50 IR Reactive Column Data, Flux 1=0.07 ml/cm$^2$.min (Continued)

| Date | Time | PV | pH | Cr(VI) (mg/l) | C/Co | Flow (ml/min) | Flux (cm/min) | % Change in Flux | v (m/year) | v (cm/day) | Eh (mV) | Total Cr (mg/l) | Cr(III) (mg/l) |
|---|---|---|---|---|---|---|---|---|---|---|---|---|---|
| 30-May | | 259.5 | 7.99 | 12 | 0.6 | 0.46 | 0.06 | 8.26 | 543.00 | 148.77 | 400.1 | 14.110 | 2.110 |
| 31-May | | 269.6 | 7.85 | 13 | 0.65 | 0.44 | 0.06 | 12.22 | 519.56 | 142.35 | 405 | 15.065 | 2.065 |
| 1-Jun | | 278.15 | 7.97 | 13 | 0.65 | 0.49 | 0.07 | 1.79 | 581.33 | 159.27 | 424.6 | 15.818 | 2.818 |
| 3-Jun | | 299.2 | 8.08 | 15 | 0.75 | 0.50 | 0.07 | 0.59 | 588.42 | 161.21 | 236.6 | 16.960 | 1.960 |
| 6-Jun | | 332.7 | 8.01 | 16 | 0.8 | 0.49 | 0.07 | 1.93 | 580.45 | 159.03 | 341.6 | 17.583 | 1.583 |
| 7-Jun | | 345.57 | 7.99 | 16 | 0.8 | 0.50 | 0.07 | 0.40 | 589.53 | 161.52 | 409.1 | 17.433 | 1.433 |
| 10-Jun | | 374.37 | 8.01 | 16 | 0.8 | 0.46 | 0.06 | 8.39 | 542.22 | 148.55 | 422.22 | 16.975 | 0.975 |
| 13-Jun | | 409.83 | 7.88 | 16 | 0.8 | 0.50 | 0.07 | -0.22 | 593.20 | 162.52 | 403.8 | 18.460 | 2.460 |
| 14-Jun | | 420.25 | 7.92 | 16 | 0.8 | 0.50 | 0.07 | 0.74 | 587.51 | 160.96 | 358.8 | 18.190 | 2.190 |
| 16-Jun | | 441.25 | 7.92 | 18 | 0.9 | | | | | | 415.2 | 18.455 | 0.455 |
| 17-Jun | | 453 | 7.92 | 18 | 0.9 | | | | | | | 18.608 | 0.608 |

Table A.2. 50 IR Reactive Column Data, Flux 2=0.127 ml/cm$^2$.min

| Date | PV | pH | Cr(VI) (mg/l) | C/Co | Flow (ml/min) | Flux (cm/min) | % Change in Flux | v(m/year) | v(cm/day) | Eh | Total Cr | Cr(III) (mg/l) |
|---|---|---|---|---|---|---|---|---|---|---|---|---|
| 20-Jul | 12.5 | 7.73 | 0 | 0 | 0.86 | 0.12 | 4.10 | 1021.77 | 279.94 | 360.9 | 0 | 0 |
| 21-Jul | 33.65 | 7.87 | 0 | 0 | 0.83 | 0.12 | 7.36 | 987.00 | 270.40 | 247.3 | 0 | 0 |
| 22-Jul | 50.76 | 8.23 | 0 | 0 | 0.84 | 0.12 | 6.46 | 996.54 | 273.00 | 278.5 | 0 | 0 |
| 23-Jul | 76 | 8.16 | 0 | 0 | 0.87 | 0.12 | 3.51 | 1028.07 | 281.66 | 201.3 | 0 | 0 |
| 27-Jul | 95.75 | 8.45 | 0 | 0 | 0.81 | 0.11 | 10.00 | 958.87 | 262.66 | 283.5 | 0 | 0 |
| 28-Jul | 114.05 | 8.52 | 0 | 0 | 0.86 | 0.12 | 4.10 | 1021.76 | 279.90 | 305.3 | 0 | 0 |
| 29-Jul | 131.34 | 8.51 | 0 | 0 | 0.86 | 0.12 | 4.99 | 1012.30 | 277.34 | 312 | 0 | 0 |
| 30-Jul | 156 | 8.5 | 0 | 0 | 0.86 | 0.12 | 4.10 | 1021.76 | 279.93 | 350.7 | 0 | 0 |
| 31-Jul | 172.25 | 8.35 | 0.75 | 0.04 | 0.86 | 0.12 | 4.39 | 1018.60 | 279.00 | 328.9 | 1.388 | 0.638 |
| 1-Aug | 190.15 | 8.29 | 3.75 | 0.19 | | | | | | 271.3 | 5.38 | 1.63 |
| 2-Aug | 211.75 | 8.01 | 5.25 | 0.26 | 0.86 | 0.12 | 4.66 | 1015.72 | 278.28 | 281.8 | 5.645 | 0.395 |
| 3-Aug | 228.85 | 8.07 | 7 | 0.35 | 0.84 | 0.12 | 6.42 | 997.00 | 273.17 | 344.7 | 9.035 | 2.035 |
| 4-Aug | 249.65 | 8.01 | 8 | 0.4 | 0.86 | 0.12 | 4.80 | 1014.25 | 277.88 | 302.4 | 9.76 | 1.76 |
| 5-Aug | 266.3 | 7.89 | 9 | 0.45 | 0.87 | 0.12 | 3.11 | 1032.32 | 282.88 | 298.3 | 16.785 | 7.785 |
| 7-Aug | 305.6 | 7.66 | 10 | 0.5 | 0.86 | 0.12 | 4.58 | 1016.63 | 278.53 | 371.6 | 14.2525 | 4.2525 |
| 9-Aug | 339.8 | 7.67 | 13 | 0.65 | 0.81 | 0.12 | 9.57 | 963.50 | 263.97 | 372.4 | 13.625 | 0.625 |
| 11-Aug | 377.75 | 7.7 | 12 | 0.6 | 0.80 | 0.11 | 11.19 | 946.24 | 259.24 | 301.5 | 13.9675 | 1.9675 |
| 13-Aug | 394.07 | 7.71 | 14 | 0.7 | 0.78 | 0.11 | 13.21 | 924.72 | 253.35 | 382.8 | | -14 |
| 15-Aug | 446.55 | 7.35 | 14 | 0.7 | 0.79 | 0.11 | 12.52 | 932.00 | 255.35 | 331.7 | 12.815 | -1.185 |
| 16-Aug | 465.05 | 7.62 | 13 | 0.65 | 0.75 | 0.11 | 17.05 | 883.76 | 242.13 | 347.3 | 14.5925 | 1.5925 |
| 17-Aug | 481.05 | 7.79 | 14 | 0.7 | 0.72 | 0.10 | 19.46 | 858.10 | 235.10 | 347 | 15.395 | 1.395 |

Table A.3. 50 IR Reactive Column Data, Flux 3=0.17 ml/cm$^2$.min

| Date | PV | pH | Cr(VI)(mg/l) | C/Co | v(m/year) | v(cm/day) | Eh | Total Cr | Cr(III) |
|---|---|---|---|---|---|---|---|---|---|
| 11/12/2005 | 22.28 | 9.12 | 2 | 0.10 | | | 366.1 | 2.24 | 0.24 |
| 11/12/2005 | 32.68 | 8.08 | 12 | 0.57 | | | 371.2 | 15.0875 | 3.0875 |
| 11/13/2005 | 48 | 8.11 | 15 | 0.71 | | | 376.4 | 14.72 | -0.28 |
| 11/13/2005 | 51.44 | 8.1 | 19 | 0.90 | | | 373 | 17.0825 | -1.9175 |
| 11/13/2005 | 58.67 | 7.99 | 16 | 0.76 | | | 392.3 | 18.1125 | 2.1125 |
| 11/14/2005 | 75.67 | 7.93 | 21 | 1.00 | | | 384.2 | 18.9375 | -2.0625 |
| 11/15/2005 | 100.77 | 7.76 | 21 | 1.00 | | | 378.4 | 20.64 | -0.36 |
| 11/16/2005 | 129.93 | 7.84 | 18 | 0.86 | | | 370.5 | 19.8475 | 1.8475 |
| 11/17/2005 | 151.63 | 7.88 | 21 | 1.00 | | | 356.63 | 20.11 | -0.89 |

Table A. 4. 25 IR Reactive Column Data, Flux 1=0.07 ml/cm$^2$.min

| Date | PV | pH | Cr(VI) (mg/l) | C/Co | Flow (ml/min) | Flux (cm/min) | % Change in Flux | v(m/year) | v(cm/day) | Eh | Total Cr | Cr(III) (mg/l) |
|---|---|---|---|---|---|---|---|---|---|---|---|---|
| 20-Jul | 12.5 | 7.73 | 0 | 0 | 0.86 | 0.12 | 4.10 | 1021.77 | 279.94 | 360.9 | 0 | 0 |
| 21-Jul | 33.65 | 7.87 | 0 | 0 | 0.83 | 0.12 | 7.36 | 987.00 | 270.40 | 247.3 | 0 | 0 |
| 22-Jul | 50.76 | 8.23 | 0 | 0 | 0.84 | 0.12 | 6.46 | 996.54 | 273.00 | 278.5 | 0 | 0 |
| 23-Jul | 76 | 8.16 | 0 | 0 | 0.87 | 0.12 | 3.51 | 1028.07 | 281.66 | 201.3 | 0 | 0 |
| 27-Jul | 95.75 | 8.45 | 0 | 0 | 0.81 | 0.11 | 10.00 | 958.87 | 262.66 | 283.5 | 0 | 0 |
| 28-Jul | 114.05 | 8.52 | 0 | 0 | 0.86 | 0.12 | 4.10 | 1021.76 | 279.90 | 305.3 | 0 | 0 |
| 29-Jul | 131.34 | 8.51 | 0 | 0 | 0.86 | 0.12 | 4.99 | 1012.30 | 277.34 | 312 | 0 | 0 |
| 30-Jul | 156 | 8.5 | 0 | 0 | 0.86 | 0.12 | 4.10 | 1021.76 | 279.93 | 350.7 | 0 | 0 |
| 31-Jul | 172.25 | 8.35 | 0.75 | 0.04 | 0.86 | 0.12 | 4.39 | 1018.60 | 279.00 | 328.9 | 1.388 | 0.638 |
| 1-Aug | 190.15 | 8.29 | 3.75 | 0.19 | | | | | | 271.3 | 5.38 | 1.63 |
| 2-Aug | 211.75 | 8.01 | 5.25 | 0.26 | 0.86 | 0.12 | 4.66 | 1015.72 | 278.28 | 281.8 | 5.645 | 0.395 |
| 3-Aug | 228.85 | 8.07 | 7 | 0.35 | 0.84 | 0.12 | 6.42 | 997.00 | 273.17 | 344.7 | 9.035 | 2.035 |
| 4-Aug | 249.65 | 8.01 | 8 | 0.4 | 0.86 | 0.12 | 4.80 | 1014.25 | 277.88 | 302.4 | 9.76 | 1.76 |
| 5-Aug | 266.3 | 7.89 | 9 | 0.45 | 0.87 | 0.12 | 3.11 | 1032.32 | 282.83 | 298.3 | 16.785 | 7.785 |
| 7-Aug | 305.6 | 7.66 | 10 | 0.5 | 0.86 | 0.12 | 4.58 | 1016.63 | 278.53 | 371.6 | 14.2525 | 4.2525 |
| 9-Aug | 339.8 | 7.67 | 13 | 0.65 | 0.81 | 0.12 | 9.57 | 963.50 | 263.97 | 372.4 | 13.625 | 0.625 |
| 11-Aug | 377.75 | 7.7 | 12 | 0.6 | 0.80 | 0.11 | 11.19 | 946.24 | 259.24 | 301.5 | 13.9675 | 1.9675 |
| 13-Aug | 394.07 | 7.71 | 14 | 0.7 | 0.78 | 0.11 | 13.21 | 924.72 | 253.35 | 382.8 | | -14 |
| 15-Aug | 446.55 | 7.35 | 14 | 0.7 | 0.79 | 0.11 | 12.52 | 932.00 | 255.35 | 331.7 | 12.815 | -1.185 |
| 16-Aug | 465.05 | 7.62 | 13 | 0.65 | 0.75 | 0.11 | 17.05 | 883.76 | 242.13 | 347.3 | 14.5925 | 1.5925 |
| 17-Aug | 481.05 | 7.79 | 14 | 0.7 | 0.72 | 0.10 | 19.46 | 858.10 | 235.10 | 347 | 15.395 | 1.395 |

Table A. 5. 25 IR Reactive Column Data, Flux 2=0.127 ml/cm$^2$.min

| Date | PV | pH | Cr(VI) (mg/l) | C/Co | Flow (ml/min) | Flux (cm/min) | % Change in Flux | v (m/year) | v (cm/day) | Eh (mV) | Total Cr(mg/l) | Cr(III) (mg/l) |
|---|---|---|---|---|---|---|---|---|---|---|---|---|
| 27-Jul | 5.77 | 8.21 | 0 | 0 | 0.89 | 0.13 | 0.71 | 1267.75 | 347.32 | 342.9 | 0 | 0.00 |
| 28-Jul | 27.56 | 8.54 | 0 | 0 | 0.87 | 0.12 | 3.44 | 1233.00 | 337.82 | 346 | 0 | 0.00 |
| 29-Jul | 47.86 | 8.44 | 4 | 0.2 | 0.84 | 0.12 | 6.89 | 1188.90 | 325.73 | 353 | 9.815 | 5.82 |
| 30-Jul | 75.26 | 8.24 | 10 | 0.5 | 0.80 | 0.11 | 11.09 | 1135.29 | 311.00 | 363.2 | | |
| 31-Jul | 94.8 | 8.25 | 13 | 0.65 | 0.86 | 0.12 | 3.93 | 1226.75 | 336.00 | 398.8 | 11.8925 | -1.11 |
| 1-Aug | 112.7 | 8 | 15 | 0.75 | | 0.00 | | | | 384.1 | | |
| 2-Aug | 138.6 | 7.94 | 15 | 0.75 | 0.86 | 0.12 | 4.66 | 1217.32 | 333.51 | 367.6 | 14.645 | -0.36 |
| 3-Aug | 160.2 | 7.92 | 16 | 0.8 | 0.89 | 0.13 | 1.31 | 1260.14 | 345.24 | 381.3 | 15.225 | -0.78 |
| 4-Aug | 186.1 | 7.92 | 17 | 0.85 | 0.89 | 0.13 | 1.25 | 1260.90 | 345.45 | 343.5 | 16.465 | -0.54 |
| 5-Aug | 205.3 | 7.97 | 16 | 0.8 | 0.84 | 0.12 | 6.73 | 1190.96 | 326.29 | 368.8 | 10.4075 | -5.59 |
| 7-Aug | 253.7 | 7.64 | 17 | 0.85 | 0.88 | 0.12 | 1.94 | 1252.12 | 343.05 | 372.4 | 15.615 | -1.39 |
| 9-Aug | 297.6 | 7.7 | 18 | 0.9 | 0.87 | 0.12 | 2.99 | 1238.71 | 339.37 | 209.6 | 17.2075 | -0.79 |
| 11-Aug | 346.4 | 7.66 | 17 | 0.85 | 0.88 | 0.12 | 2.67 | 1242.77 | 340.48 | 286.9 | 17.6875 | 0.69 |
| 13-Aug | 394.07 | 7.72 | 19 | 0.95 | 0.86 | 0.12 | 4.23 | 1222.89 | 335.04 | 389.4 | 16.3925 | -2.61 |

Table A. 6. 25 IR Reactive Column Data, Flux 3=0.057 ml/cm$^2$.min

| Date | PV | pH | Cr(VI) (mg/l) | C/Co | Flow (ml/min) | Flux (cm/min) | % Change in Flux | v (m/year) | v (cm/day) | Eh (mV) | Total Cr (mg/L) | Cr(III) (mg/l) |
|---|---|---|---|---|---|---|---|---|---|---|---|---|
| 1-Oct | 7 | 8.64 | 0 | 0 | | | | | | 429.8 | 0 | 0 |
| 3-Oct | 22.4 | 8.35 | 0 | 0 | 0.28 | 0.04 | 29.05 | 402.62 | 110.31 | 426.4 | 0 | 0 |
| 4-Oct | 32.08 | 8.24 | 0.625 | 0.03125 | 0.30 | 0.04 | 26.09 | 419.42 | 114.91 | 400 | 0.815 | 0.19 |
| 5-Oct | 39.18 | 8.18 | 2.5 | 0.125 | 0.32 | 0.04 | 20.50 | 451.15 | 123.60 | 356.1 | 3.24 | 0.74 |
| 6-Oct | 46.44 | 8.14 | 3 | 0.15 | | | | | 0.00 | 380.8 | 4.935 | 1.935 |
| 7-Oct | 52.24 | 8.12 | 4 | 0.2 | | | | | 0.00 | 404.3 | 5.3925 | 1.3925 |
| 8-Oct | 62.76 | | 6 | 0.3 | 0.34 | 0.05 | 14.45 | 485.52 | 133.02 | 379.5 | | |
| 10-Oct | 79.61 | 8.18 | 6 | 0.3 | 0.33 | 0.05 | 16.30 | 475 | 130.14 | 392.9 | | |
| 11-Oct | 90.5 | 8.08 | 8.5 | 0.425 | 0.38 | 0.05 | 5.02 | 539 | 147.67 | 368.8 | 9.975 | 1.475 |
| 12-Oct | 102.04 | 8.06 | 11.5 | 0.575 | 0.38 | 0.05 | 4.44 | 542.3 | 148.58 | 385.2 | 12.09 | 0.59 |
| 14-Oct | 121.94 | 8.1 | 11 | 0.55 | | | | | | 379.2 | 12.955 | 1.955 |
| 16-Oct | 142.89 | 8.09 | 13 | 0.65 | | | | | | 407.7 | 14.543 | 1.5425 |
| 18-Oct | 163.3 | 8.02 | 13 | 0.65 | | | | | | 408.1 | 13.583 | 0.5825 |
| 20-Oct | 182.76 | 8.12 | 13 | 0.65 | | | | | | 414.2 | 14.313 | 1.3125 |
| 21-Oct | 194.02 | 8.11 | 15 | 0.75 | | | | | | 405.7 | 14.808 | -0.1925 |
| 29-Oct | 375.68 | 7.85 | 15 | 0.75 | | | | | | 439.9 | 15.888 | 0.8875 |
| 1-Nov | 396.54 | 7.87 | 18 | 0.9 | | | | | | 400.3 | 16.163 | -1.8375 |

Table A.7. 10 IR Reactive Column Data, Flux 1=0.07 ml/cm$^2$.min

| Date | PV | pH | Cr(VI) (mg/l) | C/Co | Flow (ml/min) | Flux (cm/min) | % Change in Flux | v (m/year) | v (cm/day) | Eh (mV) | Total Cr (mg/l) | Cr(III) (mg/l) |
|------|-----|------|------|------|------|------|------|--------|--------|-------|--------|---------|
| 22-Jun | 15.26 | 7.94 | 0 | 0 | 0.47 | 0.07 | 5.99 | 719.02 | 196.99 | 430.5 | 0.000 | 0 |
| 23-Jun | 27.81 | 8.11 | 0 | 0 | | | | | | 389.3 | 0.000 | 0 |
| 24-Jun | 41.9 | 8.06 | 2 | 0.1 | | | | | | 413.8 | 2.958 | 0.9575 |
| 26-Jun | 70 | 7.94 | 9 | 0.45 | 0.47 | 0.07 | 6.82 | 712.71 | 195.26 | 326.5 | 13.173 | 4.1725 |
| 28-Jun | 95.1 | 7.86 | 16 | 0.8 | 0.46 | 0.07 | 7.64 | 706.4 | 193.5 | 321.3 | 18.488 | 2.4875 |
| 1-Jul | 135.46 | | 18 | 0.9 | 0.47 | 0.07 | 6.82 | 712.7 | 195.26 | | 17.573 | -0.4275 |
| 3-Jul | 163.76 | 7.93 | 19 | 0.95 | 0.47 | 0.07 | 5.99 | 719 | 196.99 | 384.4 | 19.755 | 0.755 |
| 6-Jul | 203.76 | | 19 | 0.95 | | | | | | 397.7 | 18.540 | -0.46 |
| 8-Jul | 229.46 | | 19 | 0.95 | | | | | | 440.2 | 20.243 | 1.2425 |
| 13-Jul | 245.32 | 7.63 | 17 | 0.85 | | | | | | 423 | 14.560 | -2.44 |
| 15-Jul | 272.23 | 7.49 | 20 | 1 | | | | | | 361.3 | 20.670 | 0.67 |

Table A.8. 10 IR Reactive Column Data, Flux 2=0.127 ml/cm$^2$.min

| Date | PV | pH | Cr(VI) (mg/l) | C/Co | Flow (ml/min) | Flux (cm/min) | % Change in Flux | v (m/year) | v (cm/day) | Eh (mV) | Total Cr (mg/l) | Cr(III) (mg/l) |
|------|-----|------|------|------|------|------|------|--------|--------|-------|--------|---------|
| 26-Aug | 23.8 | 8.41 | 1 | 0.05 | 0.86 | 0.12166 | 4.44 | 1308.8 | 358.6 | 428 | 1.104 | 0.104 |
| 27-Aug | 57.1 | 8.19 | 15 | 0.75 | 0.8 | 0.11318 | 11.11 | 1214.4 | 332.7 | 388.7 | 14.1175 | -0.8825 |
| 28-Aug | 81.6 | 8.01 | 17 | 0.85 | 0.84 | 0.11884 | 6.67 | 1284.4 | 351.9 | 444.9 | 18.69 | 1.69 |
| 29-Aug | 104.1 | 8.1 | 17 | 0.85 | 0.89 | 0.12591 | 1.11 | 1361.4 | 373 | 385.6 | 18.61 | 1.61 |
| 30-Aug | 122.4 | 8.16 | 19 | 0.95 | 0.787 | 0.11134 | 12.56 | 1203.12 | 329.62 | 384.4 | 19.2875 | 0.2875 |
| 31-Aug | 147.7 | 8.06 | 20 | 1 | 0.76 | 0.10752 | 15.56 | 1162.48 | 318.49 | 388.9 | 21.13 | 1.13 |
| 1-Sep | 167.4 | 8.04 | 19.5 | 0.975 | 0.75 | 0.1061 | 16.67 | 1153.14 | 315.93 | 376.3 | 19.455 | -0.045 |

Table A. 9. 10 IR Reactive Column Data, Flux 3=0.057 ml/cm$^2$.min

| Date | PV | pH | Cr(VI) (mg/l) | C/Co | Flow (ml/min) | Flux (cm/min) | % Change in Flux | v (m/year) | v (cm/day) | Eh (mV) | Total Cr (mg/l) | Cr(III) (mg/l) |
|------|-----|------|------|------|------|------|------|--------|--------|-------|--------|---------|
| 2-Sep | 9.10 | 8.23 | 0.0 | 0.00 | 0.38 | 0.05 | 5.00 | 579.52 | 158.78 | 378.20 | 0 | 0 |
| 4-Sep | 28.00 | 8.23 | 0.0 | 0.00 | 0.35 | 0.05 | 12.50 | 532.95 | 146.00 | 361.60 | 0.179 | 0.179 |
| 5-Sep | 38.44 | 8.22 | 2.0 | 0.10 | 0.34 | 0.05 | 15.00 | 525.39 | 143.94 | 352.50 | 2.695 | 0.695 |
| 6-Sep | 48.04 | 8.36 | 5.0 | 0.25 | 0.34 | 0.05 | 15.00 | 520.10 | 142.49 | 379.40 | 5.4025 | 0.4025 |
| 7-Aug | 58.28 | 8.36 | 8.0 | 0.40 | 0.36 | 0.05 | 10.00 | 549.39 | 150.52 | 429.80 | 8.3425 | 0.3425 |
| 8-Sep | 68.92 | 8.23 | 9.0 | 0.45 | 0.37 | 0.05 | 7.50 | 563.79 | 154.46 | 427.00 | 11.1 | 2.1 |
| 9-Sep | 78.12 | 8.20 | 12.0 | 0.60 | 0.35 | 0.05 | 12.50 | 533.07 | 146.05 | 420.90 | 12.36 | 0.36 |
| 10-Sep | 89.00 | 8.19 | 13.0 | 0.65 | 0.36 | 0.05 | 11.00 | 545.59 | 149.48 | 425.00 | 14.08 | 1.08 |
| 11-Sep | 98.40 | 8.17 | 15.0 | 0.75 | 0.35 | 0.05 | 12.50 | 532.55 | 145.90 | 400.90 | 14.685 | -0.315 |
| 13-Sep | 118.40 | | 15.5 | 0.78 | | | | | | | 15.4725 | -0.0275 |
| 15-Sep | 137.30 | | 14.5 | 0.73 | | | | | | | 15.8825 | -1.3825 |
| 16-Sep | 147.74 | | 15.5 | 0.78 | | | | | | | 16.6625 | -1.1625 |
| 19-Sep | 167.64 | 8.11 | 15.0 | 0.75 | | | | | | 412.20 | 16.3925 | 1.3925 |
| 20-Sep | 172.24 | 8.16 | 16.0 | 0.80 | | | | | | 436.70 | 15.4325 | -0.5675 |